UNIVERSITÉ DU QUÉBEC

THÈSE PRÉSENTÉE À

L'UNIVERSITÉ DU QUÉBEC À TROIS-RIVIÈRES

COMME EXIGENCE PARTIELLE

DU DOCTORAT EN GÉNIE ÉLECTRIQUE

PAR

KHALID ETTIHIR

GESTION DE L'ÉNERGIE INTÉGRANT LES VARIATIONS DE COMPORTEMENT NON MODÉLISÉES DANS UN VÉHICULE ÉLECTRIQUE À PILE À COMBUSTIBLE

OCTOBRE 2017

UNIVERSITÉ DU QUÉBEC À TROIS-RIVIÈRES

DOCTORAT EN GÉNIE ÉLECTRIQUE (PH.D.)

Programme offert par l'Université du Québec à Trois-Rivières

GESTION DE L'ÉNERGIE INTÉGRANT LES VARIATIONS DE COMPORTEMENT NON MODÉLISÉES DANS UN VÉHICULE ÉLECTRIQUE À PILE À COMBUSTIBLE

PAR

KHALID ETTIHIR

Loïc Boulon, directeur de recherche	Université du Québec à Trois-Rivières
Pierre Sicard, président du jury	Université du Québec à Trois-Rivières
Kodjo Agbossou, codirecteur de recherche	Université du Québec à Trois-Rivières
Yves Dubé, évaluateur	Université du Québec à Trois-Rivières
Daniel Hissel, évaluateur externe	Université de Franche-Comté (France)

Thèse soutenue le 07 Février 2017

Résumé

Le système pile à combustible (PAC) est une solution pleine de promesses pour le transport automobile sans émission de gaz à effet de serre. Dans la pratique, la PAC est hybridée avec des sources de puissance dans un système de traction automobile afin de récupérer l'énergie au freinage et assister la PAC dans les phases d'accélérations. Par conséquent, le couplage de la PAC avec une source annexe (par ex. des batteries) conduit à l'élaboration de stratégies de gestion d'énergie (SGE). L'objectif des SGE est, entre autres, d'assurer une répartition efficiente de l'énergie pour réduire la consommation ou pour augmenter l'autonomie de roulage. Dans cette thèse, une SGE optimale entre une PAC et un pack de batteries est développée en prenant en compte les variations des conditions opératoires de la PAC. La PAC est un système multiphysique et, par conséquent, ses performances varient selon les conditions opératoires (i.e, température, humidité relative, stœchiométrie et pression des gaz, et le degré de dégradation). De ce fait, des techniques spécifiques doivent être développées pour atteindre les meilleures performances de la PAC tout en assurant les performances de roulage. Dans cette thèse, une méthode basée sur l'identification en ligne des paramètres d'un modèle de PAC est établie afin de retranscrire les performances de la PAC en ligne. Ensuite, un algorithme d'optimisation est couplé à l'identification en ligne afin de rechercher les maximums de rendement et de puissance de la PAC. Ce procédé est utilisé dans une SGE globale optimale basée sur le principe du minimum de Pontriaguine. Cette thèse, démontre que la SGE optimale adaptative permet de réduire la consommation d'hydrogène tout en préservant la PAC pendant son fonctionnement.

Table des matières

Liste des figures

Chapitre 1 - Introduction

1.1 Contexte : Développement durable ou consumérisme ?

Les besoins énergétiques mondiaux grandissants et dus à la forte croissance des pays émergents constituent une problématique majeure pour la communauté internationale. Le secteur du transport est particulièrement dépendant des combustibles fossiles et spécifiquement du pétrole. L'agence internationale de l'énergie a mis en lumière qu'à l'horizon 2040 le prix du baril de pétrole serait fatalement élevé malgré les avancées technologiques en matière d'extraction et une politique favorable à l'amélioration du rendement énergétique [1]. La pérennité de l'économie mondiale est menacée, de plus l'utilisation des combustibles fossiles impactes de plus en plus les changements climatiques. En effet, les combustibles fossiles sont responsables en grande partie des émissions de Gaz à Effet de Serre Anthropologique (GESA), conduisant ainsi à la modification des écosystèmes.

Le secteur automobile constitue une part importante dans les émissions de GESA au Québec [2]. D'après le Ministère du Développement durable, de l'Environnement et des Parcs, le secteur du transport des biens et personnes est responsable de 44.7% des émissions de GESA au Québec (figure 1). Le Québec importe la totalité de son pétrole pour le raffiner par la suite[1]. Cela représente selon l'institut statistique du Québec une facture annuelle de

[1] Énergie et ressources naturelles du Québec [consulté le 17 septembre 2015]. Disponible sur : http://www.mern.gouv.qc.ca/energie/statistiques/statistiques-import-export-petrole.jsp

10 998 millions de dollars canadiens. Le pétrole est majoritairement responsable de la balance commerciale énergétique négative (charbon : 212 M$ et gaz naturels : 1 160 M$). Avec le temps, la balance énergétique négative québécoise croit fatalement et des solutions énergétiques alternatives pour le transport doivent émerger.

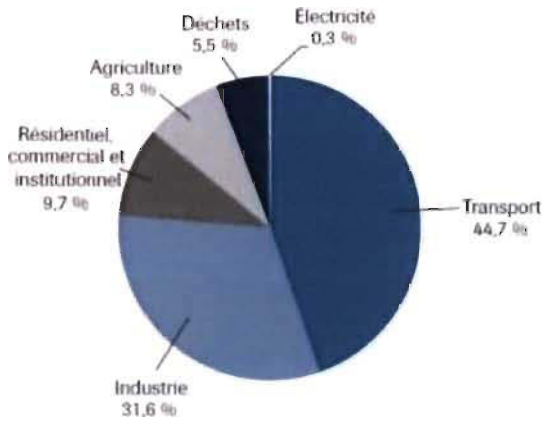

Figure 1: Répartition des émissions de GESA par secteur au Québec [2].

Actuellement, le véhicule électrique hybride à moteur à combustion interne (VEH) est une solution viable, mais toujours dépendante des énergies fossiles. Le véhicule tout électrique (VTE) à batterie (VB) est une alternative sérieuse au VEH. Cependant, la problématique du temps de recharge, la basse capacité, le coût, la faible plage de température de fonctionnement et le nombre de cycles des batteries sont un frein à l'implantation du VB [3].

Une des solutions prometteuses est le véhicule hybride pile à combustible (VHPAC) et en particulier le VHPAC à pile PEM (Proton Exchange Membrane). Ce type de véhicule se caractérise par une émission locale de polluant nulle, une efficacité énergétique supérieure au moteur à combustion (dans les VEH), et un temps de recharge faible (quelques minutes,

contrairement aux batteries qui demandent plusieurs dizaines de minutes, pour les meilleures recharges rapides) [4].

Dans le transport, la pile PEM est généralement retenue, car cette dernière possède des avantages par rapport aux autres technologies (ex : solide oxyde, alcalin, direct methanol…) telles que la basse température de fonctionnement, une tolérance au CO_2 (utilisation de l'air comme comburant), ainsi que des densités de puissance élevées. Par contre, la pile PEM souffre d'une forte sensibilité à la pureté de l'hydrogène, d'une nécessité forte d'équilibrer l'humidification et d'un prix de catalyseur élevé, d'où la nécessité d'auxiliaires performants [5, 6].

La pile PEM pâtie aussi d'une limitation dynamique et devrait être surdimensionnée, en puissance notamment, pour répondre seule aux transitoires de la charge (par exemple : démarrage du véhicule). La cause est que la pile PEM est limitée par la dynamique fluidique et un phénomène de famine est observé quand une consigne de puissance de dynamique et d'amplitude élevées est imposée à la pile. Dans une architecture de véhicule pile à combustible, il est nécessaire d'hybrider avec une source secondaire (batterie de puissance, supercondensateur, volant inertiel...) pour répondre aux fortes dynamiques et satisfaire la demande du conducteur ainsi que pour récupérer l'énergie au freinage [7]. Comme l'hybridation induit une répartition de l'énergie entre au moins deux sources, la recherche de Stratégies de Gestion de l'Énergie (SGE) s'impose.

1.2 Stratégies de gestion d'énergie pour les véhicules à pile à combustible : importance des variations de performances de la PAC et nécessité d'une gestion adaptative

1.2.1 Problématique

Dans la littérature, les SGE pour le VHPAC peuvent se définir en deux classes : les SGE basées sur des règles et celles basées sur le contrôle optimal [8].

Les SGE basées sur des règles sont développées à partir des connaissances des experts sur un système donné (par ex. : le VHPAC). Ces types de SGE sont basées sur des heuristiques, qui prennent une forme déterministe (par ex : SGE thermostatique ou on/off), adaptative ou prédictive et sont facilement intégrables ainsi qu'efficientes sur un système en temps réel.

La seconde approche sur les SGE qui est basée sur l'optimisation se scinde en deux parties : l'optimisation globale et l'optimisation en temps réel. Ces deux méthodes s'appuient sur l'optimisation d'une fonction coût traduite soit par la consommation de carburant (par ex. : hydrogène), par l'efficacité ou par la puissance du système (par ex. : rendement du système pile à combustible).

La littérature abonde de SGE sur les véhicules hybrides, cependant, ce travail de thèse met une emphase sur les SGE temps réel appliquées au VHPAC. À cet effet, Payman et al. [9] propose une commande par platitude afin de réguler le bus continu et réalise une validation expérimentale. Feroldi et al. [10] développe une SGE basée sur la cartographie du rendement et intègre ce travail dans un banc test en temps réel. Leurs études montrent que la consommation d'hydrogène est drastiquement réduite. Hemi et al. [11] développe

une SGE basée sur la répartition optimale de la puissance avec l'application du principe du de Pontriaguine. Une étude de simulation est faite sur un système VHPAC complet. Bernard et al. [12] conçoie une SGE dérivée de la théorie de commande optimale (principe de Pontriaguine) afin de minimiser la consommation d'hydrogène et fournie des résultats expérimentaux. Farouk et al. [13] propose une étude comparative entre une SGE basée sur la logique floue et une autre basée sur la commande optimale adaptée en ligne. La conclusion de ce travail validé expérimentalement, montre que de meilleures performances sont obtenues avec la commande optimale puisque la consommation d'hydrogène est plus faible.

Cependant dans ces études, les SGE sont développées à partir d'un modèle ou d'une cartographie valide dans une plage de fonctionnement donnée. Ce qui constitue une limitation importante des SGE classiques. Cette thèse se focalise sur l'aspect adaptatif des SGE afin de réduire la consommation d'hydrogène et de surcroit augmenter l'autonomie du véhicule (figure 2)

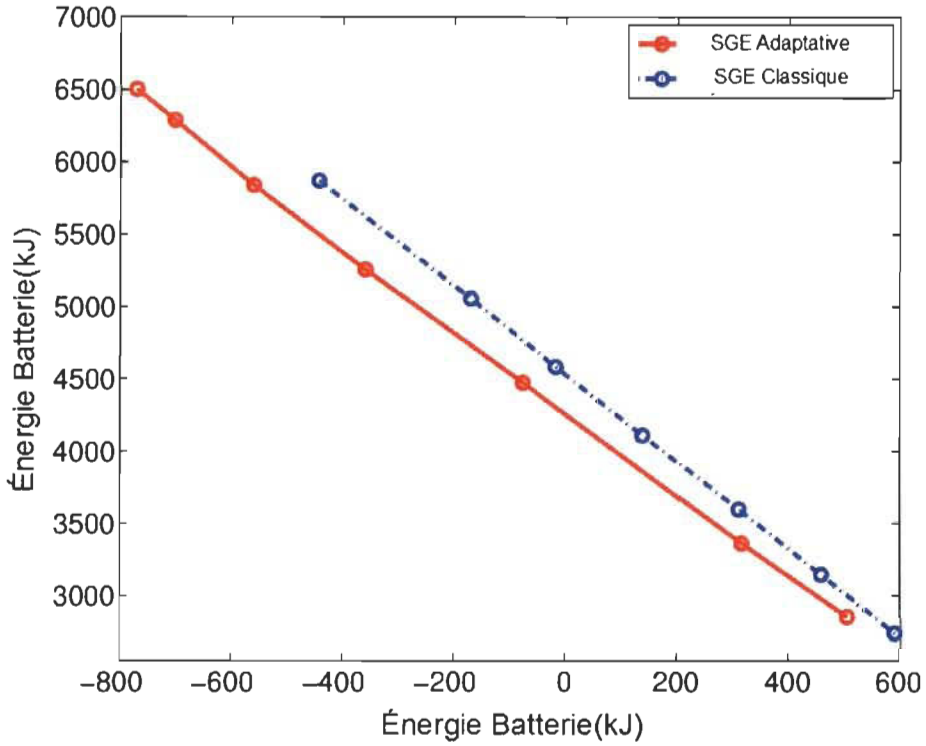

Figure 2 : Énergie d'hydrogène utilisée versus l'énergie des batteries pour deux SGE données

La problématique de cette thèse est la limitation importante des SGE classiques lorsque les performances de la pile à combustible varient en fonction des conditions opératoires (températures, pressions, stœchiométries) et de dégradations.

En effet, la pile à combustible est un système multiphysique, et en conséquence la puissance et le rendement de la pile sont fortement dépendants des conditions opératoires et de dégradations. Les figures 3 et 4 montrent les variations des performances de deux piles PEM de modèle identique[2], mais avec une durée de fonctionnement différente. Les performances en puissance maximum chutent de 30% et le rendement maximum baisse de

[2] Horizon Fuel Cell Technologies [consulté le 11 janvier 2016] disponibles sur:

http://www.horizonfuelcell.com/#!h-series-stacks/c52t

9%. Également, les points d'opérations permettant d'atteindre la meilleure puissance et le meilleur rendement varient sensiblement. Par exemple, il faut un courant différent pour atteindre la meilleure puissance en début et en fin de vie. De plus, deux piles à combustible sorties d'usine et supposées identiques présentent des disparités de fonctionnement et de performance importantes (la production n'est pas encore uniforme). Dans une SGE classique, la pile à combustible avec les performances d'usine est considérée, par conséquent, la SGE n'est plus valide (ou, en tous cas, n'est plus optimale) quand les performances de la pile à combustible changent.

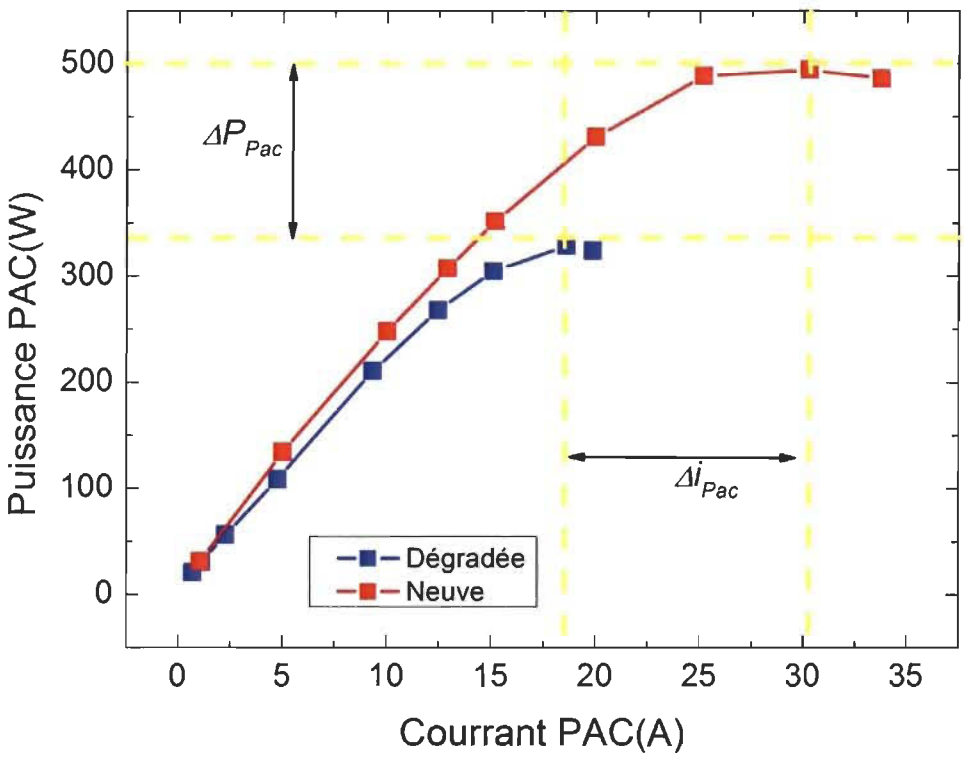

Figure 3: Courbe de puissance de deux piles PEM Horizon de 500W installées à l'IRH avec des heures de fonctionnement différentes.

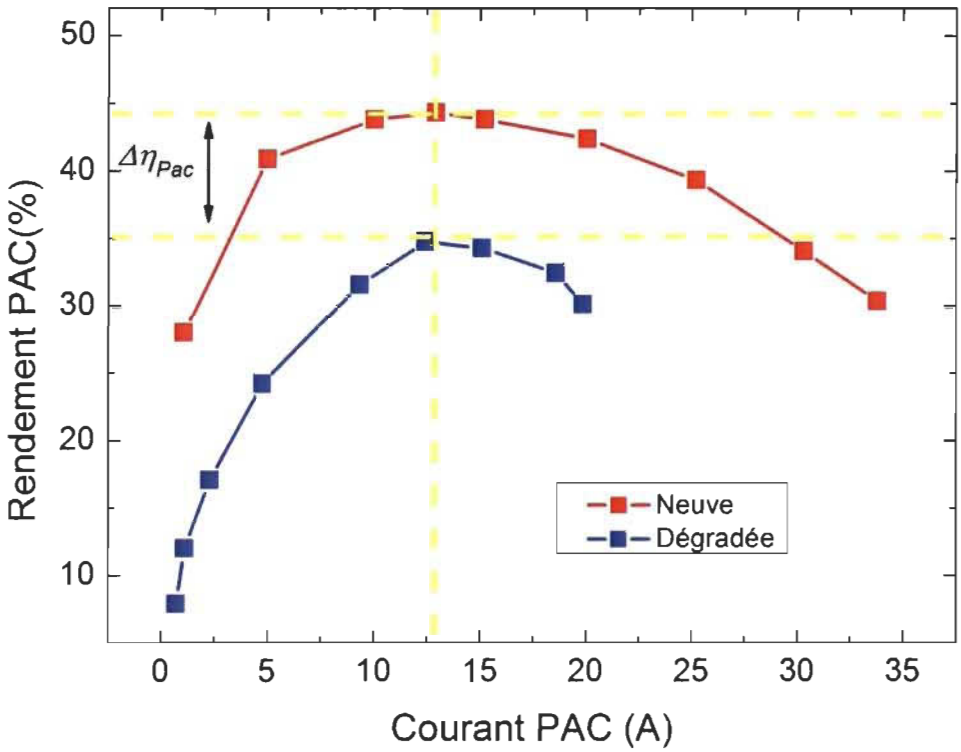

Figure 4: Courbe de rendement de deux piles PEM Horizon de 500W installées à l'IRH avec des heures de fonctionnement différentes.

1.2.2 Objectif général

L'objectif général de cette thèse est donc de développer une SGE optimale complète et en mesure de s'adapter à l'évolution des performances de la pile PEM induite par les variations de conditions d'opérations et de dégradations.

1.2.3 Méthodologie et objectif spécifiques

Pour répondre à cet objectif, cette thèse propose une méthodologie en 3 temps basée sur une identification en ligne des paramètres d'un modèle de pile PEM, la déduction des meilleurs points de fonctionnement et leur intégration dans une SGE adaptative complète (Fig. 4).

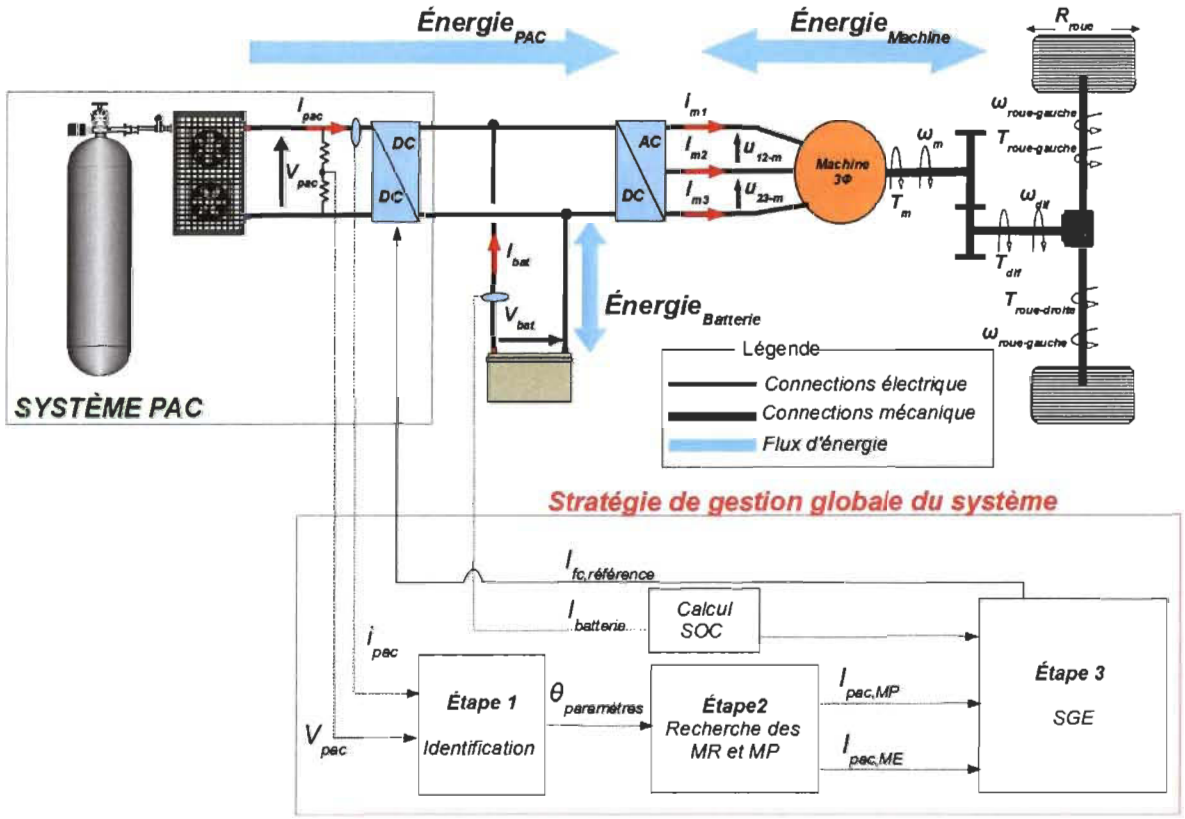

Figure 5 : Synoptique de la gestion d'énergie adaptative avec le système pile à combustible (PAC).

Dans les applications en temps réel, une solution pour pallier ces limites dans une SGE est l'utilisation de modèles complexes afin de considérer l'aspect multiphysique du système pile à combustible [14]. Cependant, le développement et la validation de ce type de modèle sont ardus et il n'existe pas encore de modèles matures de dégradation de la pile à combustible [14]. De plus, la complexité du modèle fait exploser les temps de calcul, ce qui est rédhibitoire pour une implantation de SGE en temps réel.

Une autre solution est l'emploi de modèles de type boite noire et d'adapter les paramètres en ligne en fonction des fluctuations des conditions opératoires et de dégradations. Beaucoup de modèles de pile à combustible dans la littérature répondent aux contraintes du

temps réel et possèdent des paramètres identifiables en ligne. Meiler et al. [15] classifie les modèles temps réel de pile PEM pour les SGE et montre que parmi tous les modèles étudiés dans ces travaux (logique floue, réseau de neurones, auto régressive, de Wiener…), les meilleurs résultats sont obtenus par le modèle d'Uryson. Raga et al. [16] propose d'étudier un modèle de pile PEM de type boite noire afin de développer une méthodologie d'identification expérimentale des paramètres empiriques hors ligne. Les résultats montrent un écart de 2% entre les résultats de simulation et expérimentaux de, ce qui rend possible l'utilisation de ce modèle pour la conception de commandes basées sur des modèles. Valdivia et al. [17] utilisent des modèles de type boîte noire afin d'émuler le comportement d'une source hybride (pile PEM couplée avec un pack de batteries à travers un convertisseur DC-DC). Cette étude démontre la possibilité d'identifier hors ligne le comportement de la source hybride pour la conception de commande. Torreglosa et al. [18] développe dans son étude une comparaison entre un modèle de pile PEM linéaire et un modèle de Wiener pour prendre en compte la non-linéarité du comportement de la pile à combustible. Les paramètres des modèles sont déterminés hors ligne et la conclusion de l'article pointe sur la nécessité de la prise en compte de la non-linéarité de la caractéristique de la pile à combustible pour une meilleure précision du modèle pour le contrôle. Kunusch et al. [19] propose pour sa part un modèle paramétrique traduisant la quantité d'eau dans la membrane de la pile à combustible. Ce travail démontre la possibilité d'estimer en ligne la quantité d'eau dans la membrane. Les travaux de Xu et al. [20] constitue une base solide pour les travaux de cette thèse car une SGE optimale adaptative est développée pour un système PAC. Les paramètres d'un modèle très simple de la PAC sont déterminés grâce à un algorithme des moindres carrés pour mettre un jour des cartographies représentant la

dynamique temporelle de la PAC. Le point négatif de cette SGE réside justement dans l'utilisation de ces cartographies de constante de temps fixes.

Ces travaux montrent clairement la possibilité d'estimer les paramètres d'un modèle de pile PEM pendant son opération. Néanmoins, ces approches se basent sur des modèles mathématiques pour la plus part, sans signification physique reliée au système étudié. Cette signification physique est pour nous essentielle afin de mettre à profit notre expertise du système pour l'analyse des résultats et le développement subséquent des SGE.

D'un autre côté, la littérature montre que des modèles semi-empiriques ont la capacité de décrire le comportement de la pile PEM avec une signification physique et un temps de calcul réduit [21, 22], ce qui constitue une solution de choix pour une SGE adaptative [20].

Par conséquent, un modèle semi-empirique de pile PEM est utilisé dans ce travail de thèse, car cela offre un compromis entre la signification physique des paramètres et le temps de calcul dans le développement d'une SGE adaptative.

Objectif spécifique 1 : Développer une méthode d'identification en ligne des paramètres d'un modèle semi-empirique de pile à combustible.

Un modèle semi-empirique est donc utilisé pour suivre les performances de la PAC en temps réel grâce à une méthode d'identification en ligne. Ce modèle peut ensuite être employé afin d'identifier les plages où la pile PEM possède ses meilleures performances. Il convient donc de définir les facteurs de performances de la pile PEM. Dans cette thèse, les indicateurs de performances de la pile à combustible se traduisent par la valeur du Maximum de Puissance (MP) et du Maximum de Rendement (MR). Ces deux critères de performance sont particulièrement intéressants. Un mode de fonctionnement au MP permet

à la pile à combustible de fournir le maximum de puissance possible. Un mode de fonctionnement MR fixe la puissance au maximum du rendement du système pile à combustible, ce qui permet de réduire la consommation d'hydrogène au minimum lors du fonctionnement. En outre, ces deux modes de fonctionnement bornent la plage de puissance de la pile PEM. Ce choix de critères de fonctionnement est soutenu pour diminuer la dégradation de la pile PEM lors du fonctionnement. En effet, la littérature montre que le taux de dégradation des cellules de la pile PEM est plus élevé en dehors des plages de puissance des MP et MR [10, 23].

La recherche des modes de MP et de MR se révèle être un défi puisque les performances de la pile à combustible changent en fonction des conditions opératoires et de l'état de dégradation. Dans le but d'exploiter les meilleures performances de la pile à combustible, différentes études proposent d'importantes contributions.

Zhong et al. [24] a conçu un algorithme MPPT (maximum power point tracking) afin de rechercher de manière itérative le maximum de puissance d'une pile PEM. Benyahia et al [25] a proposé une MPPT pour la pile PEM basée sur le principe du P&O (perturbation and observation). Methekar et al. [26] a décrit une commande optimale adaptative basée sur un modèle de Wiener pour déterminer en ligne le maximum de puissance et a proposé une validation numérique. Becherif et al. [27] a développé une MPPT originale afin de maximiser les performances de la pile PEM par la commande de la consommation de l'air. Dazi et al. [28] a effectué une étude numérique d'une commande prédictive afin que la pile fonctionne au maximum de puissance.

Cependant, peu d'études proposent une validation expérimentale d'une recherche de maximum (MR ou MP) pour une PAC dans une gestion complète. Par exemple, Kelouwani

et al. [29] a présenté les résultats expérimentaux d'un algorithme MEPT (maximum efficiency point tracking) qui recherche, grâce à l'identification en ligne des paramètres d'un modèle empirique, le MR de la PAC. Carlos et al. [30] a proposé une validation *hardware in the loop* d'une MPPT minimisant la consommation d'hydrogène. Somaiah et al. [31] a présenté une MPPT basée sur les moindres carrés recursifsavec une validation expérimentale. Ces études montrent des résultats probants, par contre, il faut remarquer que les modèles utilisés sont des polynômes qui ne sont pas représentatifs de la caractéristique de la pile PEM. De plus, un point commun à toutes ces études est que la problématique de tracking des extrema est toujours traitée de manière unipolaire. En effet, ces études se bornent à l'étude soit de la technique MPPT, soit de la technique du MEPT. Enfin, ces études n'inscrivent pratiquement pas leurs SGE dans un contexte automobile ou les sollicitations dynamiques sont plus contraignantes que dans le domaine stationnaire.

Dans le cas de cette thèse, un modèle semi-empirique de pile PEM est employé, les paramètres sont mis à jour grâce à une méthode d'identification en ligne. Cela permet donc d'utiliser ce modèle identifié en ligne pour déterminer les modes de fonctionnement optimaux (MR et le MP). Les modes de fonctionnement optimaux MR et MP sont recherchés simultanément.

Objectif spécifique 2 : Développer une méthode embarquée d'identification simultanée des points de MR et de MP basée sur le modèle mis à jour en temps réel de l'objectif spécifique 1.

En résumé, des SGE permettent de répartir la puissance entre deux sources dans un système hybride (par exemple batterie et pile à combustible) et des méthodes permettent de déterminer les meilleures performances (MP et MR) de la pile à combustible. Cependant, il

faut mettre en lumière qu'il n'existe pas de SGE faisant le lien entre la répartition de puissance et les méthodes de recherche de meilleures performances de la pile PEM. À ce jour, la littérature n'offre pas d'étude sur les SGE en temps réel pour un VHPAC qui établit un lien entre les meilleurs points de fonctionnement de la pile à combustible.

Objectif spécifique 3 : Développer une méthode de répartition de puissance optimale entre la pile PEM et la source auxiliaire intégrant l'évolution des meilleurs points d'opération en fonction de la variation des conditions d'opérations et de dégradations.

Ainsi, cette thèse aboutira au développement d'une SGE en temps réel prenant en compte les variations de performances de la pile à combustible dans le cadre du véhicule.

1.3 Plan de thèse

Dans cette thèse, trois articles dédiés chacun à une étape spécifique de la gestion décrite à la figure 4 sont présentés.

Dans un premier article, un travail sur les modèles semi-empiriques est réalisé pour définir le modèle capable de reproduire le comportement de la pile à combustible en temps réel. Une technique adaptative de moindres carrés est couplée au modèle afin de mettre à jour les paramètres en fonction des performances de la pile PEM. La méthode d'identification est validée sur un banc de test expérimental. Les résultats permettent de passer à l'étape suivante puisque l'article démontre que les courbes de polarisation de la pile PEM sur des températures différentes sont effectivement identifiées.

Par la suite, l'objectif du deuxième article est double. Premièrement, il est de prouver que la méthode d'identification permet de déterminer les maximums de puissance et de

rendement grâce à une optimisation sur le modèle identifié. Ensuite, démontrer que la méthode d'identification couplée à la recherche des maximums de puissance et de rendement peut s'inscrire dans une SGE simple et surtout en temps réel. L'objectif est atteint en comparant deux stratégies sur deux piles PEM avec des degrés de dégradations différents. En effet, une stratégie globale sans la méthode d'identification développée est comparée à une stratégie avec la méthode d'identification et d'optimisation. Les résultats expérimentaux montrent que la méthode développée permet bien de prendre en compte la dégradation d'une pile PEM en s'adaptant au changement de performance. Tandis que la SGE sans la méthode développée provoque l'arrêt du système.

Enfin, le troisième article décrit une SGE optimale en temps réel pour la répartition de l'énergie dans un VHPAC. Cet article constitue une réponse à la problématique générale posée. Le principe de Pontriaguine est utilisé pour formuler un problème d'optimisation sous contrainte. Comme classiquement, ce type de SGE utilise un modèle de pile à combustible fixe, le troisième article propose d'inclure la méthode d'identification dans cette SGE. Dans le deuxième article, la gestion était vue comme une machine à état qui active ou non des modes de fonctionnement de la pile PEM (maximum de puissance ou de rendement). Dans ce troisième article, la méthode d'identification des performances de la pile PEM est employée pour identifier les bornes (maximum de puissance et de rendement) de fonctionnements de la pile à combustible. D'autre part, la méthode permet aussi de mettre à jour la fonction coût (la consommation d'hydrogène). En conséquence, la gestion d'énergie est maintenant optimale, tout en s'adaptant à la variation des performances (par ex., dégradation) de la pile à combustible.

Chapitre 2 - Article 1 : Identification en ligne d'un modèle semi empirique de pile PEM

Dans cet article, une étude est menée afin d'identifier un modèle semi-empirique capable de reproduire en temps réel le comportement de la pile PEM. L'utilisation d'un modèle semi-empirique est un choix fort puisqu'une très grande partie des travaux dans la littérature s'appuie sur des modèles de type boite noire. Ce choix est motivé par la possibilité d'analyser les paramètres empiriques du modèle afin qu'un regard expert puisse évaluer la pertinence des résultats fournis par l'algorithme d'identification. Pour cela, plusieurs modèles sont comparés avec comme critère nécessaire à l'estimation du maximum de puissance : (i) la prise en compte du transport de masse (surtension la plus influente quand la pile est proche du maximum de puissance), (ii) le nombre de paramètres empirique à estimer et (iii) la signification physique des paramètres identifiés. Une fois le modèle sélectionné, une méthode adaptative des moindres carrés récursifs (ARLS) est employée. L'algorithme ARLS a pour objectif de mettre à jour les paramètres du modèle semi-empirique afin de suivre la variation des performances de la pile à combustible en temps réel. Le modèle couplé à la méthode ARLS est testé sur un banc test LabVIEW/cRio développé pour cette occasion. Le travail expérimental a permis de démontrer que le modèle sélectionné peut estimer les performances de la pile PEM en temps réel.

Deux campagnes de mesures sont conduites sous différentes conditions opératoires de la pile PEM (36 °C et 47 °C). Les mesures expérimentales montrent l'influence de la température sur les performances de la pile. Les résultats permettent également une validation expérimentale de l'estimation de la courbe de polarisation de la pile à combustible par rapport aux mesures dans les conditions données.

Une étude de sensibilité est menée afin d'évaluer l'influence des paramètres sur l'estimation de la puissance de la pile et d'évaluer la possibilité d'une simplification de modèle. Cette étude montre que le transport de masse est un facteur qui influence peu le comportement de la pile PEM puisque l'erreur d'estimation est réduite. Cela explique donc que plusieurs modèles de la littérature négligent cet aspect lors de l'utilisation de modèle semi-empirique dans la gestion d'énergie. Cependant, ces phénomènes de transport de masse sont les principaux responsables des limitations de puissance électrique dans une pile PEM. Ainsi, ce paramètre est capital dans l'estimation du maximum de puissance, comme démontré dans l'article. Ce résultat est significatif pour la suite des travaux qui repose sur l'estimation du maximum de puissance de la pile, notamment pour la recherche du maximum. Il est donc nécessaire d'appliquer un modèle semi-empirique qui tient compte de ce phénomène.

Online identification of semi-empirical model parameters for PEMFCs

Ettihir, K., Boulon, L., Becherif, M., Agbossou, K., & Ramadan, H. S. (2014). Online identification of semi-empirical model parameters for PEMFCs. *International Journal of Hydrogen Energy, 39*(36), 21165-21176.

doi: http://dx.doi.org/10.1016/j.ijhydene.2014.10.045

2.1 Introduction

The increase in worldwide use of fossil fuel energy causes faster depletion of the world reserves and it enhances greenhouse gas and particles emissions which pave the way for global warming at an alarming rate [1]. One of the promising solutions in order to produce electricity in embedded (as hybrid vehicles) or stationary systems is the Proton Exchange Membrane Fuel Cell (PEMFC) [2] as it allows a zero local emission electricity generation and the consumed hydrogen can be produced with renewable energies such as electrolysis process and biomass [3]. In the literature, the hybrid electric vehicle architecture has been classified into three categories: serial, serial-parallel and parallel. The most common architecture for Fuel Cell Vehicle (FCV) is serial [4]. In order to ensure an adequate durability of the PEMFCs, slow electric dynamics is requested. Consequently, another energy source has to be used between the PEMFC and the load such as battery, supercapacitor and/or flywheels [5]. This second device could be either the main source or a simple energetic buffer. The Hydrogen Research Institute (HRI) LSV shown in Fig.1, so-called Nemo, is a multi-source system [6]. Its architecture has been based on battery pack as the primary source and PEMFC as an auxiliary source to extend the FCV autonomy. Such a configuration leads to a decoupled operation of the PEMFC versus the load request. Therefore, very simple global energy management will start and stop the PEMFC

depending on the SOC of the second source [7]. The architecture of several PEMFC based Renewable Energy (RE) systems is quite similar[8].

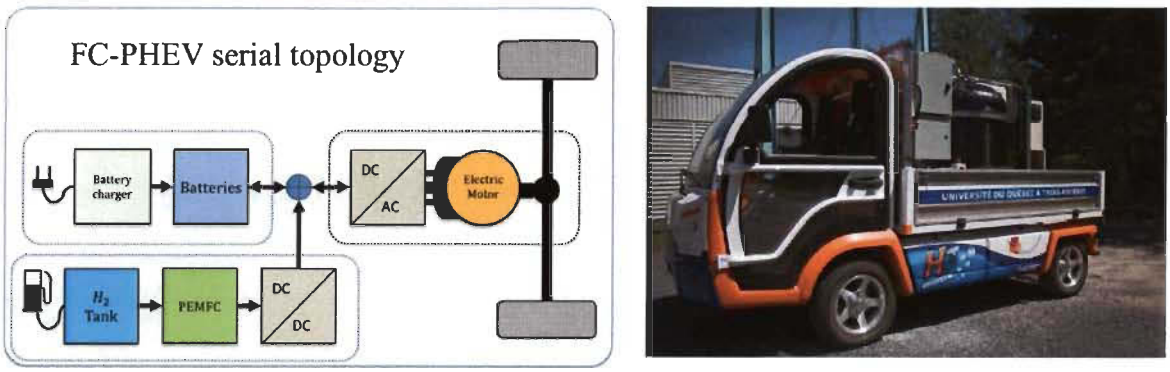

Figure 1: Synoptic of FCV Nemo of the HRI [6].

In a multi-source system, the PEMFC is generally connected through a power electronics converter and electric operating point has to be defined by the energy management [9]; [10]. This operating point can be found in order to maximize the system efficiency (and consequently the vehicle autonomy), the output power, the lifetime and so on [7]. Nevertheless, the PEMFC is a relatively complex system which make difficult to reach these operating points. As a multiphysic system, the Fuel Cell System (FCS) energetic performances are operating conditions dependent. Its performances are greatly influenced by temperature, gas relative humidity, gas stoichiometry and pressure [11, 12]. The desired operating point is constantly moving through the operating space. Therefore, this point has to be sought for different techniques. In several cases, the PEMFCs rated operating point is given by the manufacturer. It is a good compromise between energetic efficiency and durability under given standard operating conditions [13].

The Energy Management Strategies (EMS) of the FCV can be divided into two main classes: (i) rule based and (ii) optimization based. The first ones are both robust with

respect to the inaccuracy of measurement and easily adaptable in real time without a deep system understanding. However, the principal disadvantage of the rule based methods is that the performances of the EMS greatly depend on the knowledge of the designer for a stated problem [9, 14]. Optimization based strategies [15] provide interesting results; however they are deeply model quality dependent. Complex models have to be used in order to take into account the multiphysics behaviour of FCSs [16]. The model design (and validation) may be a difficult and time consuming process. The design of a complete model including ageing effect such as membrane degradation (operating point drift) is still a study limitation [17].

In order to track these issues, Maximal Power Point Tracking (MPPT) and Maximal Efficiency Point Tracking (MEPT) can be easily considered [18, 19]. Nevertheless, these techniques are limited to the FCV strategy management case with a single specific objective function (i.e. the best efficiency or/and the best power). Moreover, the implementation on a FCS can be difficult regarding the system several and different time constants such as electrochemical, fluidic, and thermal time constants that vary from the milliseconds to the minutes. As depicted in Fig.2, [7] show the relevance of a three state energy management based on the level of the battery State Of Charge (SOC). (i) the PEMFC is stopped at high SOC, (ii) the PEMFC at maximum efficiency with medium SOC, (iii) the PEMFC at maximum power with low SOC. With such an energy management, it is important to know the best efficiency point during the best power operation (and vice-versa) in order to ensure efficient switching between the modes. This feature is not possible to implement with either classic MEPT or MPPT algorithms[20].

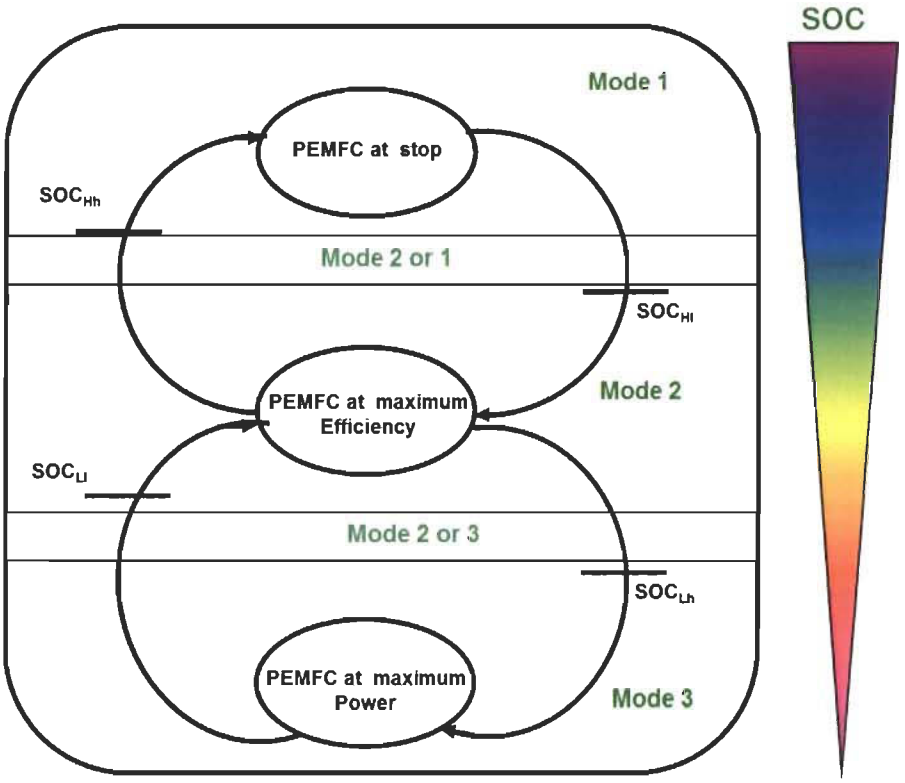

Figure 2: Simple three modes SOC based energy management [7].

In order to address these issues, a three step method is currently developed at the HRI as depicted in Fig.3. The complete process is realized online, during the FCS normal operation. The main idea is to perform a real time model identification (step 1) to find the best operating points with a light optimization algorithm (step 2). In the third step, the identified operating point is applied to the real system. The used model is relatively simple to allow real time identification, however it needs to be continuously updated. Based on this model, it is possible to identify simultaneously several operating points (best power and best efficiency for instance). In addition, higher strategy level can choose among the different identified operating points to enhance the power split in the multi-source FCV. Therefore, it will be possible to design a multi-dimensional model to seek several operating parameters such as current, temperature, pressures...etc [21] . The proposed method deals

with the concept of the extremum adaptive control [22]. This concept has been applied to a class system, usually nonlinear, whose relation between the inputs and outputs of the system admits an extremum. The objective of the control in this concept has been to maintain the state of the system relatively to this extremum. In this study, the maximum power and efficiency of the PEMFC have been considered.

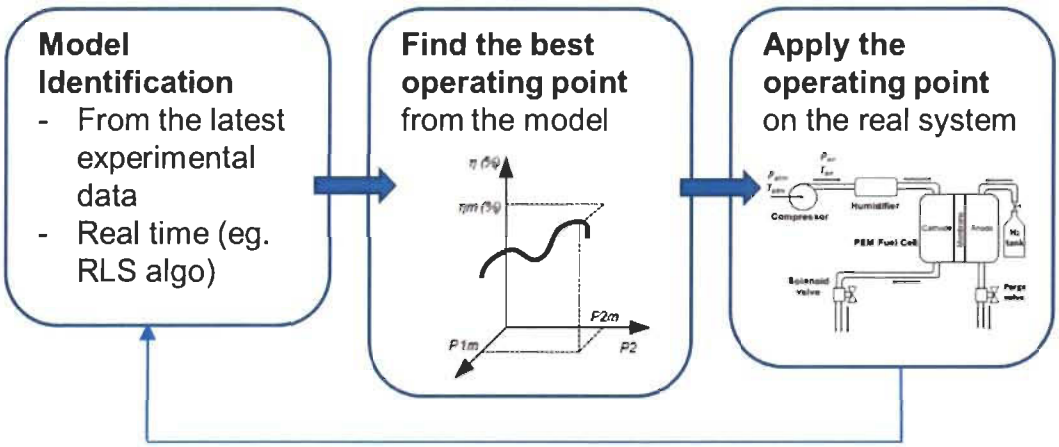

Figure 3: Three step method in order to find and track the best operating points.

This paper is organized as follows. A review of FCS model identification and PEMFC semi-empirical models is proposed. The identification algorithm dedicated to the estimation of the PEMFC model parameters is studied to extract the initial conditions for real time implementation. An experimental validation has been studied with Air Breathing PEMFC of *500W* in order to demonstrate the validity of the proposed method. The ANOVA is considered to highlight the influence of the identified parameters on the estimation of the PEMFC characteristics.

2.2 Model identification method of fuel cell systems

This paper aims at proposing the model identification step. In the parametric identification process, the number of parameters is crucial for the computational time. Relevant model architectures are considered in order to develop a convenient real-time identification method. The literature offers several models that match real time capabilities. *Meiler et al.* [23] defines some classes of model to evaluate the real time capability for different models and concludes that the best result is given by Ursyon-Model (UM). *Yang et al.* [24] uses an Auto-regressive Moving-Average (ARMAX) model to emulate the PEMFC behaviour in addition to design and validate experimentally the proposed control. *Methekar and al.* [25] proposes an adaptive optimizing control based on Wiener model and validate it with numerical simulations. *Dazi and al.* [26] investigates on simulation study of PEM-FC with a general predictive control. In this study, a semi-empirical model (polarization curve) has been considered because this type of model adequately describes PEMFC behaviour with a physical meaning and with relative short computational time [27-29]. These physical meanings such as open circuit voltage (OCV), activation, ohmic and mass transport overvoltage are very interesting to evaluate the relevance of the results. In this work, semi-empirical models are studied because the aim is to provide information to the energy management and not to design dynamic control rules.

2.3 PEMFC model overview

An important step for the model identification is to define the model. The PEMFC is subject to operating parameter variations because the physical conversion including electrochemical, thermodynamic, fluidic transport and electrical phenomena [30]. Different PEMFC models have been proposed in the literatures that emulate PEMFC behaviour

based on 0D, 1D, 2D or 3D dimension [31-33]. PEMFC model parameters have been mostly identified at a given operating condition [9, 34]. However in real time operation, the range of validity of the identified parameters is mainly influenced by the operating conditions (mainly because of the temperature) and the PEMFC health[35, 36]. Moreover, in the control field, PEMFC static maps (static models) are used for the design of management strategy [10, 14, 37]. These types of control have been no longer valid when the operating conditions change. Consequently, the choice of the convenient PEMFC model has been important. Moreover the granularity level of the model has been selected for real time operation and for reproducing the PEMFC behaviour. In case of high granularity level, the number of empirical parameters would slow down the process. In addition, fewer parameters give a lack of precision for control.

2.3.1 Srinivasan et al. model

In this model, the mass transport overvoltage has been neglected. The model has been the basis of the major semi-empirical model developed in the literature Srinivasan1988:

$$V_{cell} = Vo - b\log(i_{fc}) - ri_{fc} \qquad (1)$$

$$Vo = V_r + 2.303\frac{RT_{fc}}{\varsigma}\log(i_0) \qquad (2)$$

Based on Equation (1) and (2) *Srinivasan et al.* [38] have developed a model based on experimental data and have estimated V_r, ς, i_0, b and r that refer to the reversible potential for the cell, the transfer coefficient of the oxygen reduction, the exchange current, the Tafel slope and the slope of the linear region with nonlinear least square fits respectively.

2.3.2 *Kim et al. model*

Kim [39] has developed a semi-empirical model to fit the $V_{fc}(i_{fc})$ characteristic of the PEMFC at different operating conditions such as temperature, pressure and gas mixture. His study has focused on the following Equations:

$$V_{cell} = Vo - b\log(i_{fc}) - ri_{fc} - m\exp(ni_{fc}) \quad (3)$$

$$Vo = V_r + b\log(i_0) \quad (4)$$

where i_{fc}, V_r, b, i_0 and r are the PEMFC current, the reversible potential of the cell, the Tafel parameters for oxygen reduction and the ohmic resistance of the PEMFC respectively. The parameters *m* and *n* are constants that account for the mass transport phenomena in high current density.

2.3.3 *Lee et al. model*

Lee et al. [40] has proposed a model on the same basis of *Kim* [39]with an exponential term for the concentration loss as shown in Equation (5):

$$V_{cell} = Vo - b\log(i_{fc}) - ri_{fc} - m\exp(ni_{fc}) - b\log\left(\frac{p}{p_{O2}}\right) \quad (5)$$

In addition, a logarithmic term expressing the ratio between the total pressure *p* and the partial oxygen pressure p_{O2} has been added. The parameters *Vo*, *b*, *r*, *m* and *n* have been respectively defined as the OCV and empirical constants depending on operating condition such as temperature, total pressure, oxygen partial pressure and humidity.

2.3.4 Mann et al. model

Mann et al. [41] have considered a model with a mechanistic and an empirical approach of the PEMFC process as given in Equations (6-10):

$$V_{cell} = E_{nernst} + \eta_{act} + \eta_{ohm} \tag{6}$$

$$\begin{aligned} E_{nernst} &= 1.229 - (0.85e^{-5})(T_{fc} - 298.15) \\ &+ (4.308e^{-5})T_{fc}\left[\ln(p_{H2}) + 0.5\ln(p_{O2})\right] \end{aligned} \tag{7}$$

$$\eta_{act} = \xi_1 + \xi_2 T_{fc} + \xi_3 T_{fc}(\ln(c_{O2})) + \xi_4 T_{fc}\ln(i_{fc}) \tag{8}$$

$$\eta_{ohm} = -i_{fc}(r_{electronic} + r_{protonic}) = -i_{fc} r_{internal} \tag{9}$$

$$r_{internal} = \mu_1 + \mu_2 T_{fc} + \mu_3 i_{fc} + \mu_4 T_{fc} i_{fc} + \mu_5 T_{fc}^2 + \mu_6 i_{fc}^2 \tag{10}$$

The cell potential V_{cell} has been determined by the Nernst potential E_{nernst} and the activation η_{act} and the ohmic η_{ohm} over potential. The Nernst potential has been defined as the thermodynamic potential of the chemical reaction inside the PEMFC. It depends on the PEMFC temperature T_{fc} and the partial pressure of oxygen and hydrogen, p_{O2} and p_{H2} . The activation overpotential η_{act} is the sum of the anode and cathode overvoltage. The parameters ζ_1 ,ζ_2,ζ_3 and ζ_4 are empirical parameters related to the kinetics of the reaction. The ohmic overvoltage depends on internal resistance $r_{internal}$ and results in a fit model of the resistance of the proton and electron transfer inside the membrane and the electrodes.

2.3.5 *Squadrito et al. model*

Squadrito et al.[42]have defined a static model of PEMFC on the basis of[38, 39] as stated in Equation (11):

$$V_{cell} = Vo - b\log(i_{fc}) - ri_{fc} + \alpha i_{fc}^{\kappa}\ln(1-\beta i_{fc}) \quad (11)$$

The difference between Equation (11) and previous Equations is in the characterization of the mass transport overpotential. The parameters α and κ are fitting parameters and β is the inverse of the limiting current i_L.

2.3.6 *Kulikovsky et al. model*

Kulikovsky et al. [43, 44] have developed a static model including the oxygen stoichiometry as shown in Equations (12-15). The open circuit voltage and the ohmic overvoltage are the same as in [38-40, 42].

$$V_{cell} = Vo - b\left[\left(1+\frac{\gamma}{1+\gamma}\right)\log(\gamma) - \log(\upsilon)\right] - rj_{fc} - b\log\left(1-\frac{f_{\lambda_{O2}} j_{fc}}{j_L}\right) \quad (12)$$

$$\gamma = \frac{f_{\lambda_{O2}} j_{fc}}{j^*} \quad (13)$$

$$f_{\lambda_{O2}} = -\lambda_{O2}\log\left(1-\frac{1}{\lambda_{O2}}\right) \quad (14)$$

$$j^* = \frac{2\sigma b}{\tau} \quad (15)$$

However, the activation and the mass transport overpotential have been described by the different terms in Equation (12) including the stoichiometry. The parameters j_{fc}, j^*, j_L, υ are the PEMFC current density, the characteristic current (defined by σ, b, the proton

conductivity and the Tafel slope), the limiting current density and a parameter for the concentration overpotential respectively

2.3.7 Model selection

The criteria chosen to determine the semi-empirical model is the physical significance of the parameters, the number of parameters to be identified and the number of sensors used. Obviously, it is necessary that the model accounts for the overvoltages to characterize the PEMFC on all its measurement range. Nevertheless, the mass transport phenomena are also important in order to highlight the maximal power point of the PEMFC.

When the studied models are compared, *Squadrito et al.* model seems to be the best adapted because it has few sensors (only current and voltage measurements) and wider measurement range. The *Kim model* could be also relevant but with less physical parameter meanings as illustrated in Table 1. *Squadrito et al.* model accurately fits the experimental data and is based on the physical meaning of the parameters, and of the previous authors [39-41]. However, Equation (12) is considered not sufficient to justify the physical properties of the mass transport phenomena. *Pisani et al.* [45] have proposed a model on the basis of [39, 40, 42] and related the parameter κ with the water flooding phenomena, the parameter α to diffusion mechanism and β the inverse of the limiting current have a value of 0.99 . Moreover, the parameter has been found in 90% of cases between 2 and 4. So, *Squadrito et al.* model can be considered as a four parameter model (Vo, b, r and α).

Table 1: Implementation Equation

PEMFC semi-empirical Model	Number of fitting parameters	Number of measures	Mass transport overvoltage
Srinivasan et al. [38].	2	2	No
Kim et al.[39]	4	2	Yes
Lee et al.[40]	4	3	Yes
Amphlett et al.[30]	11	5	Yes
Squadrito et al.[42]	4	2	Yes
Kulikovsky et al.[43]	5	3	Yes

2.4 Online modeling with ARLS

2.4.1 Recursive identification algorithm

Among the different recursive methods used for online identification such as Recursive Instrumental Variable (RVA), Recursive Maximum Likelihood (RML), Recursive Correlation and Least Square (RCOR-LS), the Recursive Least Square (RLS) is considered the one that give the best results in real time[46, 47]. The RLS algorithm has been used to identify the extremum function which is suitable for real-time application based on successive updating of model parameters [22]. However, when classic RLS algorithm is implemented for tracking systems with time-varying parameters such as PEMFC, the

algorithm loses its precision during the identification process. A practical solution to maintain the precision of the algorithm is to adapt a forgetting factor ψ to account on more recent measurements. The main methods to update the forgetting factor are Exponential Forgetting (EF) and Directional Forgetting (DF) [48]. EF is well suited for persistently excited time-varying systems. However, an estimation windup phenomena appear when the system is not enough excited and the identification process becomes unreliable and sensitive to noise. DF factor is implemented to improve the performance of the RLS as developed in [49] to avoid the estimation windup phenomena [50, 51]. Moreover, the covariance matrix is decomposed (Bierman decomposition) to ensure a positive semi-definite function and avoid numerical instability [52]. The RLS algorithm coupled with DF factor is qualified as Adaptive Recursive Least Square (ARLS).

2.4.2 Adaptive RLS implementation

The ARLS is used to perform a recursive estimation of the static PEMFC model parameters as depicted in Fig.4.

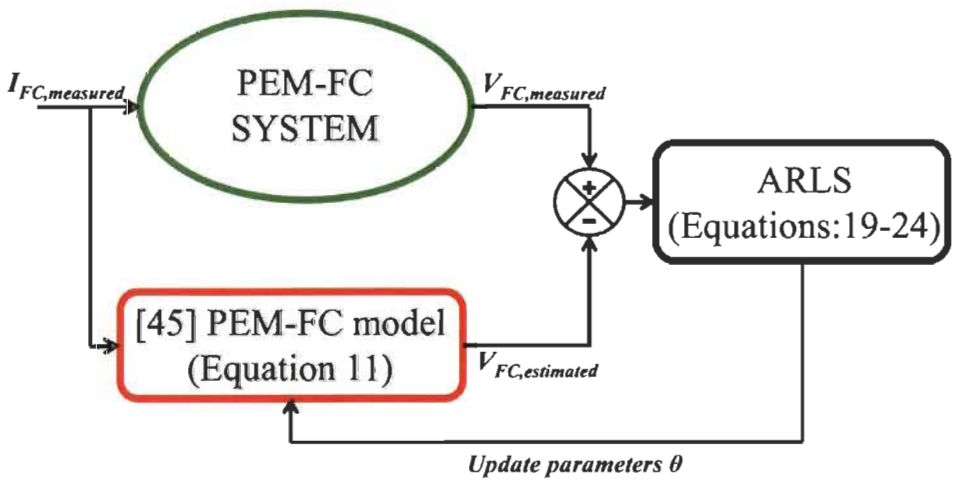

Figure 4: Synoptic of the PEMFC identification with the ARLS.

In this study, the PEMFC is considered as a Single Input Single Output (SISO) system. The model developed by *Squadrito et al.* is proposed for the ARLS algorithm using Equation (16) :

$$[y(k)] = [\phi(k)][\theta(k)]^T + [\xi(k)] \qquad (16)$$

where $\xi(k)$ is a stochastic noise variable with normal distribution and zero mean. At each time step k, the regressor vector $\varphi(k)$ defines the evolution of the measured input current . $y(k)$ is the measured PEMFC voltage . The ARLS algorithm determines online the parameter vector $\Theta(k)$ of the PEMFC behaviour under operating parameters changing with the minimization of the square error prediction $\varepsilon(k)$. Therefore the unknown parameter vector at each step time k, $\Theta(k)$ is defined by Equation (17):

$$\theta(k) = [Vo(k), b(k), r(k), \alpha(k)]^T \qquad (17)$$

The objective function $J(k)$ that should be minimized is the prediction square error of $\varepsilon(k)$ as illustrated in Equation (18):

$$J(k) = \sum_{i=1}^{k} \psi^{k-i} \varepsilon_i^2 \qquad (18)$$

where ψ is the forgetting factor which is necessary to track the variation of the parameters during time variation (ageing drift). ψ is a value between [0;1] and $\varepsilon(k)$ is the prediction error. ψ is initialized at 0.9 and is actualized in Equation 21. The implementation of the ARLS is attained using Equations (19-24):

$$K(k+1) = \frac{P(k)\phi(k+1)}{1 + \phi^T(k+1)P(k)\phi(k+1)} \qquad (19)$$

$$P(k+1) = P(k) - \frac{\left(P(k) - K(k+1)\phi^{T}(k+1)P(k)\right)}{\left(\mu(k)^{-1} + \phi^{T}(k+1)P(k)\phi(k+1)\right)} \quad (20)$$

$$\mu(k+1) = \begin{cases} \psi(k+1) - \dfrac{1-\psi(k+1)}{\phi^{T}(k+1)P(k)\phi(k+1)}; & if\ \phi^{T}(k+1)P(k)\phi(k+1) > 0 \\ 1 & ;\ if\ \phi^{T}(k+1)P(k)\phi(k+1) = 0 \end{cases} \quad (21)$$

$$\varepsilon(k+1) = y(k+1) - \phi^{T}(k+1)\theta(k) \quad (22)$$

$$\theta(k+1) = \theta(k) + K(k+1)\varepsilon(k+1) \quad (23)$$

$$P(k) = U(k)D(k)U(k)^{T} \quad (24)$$

where *K(k)* is the Kalman gain, *P(k)* is the covariance matrix of the prediction error *ε(k)*. The Biermann factorized components are *U(k)* which is an upper triangular matrix with ones in the diagonal,and *D(k)* which is a diagonal matrix. Equations (19-24) are solved recursively to determine $\theta(k)$.

2.4.3 Determination of the experimental initial parameters

The experimental initial parameters of the ARLS should be properly chosen close to the reality to avoid algorithm divergence. Thus, a PEMFC dynamic model is introduced to emulate the *500W* PEMFC behaviour in simulation [21, 53]. This model is parametrized with classical literature values as there is no need preliminary experiment. This model is implemented in Matlab/Simulink. Thereafter, the ARLS algorithm is used for fitting the parameters of the static model as previously described in Fig.2. However, the real PEMFC is replaced by the dynamic model. The determination of the initial operating point is realized during simulation. Consequently, a pseudo random binary current can be injected in the model to maximize the performances of the ARLS algorithm (fitting parameters

depicted in Table 2). The parameters extracted are experimentally used as the initial data of the ARLS.

Table 2: Initialization of the parameters using the ARLS algorithm.

Empirical parameters	*Vo*	*b*	*R*	*α*
Value	33.0694	-0.02594	-26.0395	0.2492

2.5 Experimental validation

2.5.1 Test-bench description

The ARLS algorithm is verified using the initial conditions determined from the numerical simulation. The experiment is performed with an air breathing *500W* PEMFC Horizon composed of *36 cells*. The test bench Fig.5 is a reduced scale of the powertrain of the LSV Nemo of the HRI.

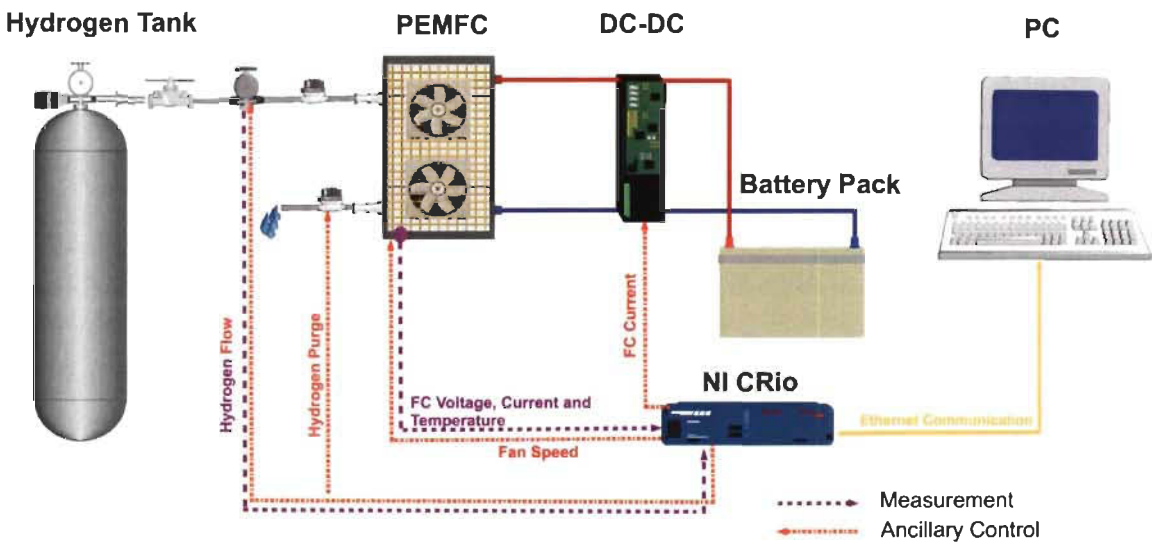

Figure 5: Experimental test bench at the HRI.

The PEMFC works with ancilaries to regulate the pressure and the temperature. The pressure is regulated at *1.5 bars* at the anode side for the hydrogen. The fans have two main roles. The first is to bring the air to the reduction reaction of oxygen on the cathode side. In practice, such a system works with very high stoichoimetry ratio from *10* to *30[54]*. The second is the regulation of the temperature within its operating range between *0* and *65*. Moreover, purge valve evacuates the water produced each *ten seconds* during *ten miliseconds*. The PEMFC current is controlled using *1kW* Zahn Electronics power converter and connected to the lead acid battery pack of *3.9kWh*. The embedded computer compact CRio *9022* of National Instrument is used to control the PEMFC power through the power converter. In addition, control of fan speed, the hydrogen purge, and the data acquisition is performed by this module.

2.5.2 Experimental study under load variation

A current profile has been imposed to the PEMFC on the complete operating range (*0-30A*) as illustrated in Fig.6. The measured and estimated voltages $V_{fc,measured}$, $V_{fc,estimated}$, respectively, have been compared. Percentage error curve has been shown adequate results for the ARLS even for operating parameters variation as demonstrated in Fig.6 and Fig.7. The *Vo*, *b*, *r* and α are the updated fitting parameters of the implemented semi-empirical model during the test as shown in Fig.8.

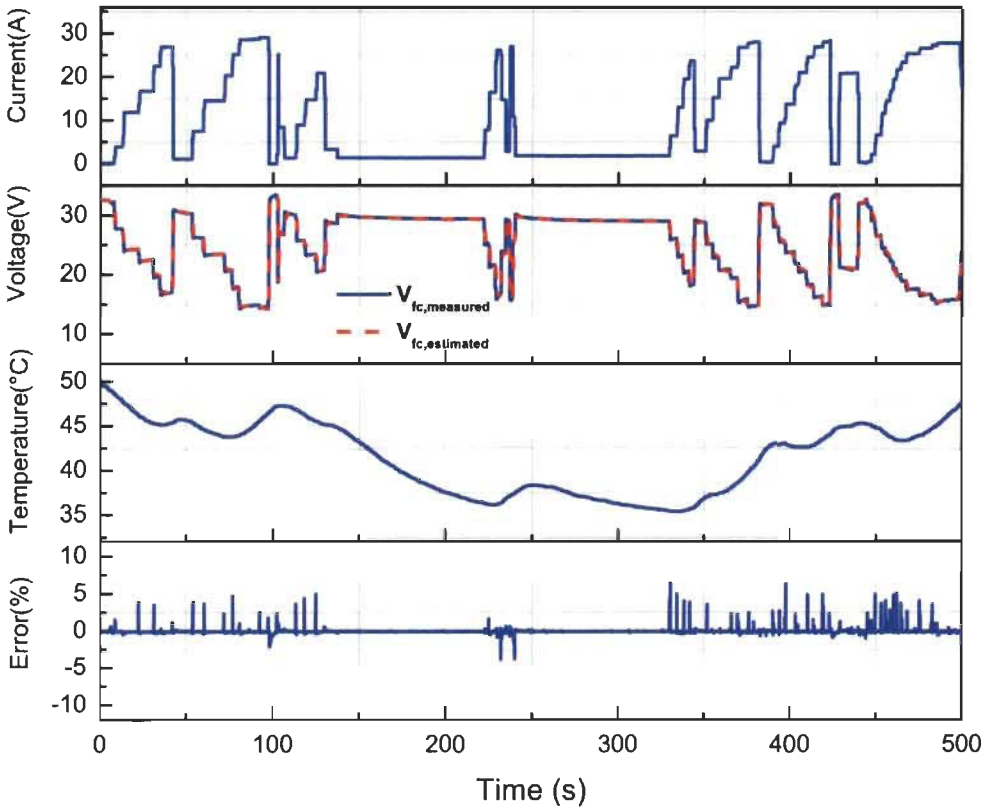

Figure 6: Experimental validation of the ARLS under load and temperature variation.

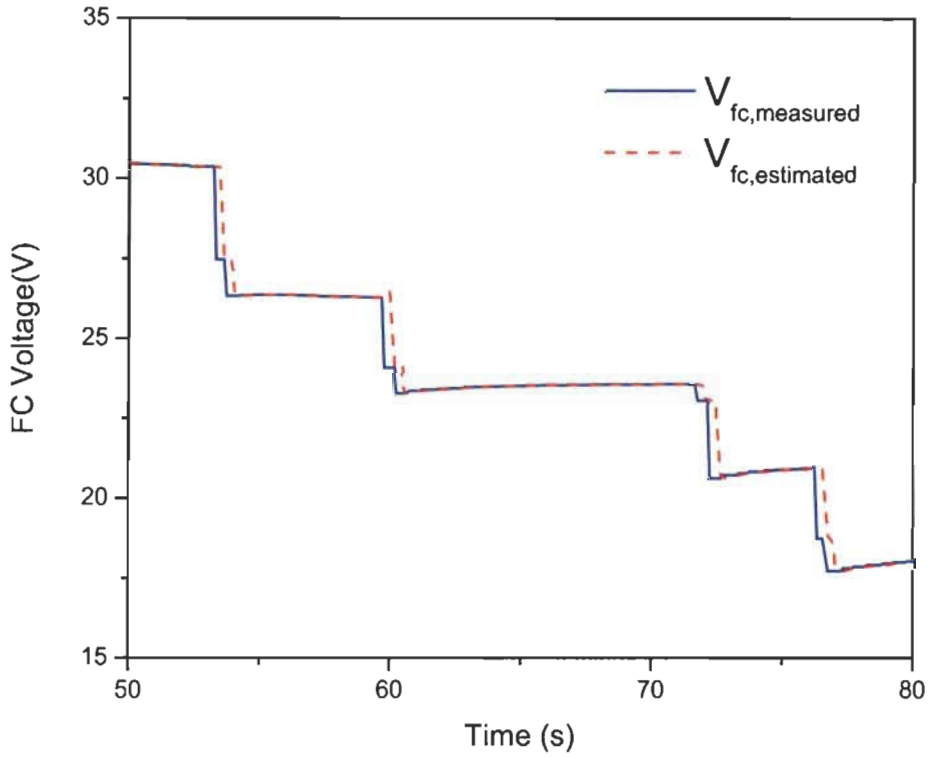

Figure 7: Zoom on the variation of the PEMFC voltage with the ARLS estimation.

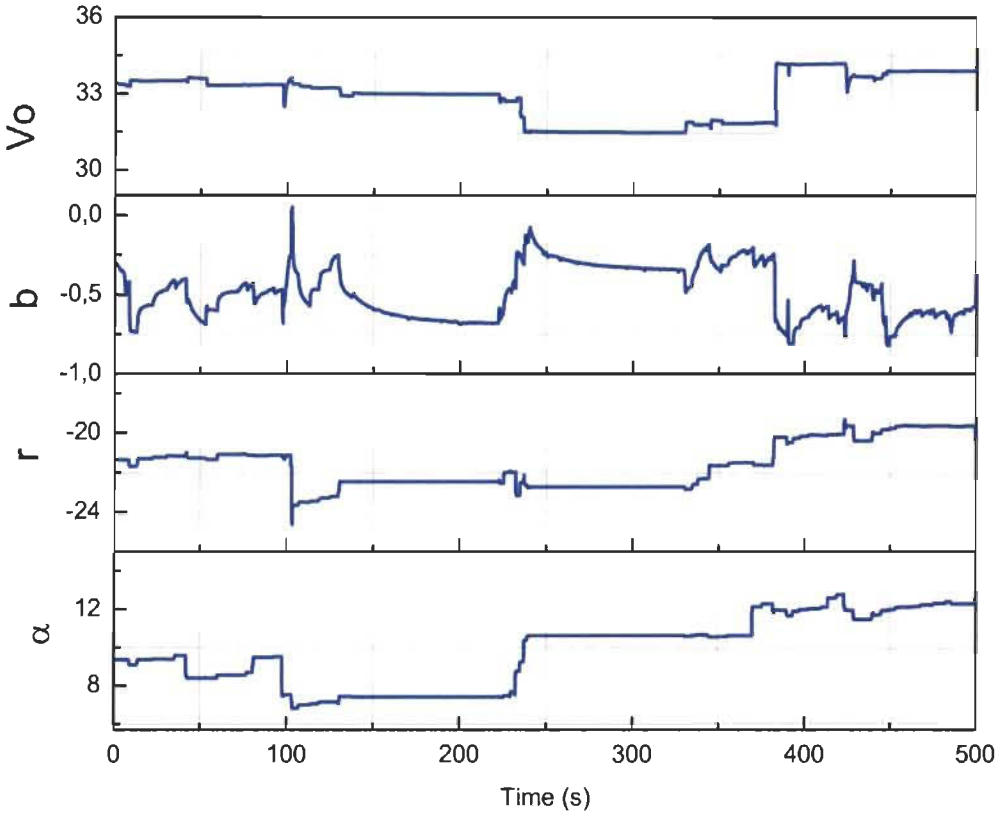

Figure 8: Variation of the empirical parameters considering load and temperature variation.

The experimental test allows plotting the PEMFC characteristics, PEMFC power curves, at two different temperatures T_{fc} to highlight the behaviour of the fitting parameters. Accordingly, two parameter sets are chosen during the previous experiment: (i) when the fans are controlled to achieve maximum speed the temperature of the PEMFC drops to *36°C*, (ii) when the fans are controlled to achieve the minimum speed, the temperature of the PEMFC rises to *47°C*. The two parameter sets are used to plot the PEMFC power curve characteristics at each temperature as demonstrated in Fig.9. As expected from the literature, the temperature increase leads to not only a PEMFC power rise but also an increase in its maximum current [55]. Thus, the ARLS distinguishes the

PEMFC power at different temperatures (at *36°C* and *47°C*) by updating the parameters corresponding to the operating conditions. Finally, polarization curves plot is performed after the ARLS experiment in order to show the relevance of the estimated parameters as shown in Fig.10. For this purpose, a new trial for each polarization curve is done.

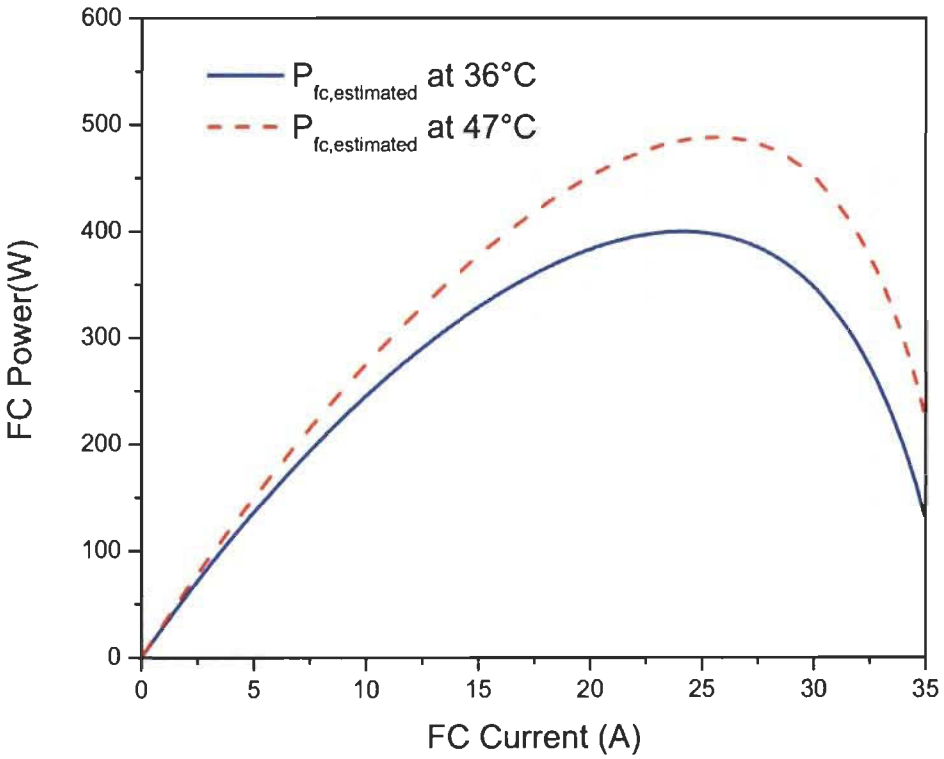

Figure 9: PEMFC power curve identified with ARLS under different operating conditions.

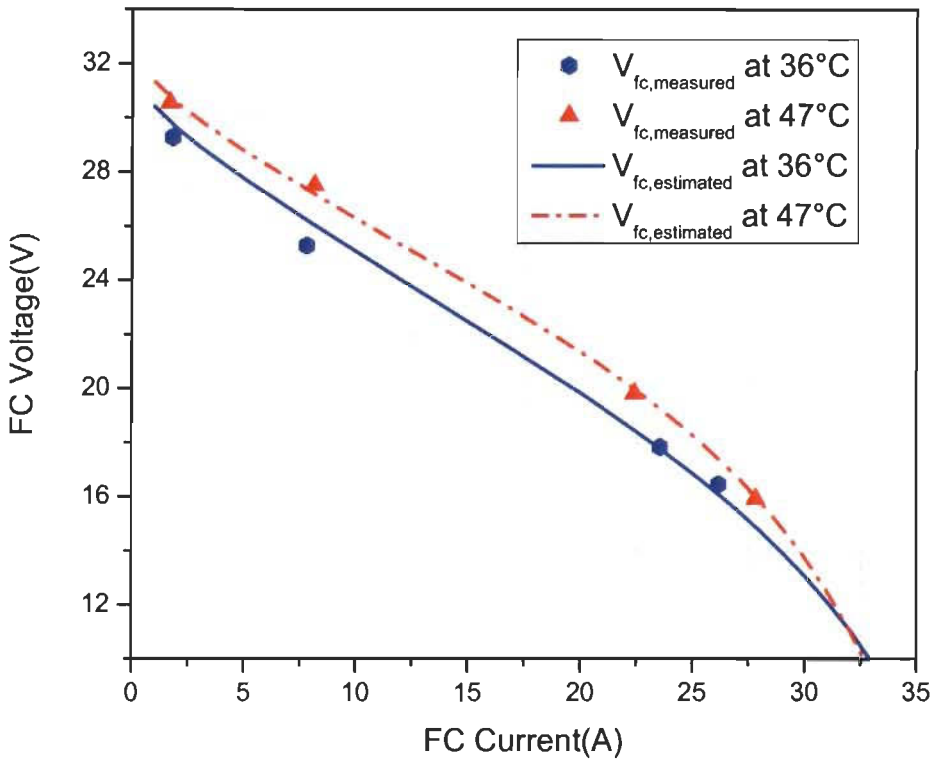

Figure 10: Comparison between the estimated polarization curves and the experimental operating points at different temperature.

2.6 Simulation and experimental results discussion

The use of the static model enables matching with experimental measurement. In the study, four parameters are identified in real time by the ARLS using *Squadrito et al model [42]*. Therefore studying the influence of each parameter on the PEMFC characterization such as OCV, activation (AL), ohmic (OL) and concentration (CL) loss (mass transport phenomena) becomes possible. The decomposition by ANOVA with the Sobol method is

considered to highlight and quantify the parameter that has the greatest effect on the estimated PEMFC voltage [56]. Using Equation (25), the set of results that defines the PEMFC voltage has been calculated as shown in Table 3:

$$V_{FC,w,x,y,z} = Vo_{w} - b_{x}\log(i_{fc}) - r_{y}i_{fc} + \alpha_{z}i_{fc}^{\kappa}\log(l)(1-\beta i_{fc}) \qquad (25)$$

The model used for the online identification is employed to characterize the total variance of the PEMFC voltage and the variance of each factor (Vo, b, r, α) as given in Equations (26-30).

Table 3: Example of the values of the FC Voltage with different parameter level (N=5).

$y=1; z=1$	$Vo_{\|w=1}$	$Vo_{\|w=2}$	$Vo_{\|w=3}$	$Vo_{\|w=4}$	$Vo_{\|w=5}$	Means
$b_{\|x=1}$	$V_{FC,1,1,1,1}$	$V_{FC,2,1,1,1}$	$V_{FC,3,1,1,1}$	$V_{FC,4,1,1,1}$	$V_{FC,5,1,1,1}$	$\overline{V_{FC,.,1,1,1}}$
$b_{\|x=2}$	$V_{FC,1,2,1,1}$	$V_{FC,2,2,1,1}$	$V_{FC,3,2,1,1}$	$V_{FC,4,2,1,1}$	$V_{FC,5,2,1,1}$	$\overline{V_{FC,.,2,1,1}}$
$b_{\|x=3}$	$V_{FC,1,3,1,1}$	$V_{FC,2,3,1,1}$	$V_{FC,3,3,1,1}$	$V_{FC,4,3,1,1}$	$V_{FC,5,3,1,1}$	$\overline{V_{FC,.,3,1,1}}$
$b_{\|x=4}$	$V_{FC,1,4,1,1}$	$V_{FC,2,4,1,1}$	$V_{FC,3,4,1,1}$	$V_{FC,4,4,1,1}$	$V_{FC,5,4,1,1}$	$\overline{V_{FC,.,4,1,1}}$
$b_{\|x=5}$	$V_{FC,1,5,1,1}$	$V_{FC,2,5,1,1}$	$V_{FC,3,5,1,1}$	$V_{FC,4,5,1,1}$	$V_{FC,5,5,1,1}$	$\overline{V_{FC,.,5,1,1}}$
Means	$\overline{V_{FC,1,.,1,1}}$	$\overline{V_{FC,2,.,1,1}}$	$\overline{V_{FC,3,.,1,1}}$	$\overline{V_{FC,4,.,1,1}}$	$\overline{V_{FC,5,.,1,1}}$	$\overline{V_{FC,.,.,1,1}}$

$$Var(V_{FC,w,x,y,z}) = \frac{\sum_{w=1}^{N}\sum_{x=1}^{N}\sum_{y=1}^{N}\sum_{z=1}^{N}(V_{FC,w,x,y,z} - \overline{V_{FC,\dots}})^2}{N^4} \tag{26}$$

$$Var(Vo) = \frac{\sum_{w=1}^{N}(\bar{V}_{FC,w,\dots} - \bar{V}_{FC,\dots})^2}{N} \tag{27}$$

$$Var(b) = \frac{\sum_{x=1}^{N}(\bar{V}_{FC,\dots,x,\dots} - \bar{V}_{FC,\dots})^2}{N} \tag{28}$$

$$Var(r) = \frac{\sum_{y=1}^{N}(\bar{V}_{FC,\dots,y,\dots} - \bar{V}_{FC,\dots})^2}{N} \tag{29}$$

$$Var(\alpha) = \frac{\sum_{z=1}^{N}(\bar{V}_{FC,\dots,z} - \bar{V}_{FC,\dots})^2}{N} \tag{30}$$

As illustrated in Fig.11, the parameters that have the greatest effect on the static model are the OCV and the OL using ANOVA. The PEMFC system model is less sensitive to α than all other parameters. Thus the CL term (mass transport) could be assumed constant and removed from the online identification process in order to reduce the computational time. From a statistical point of view, the PEMFC model is nearby similar to the model of *Srinivasan et al.* extensively discussed in Section 2 [38]. However, if the mass transport is

neglected, the PEMFC maximum power point is no longer identifiable as demonstrated in Fig.12. This operating point is very important for the FCV energy management strategy.

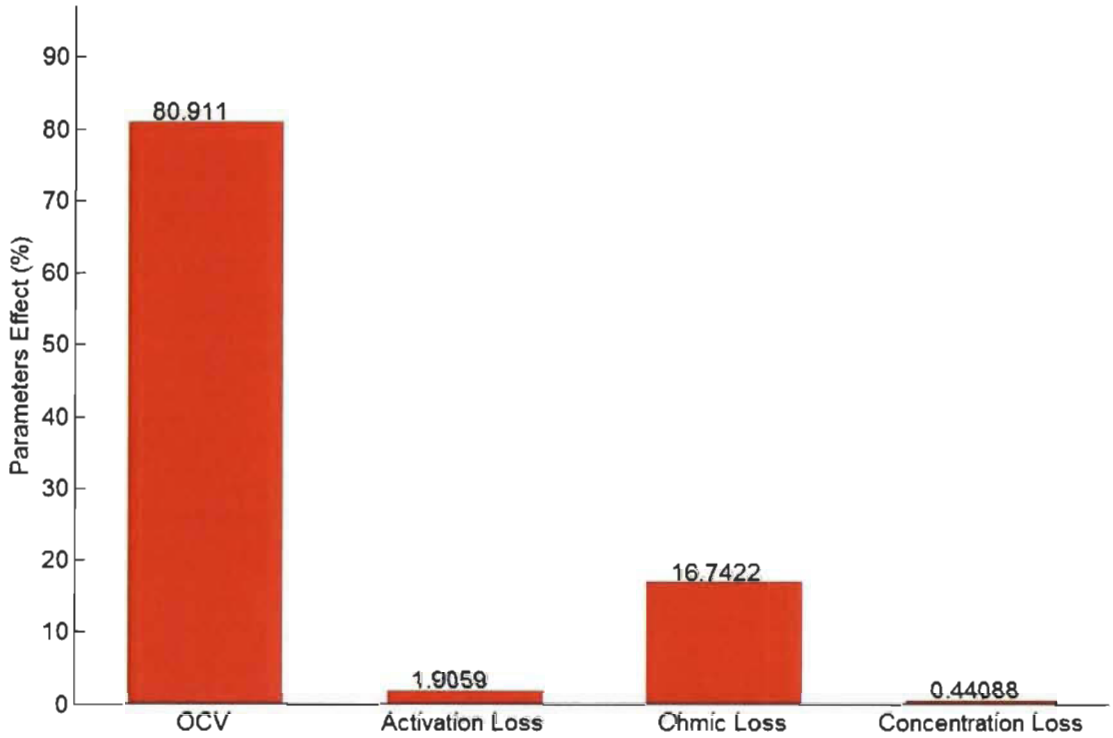

Figure 11: Influence of each fitting parameters on the PEMFC voltage estimation.

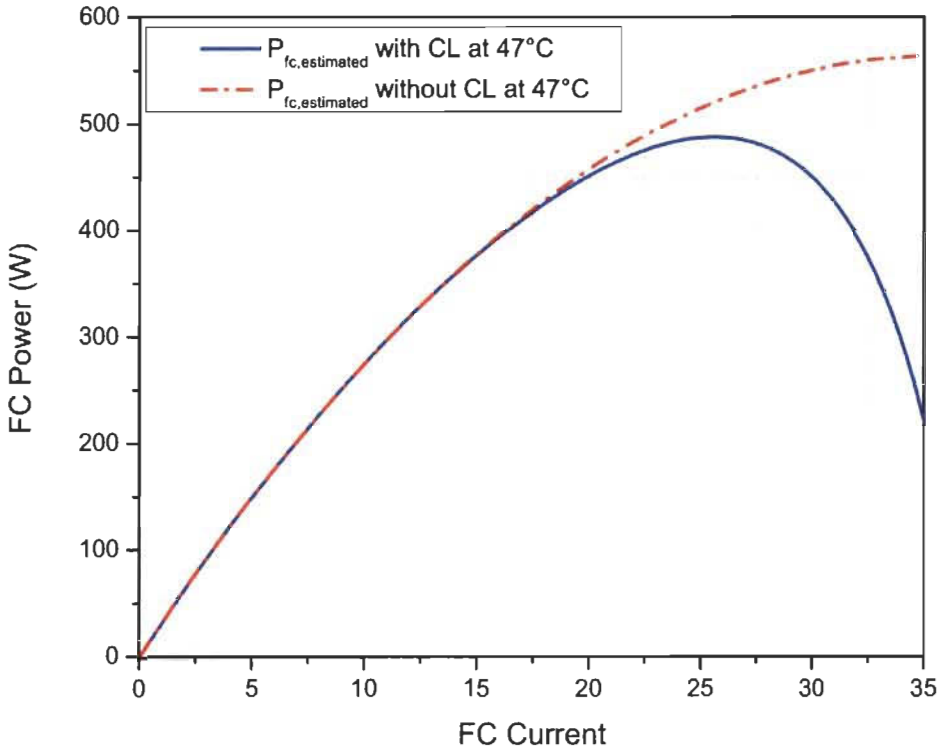

Figure 12: PEMFC power curves with and without mass transport overvoltage (CL).

2.7 Conclusion

In this paper, an online identification approach for the PEMFC air breathing behaviour with semi-empirical model has been presented. For this purpose, *Squadrito et al.* model has been used in favor of its relative simplicity, the physical meaning of the empirical parameters and its reduced number of sensors necessary for the current and the voltage estimation in comparison with the other studied models. The initial parameters have been defined by simulation with a dynamic model of PEMFC. Then, the ARLS has been used because of its suitability for time varying system. The ARLS algorithm has been applied in

real time and the parameters are well identified. The characteristics of the PEMFC have been plotted. Finally, a statistical sensitivity analysis (ANOVA) has been performed to highlight the impact of each parameter on the PEMFC characteristic. The OCV, AL and OL are the most significant parameters on the characterization of the PEMFC with semi-empirical model. Moreover, the CL should be considered owing to its importance in the energy management strategy purposes.

Future works will follow two main axes. Firstly, the identification method will be improved to design a multi-dimensional model to seek several operating parameters such as current, temperature, pressures Secondly, this identification method will be optimally developed on the test bench and then implemented on a real FCV.

Acknowledgments

This work has been supported by the "Bureau de l'efficacité et de l'innovation énergétique", the "Ministère des Ressources naturelles et de la Faune du Québec", the Natural Sciences and Engineering Research Council of Canada, LTE Hydro-Québec, the "Fonds de Recherche Québécois " Nature et Technologie" (FRQNT).

References

[1] I. E. Agency. (2013, 12 Nov 2013). *World Energy Outlook. International Energy Agency.*

[2] R. H. Borgwardt, "Platinum, fuel cells, and future US road transport," *Transportation Research Part D: Transport and Environment,* vol. 6, pp. 199-207, 5// 2001.

[3] T. Azib, O. Bethoux, G. Remy, and C. Marchand, "Saturation Management of a Controlled Fuel-Cell/Ultracapacitor Hybrid Vehicle," *Vehicular Technology, IEEE Transactions on,* vol. 60, pp. 4127-4138, 2011.

[4] C. C. Chan, "The State of the Art of Electric, Hybrid, and Fuel Cell Vehicles," *Proceedings of the IEEE,* vol. 95, pp. 704-718, 2007.

[5] L. Andaloro, G. Napoli, F. Sergi, G. Dispenza, and V. Antonucci, "Design of a hybrid electric fuel cell power train for an urban bus," *International Journal of Hydrogen Energy,* vol. 38, pp. 7725-7732, 6/18/ 2013.

[6] S. Kelouwani, K. Adegnon, K. Agbossou, and Y. Dube, "Online System Identification and Adaptive Control for PEM Fuel Cell Maximum Efficiency Tracking," *Energy Conversion, IEEE Transactions on,* vol. 27, pp. 580-592, 2012.

[7] K. Ettihir, L. Boulon, K. Agbossou, S. Kelouwani, and M. Hammoudi, "Design of an Energy Management Strategy for PEM Fuel Cell Vehicles," *2012 IEEE International Symposium on Industrial Electronics (ISIE),* pp. 1714-1719, 2012.

[8] O. Erdinc and M. Uzunoglu, "Recent trends in PEM fuel cell-powered hybrid systems: Investigation of application areas, design architectures and energy management approaches," *Renewable and Sustainable Energy Reviews,* vol. 14, pp. 2874-2884, 2010.

[9] S. Caux, W. Hankache, M. Fadel, and D. Hissel, "On-line fuzzy energy management for hybrid fuel cell systems," *International Journal of Hydrogen Energy,* vol. 35, pp. 2134-2143, 2010.

[10] D. Feroldi, M. Serra, and J. Riera, "Energy Management Strategies based on efficiency map for Fuel Cell Hybrid Vehicles," *Journal of Power Sources,* vol. 190, pp. 387-401, 2009.

[11] L. Wang, A. Husar, T. Zhou, and H. Liu, "A parametric study of PEM fuel cell performances," *International Journal of Hydrogen Energy,* vol. 28, pp. 1263-1272, 2003.

[12] A. Husar, S. Strahl, and J. Riera, "Experimental characterization methodology for the identification of voltage losses of PEMFC: Applied to an open cathode stack," *International Journal of Hydrogen Energy,* vol. 37, pp. 7309-7315, 4// 2012.

[13] A. Kazim, "A novel approach on the determination of the minimal operating efficiency of a PEM fuel cell," *Renewable Energy,* vol. 26, pp. 479-488, 7// 2002.

[14] C.-Y. Li and G.-P. Liu, "Optimal fuzzy power control and management of fuel cell/battery hybrid vehicles," *Journal of Power Sources,* vol. 192, pp. 525-533, 7/15/ 2009.

[15] F. R. Salmasi, "Control Strategies for Hybrid Electric Vehicles: Evolution, Classification, Comparison, and Future Trends," *Vehicular Technology, IEEE Transactions on,* vol. 56, pp. 2393-2404, 2007.

[16] X.-F. Wang, F. Peng, B.-B. Mao, and W.-R. Chen, "On power following energy management strategy based on fuzzy optimization," in *Control Conference (CCC), 2011 30th Chinese*, 2011, pp. 5073-5077.

[17] O. Z. Sharaf and M. F. Orhan, "An overview of fuel cell technology: Fundamentals and applications," *Renewable and Sustainable Energy Reviews,* vol. 32, pp. 810-853, April 2014.

[18] Z.-d. Zhong, H.-b. Huo, X.-j. Zhu, G.-y. Cao, and Y. Ren, "Adaptive maximum power point tracking control of fuel cell power plants," *Journal of Power Sources,* vol. 176, pp. 259-269, 2008.

[19] N. Bizon, "On tracking robustness in adaptive extremum seeking control of the fuel cell power plants," *Applied Energy,* vol. 87, pp. 3115-3130, 2010.

[20] X. Zhang, X. Chen, B. Lin, and J. Chen, "Maximum equivalent efficiency and power output of a PEM fuel cell/refrigeration cycle hybrid system," *International Journal of Hydrogen Energy,* vol. 36, pp. 2190-2196, 2// 2011.

[21] J. Wishart, Z. Dong, and M. Secanell, "Optimization of a PEM fuel cell system based on empirical data and a generalized electrochemical semi-empirical model," *Journal of Power Sources,* vol. 161, pp. 1041-1055, 10/27/ 2006.

[22] D. E. Seborg, T. F. Edgar, and S. L. Shah, "Adaptive-Control Strategies for Process-Control - a Survey," *Aiche Journal,* vol. 32, pp. 881-913, Jun 1986.

[23] M. Meiler, O. Schmid, M. Schudy, and E. P. Hofer, "Dynamic fuel cell stack model for real-time simulation based on system identification," *Journal of Power Sources,* vol. 176, pp. 523-528, 2008.

[24] Y.-P. Yang, F.-C. Wang, H.-P. Chang, Y.-W. Ma, and B.-J. Weng, "Low power proton exchange membrane fuel cell system identification and adaptive control," *Journal of Power Sources,* vol. 164, pp. 761-771, 2007.

[25] R. N. Methekar, S. C. Patwardhan, R. D. Gudi, and V. Prasad, "Adaptive peak seeking control of a proton exchange membrane fuel cell," *Journal of Process Control,* vol. 20, pp. 73-82, 2010.

[26] L. Dazi, Y. Yadi, J. Qibing, and G. Zhiqiang, "Maximum power efficiency operation and generalized predictive control of \{PEM\} (proton exchange membrane) fuel cell," *Energy,* vol. 68, pp. 210 - 217, 2014.

[27] X. Li, J. Li, L. Xu, F. Yang, J. Hua, and M. Ouyang, "Performance analysis of proton-exchange membrane fuel cell stacks used in Beijing urban-route buses trial project," *International Journal of Hydrogen Energy,* vol. 35, pp. 3841-3847, 2010.

[28] J. P. Torreglosa, F. Jurado, P. García, and L. M. Fernández, "PEM fuel cell modeling using system identification methods for urban transportation applications," *International Journal of Hydrogen Energy,* vol. 36, pp. 7628-7640, 7// 2011.

[29] X. Xu, S. Wang, Z. Sun, and F. Xiao, "A model-based optimal ventilation control strategy of multi-zone VAV air-conditioning systems," *Applied Thermal Engineering,* vol. 29, pp. 91-104, 2009.

[30] J. C. Amphlett, "Performance Modeling of the Ballard Mark IV Solid Polymer Electrolyte Fuel Cell," *Journal of The Electrochemical Society,* vol. 142, p. 1, 1995.

[31] D. Cheddie and N. Munroe, "Review and comparison of approaches to proton exchange membrane fuel cell modeling," *Journal of Power Sources,* vol. 147, pp. 72-84, 2005.

[32] L. Boulon, D. Hissel, A. Bouscayrol, and M. Pera, "From Modeling to Control of a PEM Fuel Cell Using Energetic Macroscopic Representation," *Industrial Electronics, IEEE Transactions on,* vol. 57, pp. 1882-1891, 2010.

[33] L. Boulon, K. Agbossou, D. Hissel, P. Sicard, A. Bouscayrol, and M. C. Péra, "A macroscopic PEM fuel cell model including water phenomena for vehicle simulation," *Renewable Energy,* vol. 46, pp. 81-91, 10// 2012.

[34] S. Caux, W. Hankache, M. Fadel, and D. Hissel, "PEM fuel cell model suitable for energy optimization purposes," *Energy Conversion and Management,* vol. 51, pp. 320-328, 2010.

[35] X. Cheng, Z. Shi, N. Glass, L. Zhang, J. Zhang, D. Song, *et al.*, "A review of PEM hydrogen fuel cell contamination: Impacts, mechanisms, and mitigation," *Journal of Power Sources,* vol. 165, pp. 739-756, 2007.

[36] Y.-J. Sohn, G.-G. Park, T.-H. Yang, Y.-G. Yoon, W.-Y. Lee, S.-D. Yim, *et al.*, "Operating characteristics of an air-cooling PEMFC for portable applications," *Journal of Power Sources,* vol. 145, pp. 604-609, 2005.

[37] D. Feroldi, M. Serra, and J. Riera, "Design and Analysis of Fuel-Cell Hybrid Systems Oriented to Automotive Applications," *Vehicular Technology, IEEE Transactions on,* vol. 58, pp. 4720-4729, 2009.

[38] S. Srinivasan, E. A. Ticianelli, C. R. Derouin, and A. Redondo, "Advances in solid polymer electrolyte fuel cell technology with low platinum loading electrodes," *Journal of Power Sources,* vol. 22, pp. 359-375, 1988.

[39] J. Kim, S. M. Lee, S. Srinivasan, and C. E. Chamberlin, "Modeling of proton exchange membrane fuel cell performance with an empirical equation," *Journal of the Electrochemical Society,* vol. 142, pp. 2670-2674, 1995.

[40] J. H. Lee, T. R. Lalk, and A. J. Appleby, "Modeling electrochemical performance in large scale proton exchange membrane fuel cell stacks," *Journal of Power Sources,* vol. 70, pp. 258-268, 1998.

[41] R. F. Mann, J. C. Amphlett, M. A. I. Hooper, H. M. Jensen, B. A. Peppley, and P. R. Roberge, "Development and application of a generalised steady-state electrochemical model for a PEM fuel cell," *Journal of Power Sources,* vol. 86, pp. 173-180, Mar 2000.

[42] G. Squadrito, G. Maggio, E. Passalacqua, F. Lufrano, and A. Patti, "An empirical equation for polymer electrolyte fuel cell (PEFC) behaviour," *Journal of Applied Electrochemistry,* vol. 29, pp. 1449-1455, 1999.

[43] A. A. Kulikovsky, "Semi-analytical 1D+1D model of a polymer electrolyte fuel cell," *Electrochemistry Communications,* vol. 6, pp. 969-977, 2004.

[44] A. A. Kulikovsky, T. Wüster, A. Egmen, and D. Stolten, "Analytical and Numerical Analysis of PEM Fuel Cell Performance Curves," *Journal of The Electrochemical Society,* vol. 152, p. A1290, 2005.

[45] L. Pisani, G. Murgia, M. Valentini, and B. D'Aguanno, "A new semi-empirical approach to performance curves of polymer electrolyte fuel cells," *Journal of Power Sources,* vol. 108, pp. 192-203, 2002.

[46] R. Isermann, "Practical aspects of process identification," *Automatica,* vol. 16, pp. 575-587, 9// 1980.

[47] H. Kurz, R. Isermann, and R. Schumann, "Experimental comparison and application of various parameter-adaptive control algorithms," *Automatica,* vol. 16, pp. 117-133, 3// 1980.

[48] C. Liyu and S. Howard, "A directional forgetting algorithm based on the decomposition of the information matrix," *Automatica,* vol. 36, pp. 1725 - 1731, 2000.

[49] R. Kulhavý, "Restricted exponential forgetting in real-time identification," *Automatica,* vol. 23, pp. 589-600, 9// 1987.

[50] S. Bittanti, P. Bolzern, and M. Campi, "Exponential convergence of a modified directional forgetting identification algorithm," *Systems & Control Letters,* vol. 14, pp. 131-137, 2// 1990.

[51] S. Bittanti, P. Bolzern, and M. Campi, "Convergence and exponential convergence of identification algorithms with directional forgetting factor," *Automatica,* vol. 26, pp. 929-932, 9// 1990.

[52] G. J. Bierman, "Measurement updating using the U-D factorization," *Automatica,* vol. 12, pp. 375-382, 7// 1976.

[53] K. Ettihir, L. Boulon, K. Agbossou, and S. Kelouwani, "MPPT control strategy on PEM Fuel Cell Low Speed Vehicle," in *Vehicle Power and Propulsion Conference (VPPC), 2012 IEEE*, 2012, pp. 926-931.

[54] H.-i. Kim, C. Y. Cho, J. H. Nam, D. Shin, and T.-Y. Chung, "A simple dynamic model for polymer electrolyte membrane fuel cell (PEMFC) power modules: Parameter estimation and model prediction," *International Journal of Hydrogen Energy,* vol. 35, pp. 3656-3663, 4// 2010.

[55] M. G. Santarelli, M. F. Torchio, and P. Cochis, "Parameters estimation of a PEM fuel cell polarization curve and analysis of their behavior with temperature," *Journal of Power Sources,* vol. 159, pp. 824-835, 2006.

[56] A. Saltelli, M. Ratto, T. Andres, F. Campolongo, J. Cariboni, D. Gatelli, *et al.*, *Global sensitivity analysis: the primer*: Wiley. com, 2008.

Chapitre 3 - Article 2 : Validation de la méthode de recherche des maximums avec une stratégie simple

L'article décrit dans le chapitre 1 a permis de montrer que la méthode permet de prendre en compte des variations de conditions d'opération ou de dégradation. La méthode est validée sur l'exemple spécifique de la prise en compte de l'influence de la variation de la température sur la caractéristique de la pile PEM. Dans cet article, il s'agit de capitaliser sur ce travail en développant une couche supplémentaire à la méthode. Le modèle semi-empirique couplé à l'ARLS permet d'estimer la courbe de polarisation de la pile PEM. Un algorithme d'optimisation est ajouté pour rechercher les maximums de puissance et de rendement à partir de l'identification en ligne. Cela permet dans ce travail d'estimer la puissance de la pile et de reproduire la caractéristique tension-courant de la PAC en temps réel. De plus, la recherche du maximum de rendement est introduite grâce à l'estimation du débit d'hydrogène consommé par la pile à combustible et donc, de la courbe de rendement.

Le sous-problème traité dans cet article est que les stratégies classiques basées sur une cartographie fixe de la pile à combustible ne sont plus valides quand les performances de la pile changent (dans ce cas d'étude, en raison du vieillissement du système). Dans le cadre d'une stratégie globale, il est donc nécessaire d'inclure cette variation de performances afin de garder la pile PEM dans sa bonne plage de fonctionnement.

En premier lieu, la validation expérimentale de la recherche du maximum de puissance et de rendement de la pile à l'aide des algorithmes est développée (cas de la pile en bonne santé). Les résultats expérimentaux prouvent que les maximums de puissance et de rendement peuvent d'être déterminés en temps réel.

Par la suite, une stratégie de répartition basée sur l'hystérésis (machine à états) est développée pour placer la recherche des maximums dans le cadre d'une gestion d'énergie sur le VHPAC. Cette stratégie hystérésis se base sur un article développé précédemment [32]. Les modes de fonctionnement qui placent le fonctionnement de la pile PEM au maximum de rendement et de puissance sont déterminés en ligne par l'algorithme de recherche des maximums. Deux piles PEM avec un degré de dégradation différent sont utilisées pour démontrer la capacité de l'algorithme hystérésis à activer les modes de recherche du maximum de rendement et de puissance selon le niveau de charge des batteries.

Energy Management Strategy for a Fuel Cell Hybrid Vehicle based on Maximum Efficiency and Maximum Power identification

Ettihir, Khalid, Boulon, Loïc, & Agbossou, Kodjo. (2016). Energy management strategy for a fuel cell hybrid vehicle based on maximum efficiency and maximum power identification. *IET Electrical Systems in Transportation, 6*(4), 261-268. http://digital-library.theiet.org/content/journals/10.1049/iet-est.2015.0023

3.1 Introduction

The most used fuel cell system (FCS) for embedded applications is the proton exchange membrane fuel cell (PEM-FC) because of its low operating temperature and pressure, tolerance to carbon dioxide and solid membrane [1]. A PEM-FC allows a zero local emission electricity generation, and the consumed hydrogen can be produced with renewable energies, such as electrolysis and biomass processes [2]. To ensure a good durability of the PEM-FC, slow load dynamics are requested, and consequently, another energy source must be used between the PEM-FC and the load to satisfy the fast dynamic load for the traction power on a vehicle DC bus [3]. This second device could be the main source or a simple energetic buffer (battery, supercapacitor, and flywheel). Consequently, the supplied PEM-FC power can be different from the load request and can be used in specific operating modes (maximum efficiency or maximum power for instance). This work addresses the energy management strategy (EMS) of embedded systems and more specifically the fuel cell hybrid electric vehicle (FC-HEV) (the architecture is defined in section 2).

In the literature, the EMS of the FC-HEV is divided in two classes: rule-based controls and optimisation-based controls [4]. The rule-based controls use expert knowledge, appear in deterministic (for example, thermostatic EMS), adaptive or predictive forms and

are easily adaptable in real-time systems. The second approach based on optimisation is divided into two parts: global optimisation and real-time optimisation. These two methods optimize a cost function, which frequently defines the criterion of the fuel consumption, system efficiency, or system power.

Payman et al. [5] propose a flatness based control to regulate the dc bus and perform experimental validation. Feroldi et al. [6] develop strategies based on the static efficiency map and implement them in real time. Their study shows that the hydrogen consumption could be reduced drastically. Hemi et al. [7] design an optimal power split strategy based on the Pontryagin's principle. A simulation study of a complete real time EMS is realized. Bernard et al. [8] design a strategy derived from an optimal control theory to minimize the hydrogen consumption and perform experimental validation. Recently, Farouk et al. [9] propose the study of two strategies: one strategy based on fuzzy logic and the other strategy based on optimal control theory. Their experimental study shows that optimal control can outperform the fuzzy logic power split. For the two classes of the EMS presented, the provided results are very interesting, but in most cases, they are based on a PEM-FC map or a mathematical model with constant parameters.

The drawback of these EMSs is that they depend on models (valid within a given operating range) or maps. Nevertheless, the PEM-FC is a multi-physics system [10], and consequently, its energetic performances depend on the degradation and on the operating conditions (e.g., temperature, gas relative humidity, gas stoichiometry, pressure) [11] as shown in the experimental curves obtained in Fig.1. In real time application, one solution to consider for the multi-physics behaviour of the PEM-FC is to use complex models.

However, their design (and validation) can be difficult and time-consuming processes [12]. Another solution is to use black-box models and adapt the online parameters. Several models in the literature meet the real-time capability and are given to identify the online PEM-FC parameters. Meiler et al. [13] presents a review that classifies the real-time model for the EMS and concludes that among the reviewed model (fuzzy, neural network, auto regressive, Wiener), the best results are given by the Ursyon model. However, semi-empirical models of the PEM-FC describe the PEM-FC behaviour with a physical meaning and a reduced computing time so that they can be useful for an adaptive EMS [14].

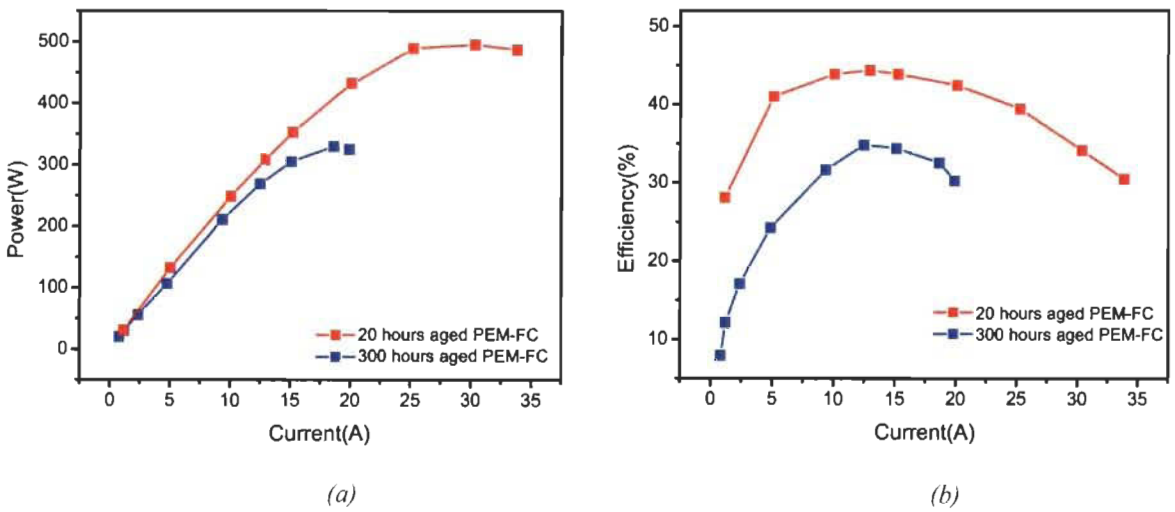

(a) *(b)*

Figure. 6. Characteristic curves for two 0.5 kW air-breathing PEM-FCs with different degrees of degradation at $T_{fc}=35$°C: (a) the power versus current; (b) the efficiency versus the current

In order to exploit the best performances of the PEM-FC, several studies have proposed important contributions on the topic of extremum-seeking control in a PEM-FC. The challenge is that the maximum power (MP) and efficiency (MP) of the PEM-FC move when the operating conditions vary. Zhong et al. [15] designs a maximum power point tracking (MPPT) algorithm. Kelouwani et al. [16] presents an experimental adaptive control approach for a maximum efficiency point tracking (MEPT) of a PEM-FC. Guo-

Rong et al. designs a MPPT algorithm based on resistance matching and implement it on a hybrid energy system. Benyahia et al. [17] proposes an MPPT based on perturb and observe technique and validate it experimentally. Methekar et al. [18] proposes an adaptive optimizing control based on the Wiener model and validated it with numerical simulations. Becherif et al. [19] designs an original MPPT to enhance the air consumption. Dazi et al. [20] investigates a simulation study on the maximum power operation of a PEM-FC with a general predictive control. However, in the previously conducted studies, few experimental extremum-seeking controls on the PEM-FC show the reliability of this type of control in real time. Carlos et al. [21] proposes specific hardware in the loop validation for an MPPT-based control. Park et al. [22] propose a hysteresis controller based on MPPT for microbial fuel cells and perform an experimental validation. Gene et al. [23] designed an experimental real-time optimisation on a solid oxide fuel cell.

To date, the literature hardly present study that offer EMS for finding the best performances of the PEM-FC, in real time, for an FC-HEV. This paper proposes a two-step extremum seeking process (ESP) for tracking specific operation points for ME and MP. The ESP is based on the online identification of a semi-empirical model followed by an optimisation process performed on this up-to-date model. The output of the ESP is the current requested for the PEM-FC through the DC/DC converter. The ESP is used in a complete EMS based on a hysteretic behaviour [24] to avoid the chattering effect and to show its effectiveness in real-time operation. The experimental results are provided with a specific emphasis on the study of the operating parameter drift by using two PEM-FCs with different levels of degradation.

The rest of the paper is organized as follows. Section 2 presents the hybrid system, whereas the EMS is described in Section 3. The experimental setup and results are presented in Sections 4 and 5. The conclusion and perspectives are discussed in Section 6.

3.2 Architecture of the hybrid system

3.2.1 FC-HEV Description

The architecture of the hybrid system used in this paper is based on the Nemo FC-HEV (low-speed vehicle (Fig.2.a). The DC bus is built around a 335 *Ah* battery pack, and a 2.5 *kW* Axane PEM-FC is used as a range extender. The powertrain is based on a 5 *kW* induction machine.

3.2.2 Description of the Test Bench

For the purpose of this work, a reduced-scale experimental test bench is designed (Fig.2.b). The experiments are performed with a Horizon 36 cells 0.5 *kW* air-breathing PEM-FC. The oxygen supply, relative humidity and temperature are managed by the fans. The hydrogen side operates in dead-end mode with a regulated pressure 0.05 *MPa*. The electric connection between the PEM-FC and the DC bus is realized by using a Zahn Electronics DC/DC converter and connected to the lead acid battery pack of 3.9*kWh* to control the PEM-FC current i_{fc}. An electronic load (Dynaload Series WCL 488 Water Cooled) and a controllable source (Sorensen SGI 100) are used to emulate the power profile recorded on the real vehicle. The embedded computer compactRIO 9022 from National Instruments is used to manage the load control, the data acquisition and the developed

control algorithms. The control of the auxiliaries, such as fan speed, anodic purges, hydrogen supply and power control, is performed by the controller (Fig.2.b).

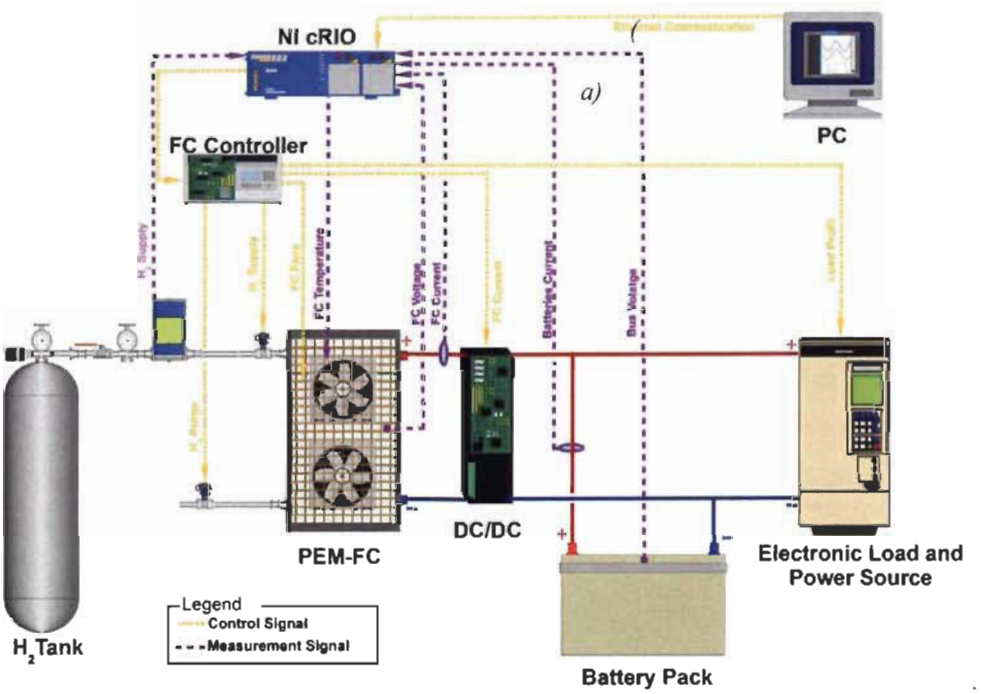

(b)

Figure. 7. The architecture of the hybrid system: (a) Nemo FC-HEV of the Hydrogen Research Institute); (b) the experimental test bench

3.3 Energy management strategy

The designed EMS is based on two layers. Fig. 3 provides a global view of the designed EMS with:

• The hysteresis power split control (HPSC) that avoids chattering and switches between different modes of PEM-FC operation

• The ESP of the optimal operating point based on the power and efficiency online estimation

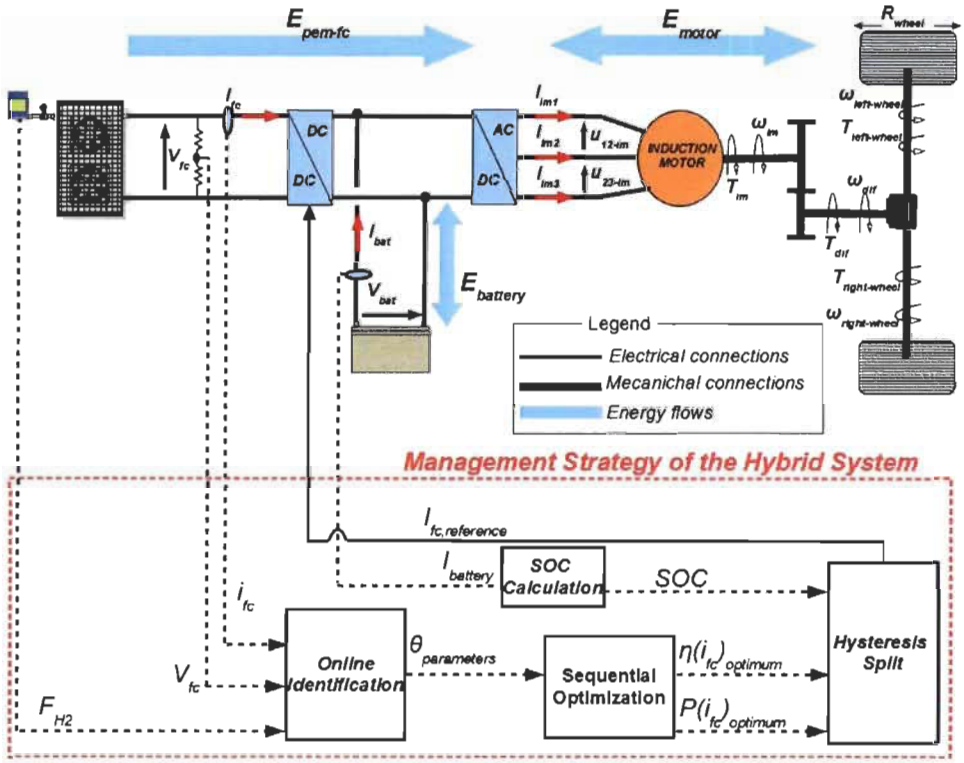

Figure. 8. Global view of the applied EMS based on ESP on the hybrid system

3.3.1 Hysteresis Power Split Strategy

The HPSC is realized with a battery state-of-charge (SoC) based strategy. It allows three operation modes for the PEM-FC: ME, MP and OFF (or ON). A double hysteresis trigger is used to avoid fast switching between the modes. The ME mode is used to ensure a lower hydrogen consumption when the PEM-FC is running. Essentially, the power range

between the open circuit voltage and the best efficiency point is the area where the hydrogen consumption is highest and is also the area where the fuel cell degrades more rapidly [6, 25]. So, when the PEM-FC is switched on, the ME mode is activated directly. The MP mode is activated to assist the battery pack in the case of a very low SoC estimation. Another use of the MP mode could be to help the batteries in the case of a high traction power operation, such as mountain slope climbing. The SoC estimation is not the aim of this paper, and a simple discrete-time approximate recurrence relation is used [26] in Equation (1):

$$SOC_{k+1} = SOC_k - \frac{i_{bat_k}}{C_n}\Delta t \tag{1}$$

where i_{bat}, C_n, k and Δt are the battery current, the battery charge capacity, the sampling instance and the time step, respectively (Table 1).

Table 1: The parameters of the SoC calculation

Parameters	i_{bat}	C_n	Δt
Value	*[0-100 A]*	*52A.h*	*1ms*

3.3.2 First step of the ESP: Adaptive Recursive Least Square Algorithm

In this section, the ARLS is the first step of the ESP to calculate the optimal points [27]. A single-input single-output system defined by Equation (2) is considered since the two models used in this article are of this type:

$$y_k = \phi_k^T \theta_k + \xi_k \tag{2}$$

where y is the output vector, ϕ is the regressor vector, θ is the system parameter vector, ξ is a stochastic noise variable with normal distribution and zero mean . Further in section 4, the models used and the respective regressors are defined. The ARLS algorithm minimizes the objective function J_k defined by the prediction error ε squared as shown in Equation (3):

$$J_k = \sum_{i=1}^{k} \lambda^{k-i} \varepsilon_i^2 \tag{3}$$

where $\lambda=0.7$ (a value between [0; 1]) is the forgetting factor, which is necessary to track the variation of the parameters (degradation drift) [28]. However, when ARLS algorithm is implemented for tracking systems with time-varying parameters such as PEM-FC, the algorithm loses its stability during the identification process. A practical solution to maintain the stability of the algorithm is to adapt a forgetting factor λ by using methods such as Exponential Forgetting (EF) and Directional Forgetting (DF). EF is well suited for persistently excited time-varying system. However, an estimation windup phenomena appear when the system is not enough excited and the identification process becomes unreliable and sensitive to noise. DF factor is implemented to improve the performance of the ARLS to avoid the estimation windup phenomena. Moreover, the covariance matrix is decomposed (Bierman decomposition) to ensure a positive semi-definite function and avoid numerical instability [27]. The implementation of the ARLS algorithm is performed by using the following equations:

$$K_{k+1} = \frac{P_k \phi_{k+1}}{1 + \phi_{k+1}^T P_k \phi_{k+1}} \tag{4}$$

$$P_{k+1} = P_k - \frac{P_k - K_{k+1} \phi_{k+1}^T P_k}{\mu_k^{-1} + \phi_{k+1}^T P_k \phi_{k+1}} \tag{5}$$

$$\mu_{k+1} = \begin{cases} \lambda - \dfrac{1-\lambda}{\phi_{k+1}^T P_k \phi_{k+1}}; & \text{if } \phi_{k+1}^T P_k \phi_{k+1}^T > 0 \\ 1; & \text{if } \phi_{k+1}^T P_k \phi_{k+1}^T = 0 \end{cases} \tag{6}$$

$$\varepsilon_{k+1} = y_{k+1} - \phi_{k+1}^T \theta_k \tag{7}$$

$$\theta_{k+1} = \theta_k + K_{k+1} \varepsilon_{k+1} \tag{8}$$

where K is the Kalman gain, P is the covariance matrix of the prediction error ε and θ are the identified parameters.

3.3.3 Second step of the ESP: the Sequential Optimisation

This section describes the step two of the ESP in which the optimum PEM-FC power and efficiency are tracked at the same time. The performance criteria are the efficiency η_{fc} and the power P_{fc}. Therefore, the role of the sequential optimisation is to determine the optimal current i_{fc} which corresponds to the maximum of the efficiency and the power of the PEM-FC. So, two optimisation problems are formulated each with an objective function (power and efficiency):

$$P_{fc}(i_{fc}) = V_{fc}\left(i_{fc}\right) i_{fc} \tag{9}$$

$$P_{h_2}(i_{fc}) = F_{h_2}(i_{fc}) HHV \tag{10}$$

$$\eta_{fc}(i_{fc}) = \frac{P_{fc}(i_{fc}) - P_{aux}}{P_{h_2}(i_{fc})} \tag{11}$$

where V_{fc}, P_{aux}, P_{h2}, F_{h2}, HHV are the PEMFC voltage (V), the auxiliary power (W) (assumed as constant), the consumed hydrogen power (W) during the electricity production, hydrogen molar flow ($mol.s^{-1}$) and the high heating value of hydrogen (286 $kJ.mol^{-1}$), respectively.

The optimisation is performed with the sequential quadratic programming (SQP) algorithm which is a local optimisation algorithm for convex problems [29]. The local optimisation is sufficient because the two objective functions are unimodal, smooth and contain one maximum, as the experimental curves show, see Fig.1. So, to obtain the current i_{fc}^{*} that yields the optimal power or efficiency, the problem is set:

Maximize i_{fc}:

$$\begin{aligned} & J(i_{fc}^{*}) = P_{fc}\left(i_{fc}^{*}\right) \\ & s.t.\ \ i_{fc,\min} \le i_{fc}^{*} \le i_{fc,\max} \end{aligned} \tag{12}$$

and maximize i_{fc} such as:

$$\begin{aligned} & J(i_{fc}^{*}) = \eta_{fc}\left(i_{fc}^{*}\right) \\ & s.t.\ \ i_{fc,\min} \le i_{fc}^{*} \le i_{fc,\max} \end{aligned} \tag{13}$$

where i_{fc}^{*} is the optimal current and $i_{fc,min}$ and $i_{fc,max}$ are the lower and upper bounds of the PEM-FC currents. For each optimal problem the Lagrangian function is set to combine all information in one function:

$$L_P = P_{fc}\left(i_{fc}\right) - l_1\left(i_{fc} - i_{fc,\min}\right) + l_2\left(i_{fc} - i_{fc,\max}\right) \tag{14}$$

$$L_\eta = \eta_{fc}\left(i_{fc}\right) - l_3\left(i_{fc} - i_{fc,\min}\right) + l_4\left(i_{fc} - i_{fc,\max}\right) \tag{15}$$

where L_P and L_η are the Lagrangian of the power criteria and efficiency criteria respectively. The parameters l_1, l_2, l_3 and l_4 are the Lagrangian multipliers. The optimal problem formulated in Equations (12) and (13) are solved using *fmincon* function in Matlab® [30].

3.4 Experimental identification and estimation of the model

3.4.1 Experimental Identification of a Semi-Empirical Model

In this section the test are conducted with the healthy (approximately 20 hours of operation) PEMFC H-500. The operating conditions for the experiments are: a PEM-FC temperature controlled near 35°*C* and an ambient temperature of 22°*C* as well as a hydrogen inlet pressure regulated at 0.05 *MPa* and a frequency purge of 0.1 *Hz*. The PEM-FC model that is suitable for real-time application is selected, and the ARLS algorithm is used to identify the model parameters. A semi-empirical model is considered because this type of model describes the PEM-FC behaviour with a physical meaning (important for the

analysis of the relevance of the identification results). Squadrito et al. [31] defines a static semi-empirical model of the PEM-FC on the basis of references [32, 33],(16):

$$V_{cell_k} = Vo_k - b_k \log(i_{fc_k}) - r_k i_{fc_k} + \alpha_k i_{fc_k}^{\sigma} \log(1 - \beta i_{fc_k}) \tag{16}$$

where i_{fc}, V_o, b, r and β are the current, open circuit voltage, Tafel slope, ohmic resistance and inverse of the limiting current, respectively. The parameters α, and σ are fitting parameters. Furthermore, the expression $\alpha_k \log(1 - \beta i_{fc_k})$ can be interpreted as an additional resistance term due to mass transport phenomena. It is necessary that the model account for the overvoltages to characterize the PEM-FC for its entire measurement range. The mass transport phenomena are also important for highlighting the maximal power point of the PEM-FC. This model has the ability to include the flooding phenomenon in the area of high current density and structural variation [31]. This aspect is important for determining the maximum power of the PEM-FC. Pisani et al. [34] provides a semi-empirical model on the same basis as references [31, 33, 35] and relates the parameters σ with the water flooding phenomena and α to the diffusion mechanism. For this model, literature provides the values of σ (between 1 and 4) and β (0.99 $A.cm^{-1}$). This model is parametrized with the online updated parameters θ_k under operating conditions changing with the minimization of the square error prediction ε_k so that the unknown parameter vector θ_k is defined at each time step by (17):

$$\theta_k = \begin{bmatrix} Vo_k & b_k & r_k & \alpha_k \end{bmatrix}^T \tag{17}$$

The initial parameters are determined off-line for selecting an initial point close to reality [27] (Table 2).

Table 2: Initialization of the parameters at time step $k=0$

Empirical parameters at $k=0$	Vo_0	b_0	r_0	α_0
Value $k=0$	*33.06*	*-0.025*	*-26.03*	*0.24*

The experimental test of the ARLS algorithm is performed with the previously defined initial parameters with a dynamic PEM-FC current i_{fc}. The measured V_{fc} and estimated $V_{fc.estimated}$ PEM-FC voltages are compared in Fig.4.a. The semi-empirical model used shows good agreement since the mean square error (MSE) between the measured and the estimated voltage calculated for this test is 2.37 %.

Fig.4.b is a representation of the parity plot obtained from the experimental identification with the ARLS algorithm. It shows the predicted performance of the PEM-FC voltage based on the semi-empirical model versus the experimentally measured PEM-FC voltage. As explained in Mann et al. [36], the accuracy of the model is shown by the proximity of the data to a 45° line (red line) passing through the origin. The good results (MSE=2.37 %) for the estimation are confirmed since the experimental points are in majority near the red line. The results are a little more far from the line after 25 *V*. It represents a voltage area close to the open circuit operation in which it is necessary to avoid working in due to a fast degradation of the PEM-FC. So, this estimated PEM-FC voltage

curve is very good in the operating area of a PEM-FC and it can be used for the maximum power and maximum efficiency estimation.

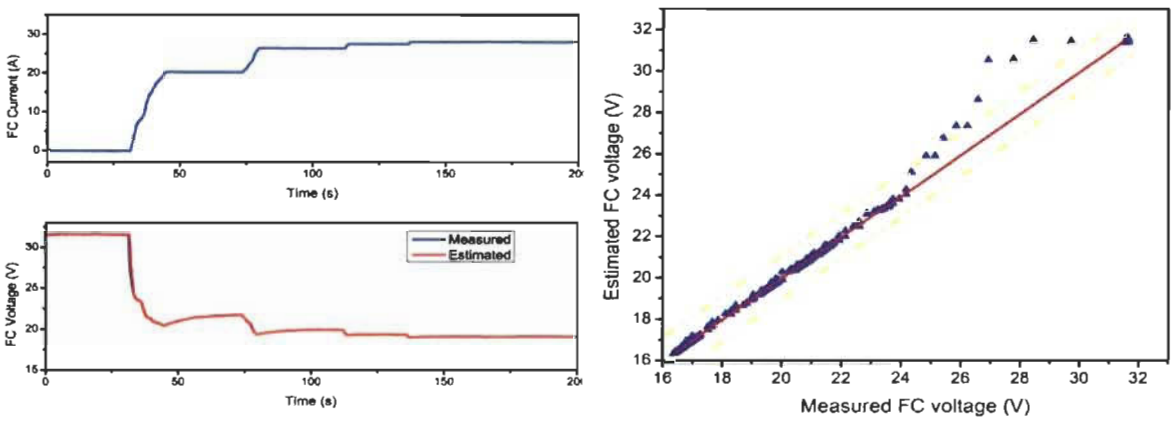

(a) *(b)*

Figure. 9. Experimental curves of the 20 hours aged PEM-FC: (a) The voltage V_{fc} estimated and measured versus time in case of dynamic current i_{fc} is imposed; (b) Representation of the parity plot(with the ± 5% envelop in yellow dashed line) from the experimental data of the 20 hours aged PEM-FC voltage as a function of the Squadrito et al. model

3.4.2 Experimental Identification of the Hydrogen Molar Flow

As defined in Bagotsky et al. [37], the operating efficiency of a PEM-FC is the ratio between the electrical power produced and the chemical power of the hydrogen oxidation. Typically, not all of the hydrogen molar flow of the reactant supplied to the PEM-FC is used for current production, and it is difficult to predict. The reasons could be due to an incomplete reactant oxidation or a diffusion of the reactant through the electrolyte. So, the hydrogen molar flow should be estimated to predict the chemical power of the hydrogen oxidation. $F_{H2,estimated}$ is the estimated hydrogen molar flow and is determined online using a second ARLS algorithm. A linear expression is used to link the hydrogen molar flow

$F_{H2.estimated}$ with the PEM-FC current i_{fc} as shown in Equation (16). Then the updated parameters θ_k used in the ARLS for hydrogen molar flow estimation are (19):

$$F_{H2,estimated} = f_1 + f_2 i_{fc} \tag{18}$$

$$\theta_k = \left[f_{1_k} \;\; f_{2_k} \right]^T \tag{19}$$

where f_1 and f_2 are the online parameters identified by the ARLS algorithm. The dynamic PEM-FC current i_{fc} is applied to highlight the behaviour of hydrogen molar flow identification process. Fig.5.a shows that the linear expression provides a relative prediction of the hydrogen molar flow since the MSE between the measured and the estimated hydrogen molar flow for this test is 4.58 %. The experimental parity plot of the hydrogen molar flow in Fig.5.b shows the accuracy of the estimation based on the proximity of the experimental data points to a 45° line (red line) passing through the origin.

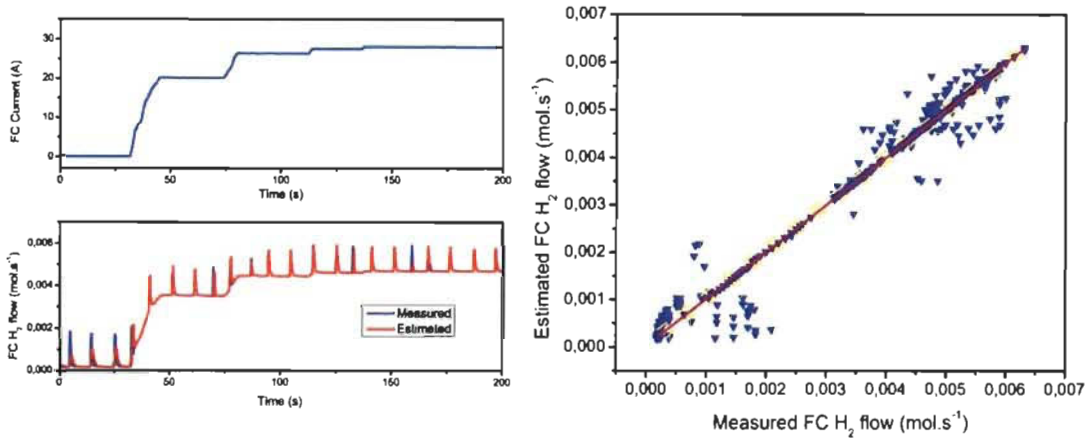

(a) *(b)*

Figure.10. Experimental curve of the 20 hours aged PEM-FC: (a) The hydrogen flow F_{H2} estimated and measured versus time in case of dynamic current i_{fc} is imposed; (b) Representation of the parity plot (with the ± 5% envelop in yellow dashed line) from the experimental data of the 20 hours aged PEM-FC molar flow as a function of Equation (18)

3.4.3 Flow Experimental Estimation of the PEM-FC Characteristics

Previous sections show that the ARLS steps converge to obtain the mathematical models of the 20 hours aged PEM-FC voltage and molar flow. The model parameters are used to plot the power and efficiency curves for the next step (sequential optimisation algorithm). Fig.6 show that the semi-empirical model coupled with the ARLS algorithm was able to predict the performance of the H-500 PEM-FC. The PEM-FC power and efficiency are determined by using the following equations:

$$P_{fc,estimated} = V_{fc,estimated} \times i_{fc} \tag{20}$$

$$\eta_{fc,estimated} = \frac{P_{fc,estimated} - P_{aux}}{P_{H2,estimated}} \tag{21}$$

where $P_{H2,estimated}$ (W) is the estimation of the consumed hydrogen power during the electricity production expressed as (23):

$$P_{H2,estimed} = F_{H2,estimated} HHV \tag{22}$$

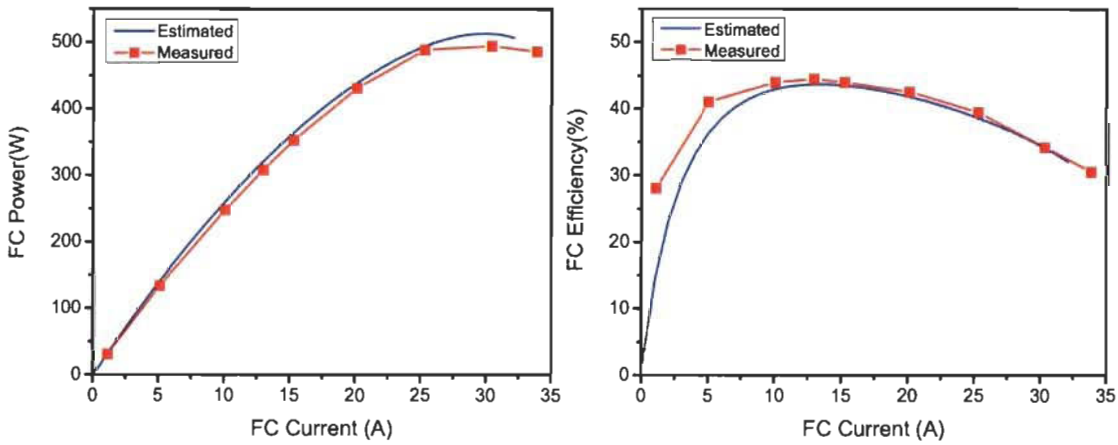

(a) *(b)*

Figure.11. Experimental characteristic curves of the 20 hours aged PEM-FC compared with the estimated characteristic curves; (a) the power versus current; (b) the efficiency versus the current.

The estimated power curve for the healthy PEM-FC in Fig.6.a provides a maximum power near 30 A and shows that it is near the maximum power of the measured PEM-FC characteristic. Additionally, Fig.6.b shows that the estimated efficiency curve of the healthy PEM-FC provides a maximum efficiency near 13 A. These results confirm that the extreme-seeking algorithm can find the optimal set point of the PEM-FC.

3.5 Experimental study

The experimental study here aims to highlight two points by considering PEM-FCs with different levels of degradation (Fig.1):

• The HPSC can switch the operating point of the PEM-FC according to the level of the SoC.

• Depending on the degree of degradation and with the same experimental protocol, the ESP can track the MP and ME modes with the identified model of the PEM-FC.

The operating conditions for the experiments are: a PEM-FC temperature controlled near 35 $°C$ and an ambient temperature of 22 $°C$ as well as a hydrogen inlet pressure regulated at 0.05 MPa and a frequency purge of 0.01 Hz. The initial parameters of the ARLS algorithm ($\theta_{initial}$), the SQP algorithm (x_{min}, x_{max} and $x_{initial}$) and the initial SoC estimation are set to the same value for every experiment. Furthermore, in the experiments, the hybrid system (PEM-FCs and battery pack) is loaded with the same current profile. The results of the HPSC based on the ESP are compared with an HPSC based on the PEM-FC maps (efficiency and power) to show the relevance of the results.

3.5.1 Case study: EMS with the 20 hours aged PEM-FC

In this experiment, a healthy (approximately 20 hours of operation) PEM- FC H-500 is used on the test bench. The healthy power and efficiency curves are provided in the previous section and correspond with the manufacturer data (Fig.1). The power curve shows that the MP P_{fc} is approximately 510 W at a current i_{fc} of 30 A. The efficiency curve provides a ME η_{fc} of 52 % at 13.5 A. Fig.7 shows the results of the PEM-FC current, power and efficiency during the test with the given load profile.

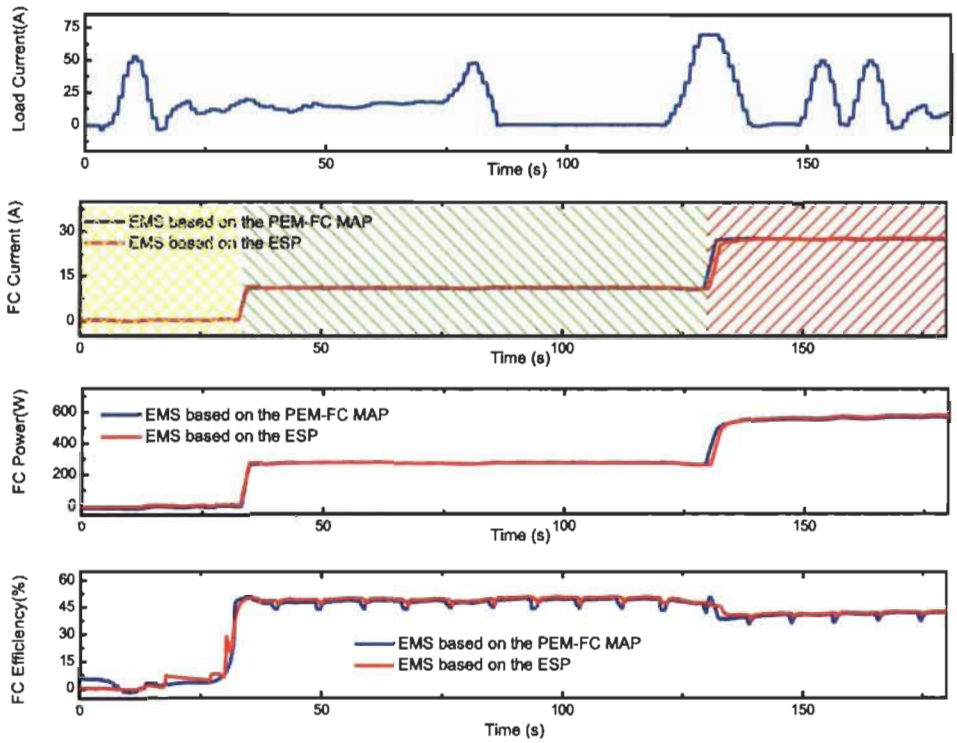

Figure.12. Experimental results of the developed EMS with the 20 hours aged PEM-FC compared with the classical strategy: yellow line, green line and red line refer to OFF mode, ME mode and MP mode respectively

It is clear that with the two EMSs designed, the power split can switch the mode of operation of the PEM-FC (ME, MP and On/Off modes) (Fig.7) depending on the SoC. The maximum current i_{fc} given by the ESP is near the maximum value of the maximum power given by the map (Fig.1) (approximately 550 W at 29.9 A). The best efficiency η_{fc} (approximately 50 % at 13.2 A) is also provided by the ESP.

3.5.2 Case study: EMS with the 300 hours aged PEM-FC

In this experiment, a degraded (approximately 300 hours of operation) PEM-FC H-500 is used on the test bench. The degraded PEM-FC power and efficiency curves are provided in the previous section (Fig.1) and show the degradation of the PEM-FC. It can be

seen that the degraded PEM-FC lost 37 % of the MP and 31 % of ME compared with a healthy H-500 PEM-FC. The power curve shows that the MP P_{fc} is approximately 320 W at a current i_{fc} of 20 A. The efficiency curve provides a ME η_{fc} of 36 % at 13.2 A and an efficiency η_{fc} of 32 % near the maximum current i_{fc}.

The results of the second test show that a HPSC based on the mapping of a healthy PEM-FC (the same as the manufacturer) is not valid when the PEM-FC is degraded. The HPSC switches well between the Off mode and ME mode, but the PEM-FC shuts down (security of the controller) when the MP mode is activated because the PEM-FC operating point is in the mass transport region and risk to degrade the PEM-FC. The requested current to obtain the MP moves as the PEM-FC ages. However, the ESP EMS avoids the shut down near the MP of the PEM-FC because it adequately seeks the optimum power (Fig.8).

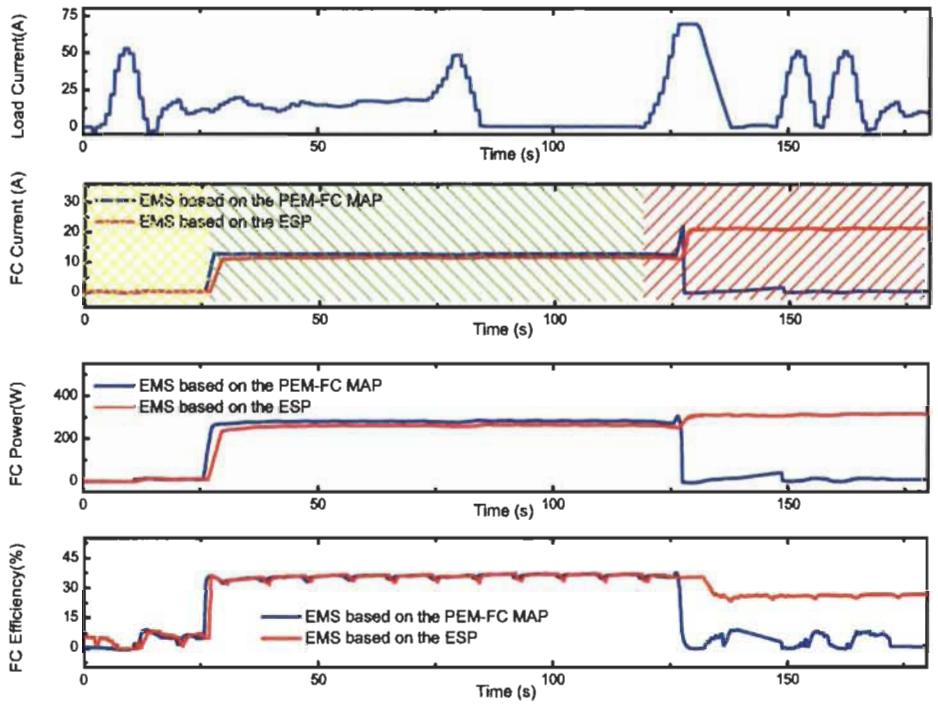

Fig.13. Experimental results of the developed EMS with the 300 hours aged PEM-FC compared with the classical strategy : yellow line, green line and red line refer to OFF mode, ME mode and MP mode respectively

The same result occurs when tracking the ME (Fig.8). The ME of the degraded PEM-FC given by the map (Fig.1.b) is determined by the ESP. Nevertheless, the ME current point does not move and the classical map strategy works. The values of power and efficiency found are the same as the values of the degraded H-500 PEM-FC maps (Fig.1).

3.6 Conclusion

An EMS based on an ESP was proposed in this paper for FC-HEV. The EMS is tested on a hybrid system test bench. The algorithms were implemented on the test bench with a NI compactRIO. The three-step method proposed shows that it is possible to match the variation of the operating condition of a PEM-FC (such as degradation) with semi-

empirical models coupled with an ARLS algorithm. It was demonstrated that the HPSC based on maps are not valid when the operating parameters change because of the operating point drift. This paper addresses to the degradation effects but similar results could be obtained with an important variation of the operating conditions, such as extreme temperature or faulty operation.

The MSE is relatively small but a misestimation can give wrong value of the PEM-FC MP or ME during a few milliseconds (the sampling time of the algorithm is 5 *kHz*). In our case, this weakness is avoided because the PEM-FC is coupled with a battery pack and then slow current dynamics are applied on the PEM-FC.

For future studies, two approaches are possible with this work. The first approach is that the proposed adaptive EMS is expected to be useful for more elaborate online EMSs based on the map and optimal power split to reduce hydrogen consumption. Because the extremum values are known in a real-time EMS, decision making can be developed. The second approach is the design of a multivariate model that provides more operating parameters, such as current, temperature, and pressure. This approach is not possible with conventional algorithms, which are limited to searching one parameter at a time. The current method could address this issue.

Acknowledgments

This work has been supported by the " Ministère des Ressources naturelles et de la Faune du Québec", the Natural Sciences and Engineering Research Council of Canada, LTE Hydro-Québec, and the "Fonds de Recherche Québécois – Nature et Technologie" (FRQNT).

References

[1] O. Z. Sharaf and M. F. Orhan, "An overview of fuel cell technology: Fundamentals and applications," *Renewable and Sustainable Energy Reviews,* vol. 32, pp. 810-853, April 2014.

[2] C. E. Thomas, "Fuel cell and battery electric vehicles compared," *International Journal of Hydrogen Energy,* vol. 34, pp. 6005-6020, 2009.

[3] L. Kumar and S. Jain, "Electric propulsion system for electric vehicular technology: A review," *Renewable and Sustainable Energy Reviews,* vol. 29, pp. 924-940, 2014.

[4] S. F. Tie and C. W. Tan, "A review of energy sources and energy management system in electric vehicles," *Renewable and Sustainable Energy Reviews,* vol. 20, pp. 82-102, 2013.

[5] A. Payman, S. Pierfederici, and F. Meibody-Tabar, "Energy control of supercapacitor/fuel cell hybrid power source," *Energy Conversion and Management,* vol. 49, pp. 1637-1644, 2008.

[6] D. Feroldi, M. Serra, and J. Riera, "Energy Management Strategies based on efficiency map for Fuel Cell Hybrid Vehicles," *Journal of Power Sources,* vol. 190, pp. 387-401, 2009.

[7] H. Hemi, J. Ghouili, and A. Cheriti, "Combination of Markov chain and optimal control solved by Pontryagin's Minimum Principle for a fuel cell/supercapacitor vehicle," *Energy Conversion and Management,* vol. 91, pp. 387-393, 2015.

[8] J. Bernard, S. Delprat, T. M. Guerra, and F. N. Büchi, "Fuel efficient power management strategy for fuel cell hybrid powertrains," *Control Engineering Practice,* vol. 18, pp. 408-417, 2010.

[9] O. Farouk, R. Jürgen, W. Lars, and H. Angelika, "Power management optimization of fuel cell/battery hybrid vehicles with experimental validation," *Journal of Power Sources,* vol. 252, pp. 333 - 343, 2014.

[10] L. Boulon, D. Hissel, A. Bouscayrol, and M. Pera, "From Modeling to Control of a PEM Fuel Cell Using Energetic Macroscopic Representation," *Industrial Electronics, IEEE Transactions on,* vol. 57, pp. 1882-1891, 2010.

[11] L. Wang, A. Husar, T. Zhou, and H. Liu, "A parametric study of PEM fuel cell performances," *International Journal of Hydrogen Energy,* vol. 28, pp. 1263-1272, 2003.

[12] C. Raga, A. Barrado, A. Lazaro, C. Fernandez, V. Valdivia, I. Quesada, *et al.*, "Black-Box Model, Identification Technique and Frequency Analysis for PEM Fuel Cell With Overshooted Transient Response," *Power Electronics, IEEE Transactions on,* vol. 29, pp. 5334-5346, 2014.

[13] M. Meiler, O. Schmid, M. Schudy, and E. P. Hofer, "Dynamic fuel cell stack model for real-time simulation based on system identification," *Journal of Power Sources,* vol. 176, pp. 523-528, 2008.

[14] L. Xu, J. Li, J. Hua, X. Li, and M. Ouyang, "Adaptive supervisory control strategy of a fuel cell/battery-powered city bus," *Journal of Power Sources,* vol. 194, pp. 360-368, 2009.

[15] Z.-d. Zhong, H.-b. Huo, X.-j. Zhu, G.-y. Cao, and Y. Ren, "Adaptive maximum power point tracking control of fuel cell power plants," *Journal of Power Sources,* vol. 176, pp. 259-269, 2008.

[16] S. Kelouwani, K. Adegnon, K. Agbossou, and Y. Dube, "Online System Identification and Adaptive Control for PEM Fuel Cell Maximum Efficiency Tracking," *Energy Conversion, IEEE Transactions on,* vol. 27, pp. 580-592, 2012.

[17] N. Benyahia, H. Denoun, A. Badji, M. Zaouia, T. Rekioua, N. Benamrouche, *et al.*, "MPPT controller for an interleaved boost dc–dc converter used in fuel cell electric vehicles," *International Journal of Hydrogen Energy,* vol. 39, pp. 15196-15205, 2014.

[18] R. N. Methekar, S. C. Patwardhan, R. D. Gudi, and V. Prasad, "Adaptive peak seeking control of a proton exchange membrane fuel cell," *Journal of Process Control,* vol. 20, pp. 73-82, 2010.

[19] M. Becherif and D. Hissel, "MPPT of a PEMFC based on air supply control of the motocompressor group," *International Journal of Hydrogen Energy,* vol. 35, pp. 12521-12530, 2010.

[20] L. Dazi, Y. Yadi, J. Qibing, and G. Zhiqiang, "Maximum power efficiency operation and generalized predictive control of \{PEM\} (proton exchange membrane) fuel cell," *Energy,* vol. 68, pp. 210 - 217, 2014.

[21] R.-P. Carlos Andrés, S. Giovanni, P. Giovanni, and M. Emilio, "A perturbation strategy for fuel consumption minimization in polymer electrolyte membrane fuel cells: Analysis, Design and FPGA implementation," *Applied Energy,* vol. 119, pp. 21 - 32, 2014.

[22] J.-D. Park and Z. Ren, "Hysteresis controller based maximum power point tracking energy harvesting system for microbial fuel cells," *Journal of Power Sources,* vol. 205, pp. 151-156, 2012.

[23] A. B. Gene, W. Zacharie, F. Grégory, N. Arata, T. Leonidas, and B. Dominique, "Experimental real-time optimization of a solid oxide fuel cell stack via constraint adaptation," *Energy,* vol. 39, pp. 54 - 62, 2012.

[24] K. Ettihir, L. Boulon, K. Agbossou, S. Kelouwani, and M. Hammoudi, "Design of an Energy Management Strategy for PEM Fuel Cell Vehicles," *2012 IEEE International Symposium on Industrial Electronics (ISIE),* pp. 1714-1719, 2012.

[25] W. Jinfeng, Y. Xiao-Zi, J. M. Jonathan, W. Haijiang, Y. Daijun, Q. Jinli, *et al.*, "Proton exchange membrane fuel cell degradation under close to open-circuit conditions: Part I: In situ diagnosis," *Journal of Power Sources,* vol. 195, pp. 1171 - 1176, 2010.

[26] G. L. Plett, "Extended Kalman filtering for battery management systems of LiPB-based HEV battery packs: Part 2. Modeling and identification," *Journal of Power Sources,* vol. 134, pp. 262-276, 2004.

[27] K. Ettihir, L. Boulon, M. Becherif, K. Agbossou, and H. S. Ramadan, "Online identification of semi-empirical model parameters for PEMFCs," *International Journal of Hydrogen Energy,* vol. 39, pp. 21165-21176, 2014.

[28] H. Y. Kuen, F. S. Mjalli, and Y. H. Koon, "Recursive Least Squares-Based Adaptive Control of a Biodiesel Transesterification Reactor," *Industrial & Engineering Chemistry Research,* vol. 49, pp. 11434-11442, 2010/11/17 2010.

[29] J.-F. Bonnans, J. C. Gilbert, C. Lemaréchal, and C. A. Sagastizábal, *Numerical optimization: theoretical and practical aspects*: Springer Science & Business Media, 2006.

[30] T. Mathworks. *Matlab Optimization Toolbox User's Guide*. Available: http://www.mathworks.co.uk/access/helpdesk/help/pdf_doc/optim/optim_tb.pdf

[31] G. Squadrito, G. Maggio, E. Passalacqua, F. Lufrano, and A. Patti, "An empirical equation for polymer electrolyte fuel cell (PEFC) behaviour," *Journal of Applied Electrochemistry,* vol. 29, pp. 1449-1455, 1999.

[32] S. Srinivasan, E. A. Ticianelli, C. R. Derouin, and A. Redondo, "Advances in solid polymer electrolyte fuel cell technology with low platinum loading electrodes," *Journal of Power Sources,* vol. 22, pp. 359-375, 1988.

[33] J. Kim, "Modeling of Proton Exchange Membrane Fuel Cell Performance with an Empirical Equation," *Journal of The Electrochemical Society,* vol. 142, p. 2670, 1995.

[34] L. Pisani, G. Murgia, M. Valentini, and B. D'Aguanno, "A new semi-empirical approach to performance curves of polymer electrolyte fuel cells," *Journal of Power Sources,* vol. 108, pp. 192-203, 2002.

[35] J. H. Lee, T. R. Lalk, and A. J. Appleby, "Modeling electrochemical performance in large scale proton exchange membrane fuel cell stacks," *Journal of Power Sources,* vol. 70, pp. 258-268, 1998.

[36] R. F. Mann, J. C. Amphlett, M. A. I. Hooper, H. M. Jensen, B. A. Peppley, and P. R. Roberge, "Development and application of a generalised steady-state electrochemical model for a PEM fuel cell," *Journal of Power Sources,* vol. 86, pp. 173-180, Mar 2000.

[37] V. S. Bagotsky, "The Working Principles of a Fuel Cell," in *Fuel Cells*, ed: John Wiley & Sons, Inc., 2012, pp. 5-24.

Chapitre 4 - Article 3 : Stratégie de contrôle optimal adaptatif

L'article du chapitre 3 proposait une SGE hystérésis simple axée sur les modes de fonctionnement de maximum de puissance ou de rendement. Cette SGE simple montre sa limite puisque les modes de fonctionnement sont activés par le niveau de charge des batteries. En effet, la SGE hystérésis bascule entre le maximum de rendement ou le maximum de puissance, des régions ou la consommation d'hydrogène est optimale et où la pile PEM se dégrade le moins. La littérature a montré à maintes reprises qu'une telle gestion reste sous-optimale [33]. Dans ce cas, ce troisième article s'appuie sur les articles précédents en proposant une SGE optimale adaptative en temps réel. La problématique traitée est que dans le cadre d'une SGE optimale, comme les conditions opératoires de la pile à combustible varient alors la SGE développée sur la base de modèle mathématique fixe n'est plus valide.. Dans cette thèse, lors de la formulation du problème d'optimisation des bornes sont définies pour le maximum et le minimum de puissance de la pile PEM. Ces bornes de puissances correspondent aux maximums de rendement (borne minimale) et de puissance (borne maximale) de la pile PEM issus de la méthode développée dans ce travail de thèse. En outr, les algorithmes de recherche des maximums de puissance et de rendement sont placés dans une SGE optimale basée sur le principe de minimum de Pontriaguine. Dans l'article suivant, la SGE optimale couplée à la recherche des maximums est décrite et des simulations sont menées afin de démontrer l'avantage de la SGE développée sur la SGE classique optimale (sans la recherche de maximums). L'article démontre que lorsque les performances de la pile PEM changent (c.-à-d., vieillissement), l'algorithme est en mesure de suivre ces variations de performances, mais également de les intégrer dans une SGE globale alors que la SGE classique est mise à défaut.

Optimization-based energy management strategy for a fuel cell/battery hybrid power system

Ettihir, K., Boulon, L., & Agbossou, K. (2016). Optimization-based energy management strategy for a fuel cell/battery hybrid power system. *Applied Energy, 163*, 142-153. doi: http://dx.doi.org/10.1016/j.apenergy.2015.10.176

4.1 Introduction

A promising solution to produce zero local emission electricity in an embedded (as hybrid vehicles) or stationary system is the fuel cell system (FCS). The most practical FCS for embedded applications is the proton exchange membrane fuel cell (PEM-FC) because of its low operating temperature and pressure, tolerance to carbon dioxide and solid membrane [1]. Furthermore, the consumed hydrogen can be produced with renewable energies through electrolysis and biomass processes to produce near zero global emission electricity [2, 3]. In practice, a good durability is ensured for the PEM-FC when slow load dynamics are applied [4]. Consequently, an energetic buffer (battery, supercapacitor, flywheel) must be used between the PEM-FC and the load to satisfy the fast dynamic load for the traction power on a vehicle DC bus [5, 6]. As the energy is distributed between two sources, energy management strategy (EMS) is required.

In the literature, two classes define the EMS of the FC-HEV: the rule-based and the optimization-based controls. The rule-based controls use expert knowledge, appear in deterministic (for example, thermostatic EMS), adaptive or predictive forms and are easily adaptable in real-time systems. The second approach is based on optimization of a cost function, which frequently defines the criterion of the fuel consumption, system efficiency, or system power [7].

Feroldi et al. [8] develop heuristic and optimal strategies based on the static efficiency map and validate them in real time. Their results show that the power split is enhanced by reducing hydrogen consumption. Bernard et al. [9] design an EMS based on Pontryagin's minimum principle (PMP) to reduce the hydrogen consumption and perform experimental validation. Farouk et al. [10] propose the study of two strategies: one strategy based on fuzzy logic and the other strategy based on the PMP. Their experimental study shows that PMP can outperform the fuzzy logic power split.

In most cases, the drawback of these strategies is that they depend on static models which are validated in a given operating range [11, 12]. Indeed, the PEM-FC is a multi-physics system [13], and its energetic performances depend on operating conditions (e.g., temperature, gas relative humidity, gas stoichiometry, pressure and ageing) [14]. It is therefore necessary to take into account these changes in operating conditions in a global EMS of the hybrid system.

There are two ways to identify the performance of a FCS, in real time. The first is the use of extremum seeking strategies, such as the maximum power point tracking (MPPT). Literature provides results on the topic regarding PEM-FCs. Zhong et al. [15] designed a MPPT algorithm based on an enhanced perturb and observe algorithm. Bizon [16] defined an additional MPPT algorithm to improve the tracking speed and display it in a numerical simulation. Guo-Rong et al. [17] designed a MPPT algorithm based on resistance matching and implement it on a hybrid energy system. The second method is to use an online identification of parameters coupled to an optimization algorithm. However, this method requires a PEM-FC model. Once again, two solutions are possible. (i) A direct solution is to consider the multi-physics behaviour of the PEM-FC in complex models. However, their

design (and validation) can be difficult and time-consuming processes [18]. (ii) Another solution is to use online parameters adaptation on black-box models. The parameters are estimated regardless of the multi-physics fluctuations. Meiler et al. [19] achieve a state of the art of the possible models for online identification of the behavior of a FCS and conclude that the best results are given by the Ursyon model. Yang et al. [20] use a model to emulate the behavior of the FCS and validated the control on test bench.

In our study, a two-step method is used. An identification algorithm is applied to a semi-empirical model of a PEM-FC. Then the identified model is used to optimize the performances (power and efficiency) of the PEM-FC. A semi-empirical model is used because it offers a trade-off between the physical meaning and the calculation cost [21]. The two-step method is chosen to enable, in future works, the identification versus several input parameters (temperature, pressure, and stoichiometry). In this study, only one parameter is optimized (the current of the PEM-FC i_{fc}).

Various studies propose contributions on the topic of online identification coupled with optimization of FCSs in order to find the best performance. Methekar et al. [22] develop an adaptive control of the FCS with a Wiener model and proposed a numerical validation. Dazi et al. [23] simulate a predictive control to determine the maximum power operation of the FCS. Ramos et al. [24] design a MPPT control, which was validated using hardwage in the loop. Gene et al. [25] conduct an experiment to validate real-time optimization of a solid oxide FCS. Kelouwani et al. [26] present an experiment on the pursuit of maximum efficiency of the PEM-FC. The study of Kelouwani et al. is based on a polynomial model of the efficiency of the PEM-FC and seeks the best efficiency by tuning the control variables (current, stoichiometry, temperature).

In summary, there are methods to split the power between two sources in a hybrid system (such as battery and PEM-FC for example) and research methods to determine the best performances of the PEM-FCs. However, it should be noted that there are few EMSs that link the power splitting in a hybrid system and extremum seeking method on PEM-FC. This work is based on a previous experimental study [21] where it has been shown that an identification algorithm which determines the performance (better efficiency and power) of a semi-empirical model of a PEM-FC is adaptable in real time. In another study, an adaptive EMS based on a hysteretic behaviour is implemented [27]. Now, the objective of this paper is to present an Adaptive EMS based on Pontryagin's Minimum Principle (A-PMP). The aim of the A-PMP strategy is to reach an optimal power split between the two sources (PEM-FC and battery pack). Furthermore this strategy will take into account the change in maximum power and efficiency of the FCS, according to the degradation of the PEM-FCs. A specific emphasis is placed on the operating parameter drift by using two PEM-FCs with different levels of degradation. Through this test bench, the maps of two PEM-FCs were obtained in experimentation. One PEM-FC is healthy with approximately 20 hours of operation while the second is degraded with approximately 300 hours of operation as shown in Fig.1 and Fig.2. In the following chapters, these maps are employed to validate the developed algorithms.

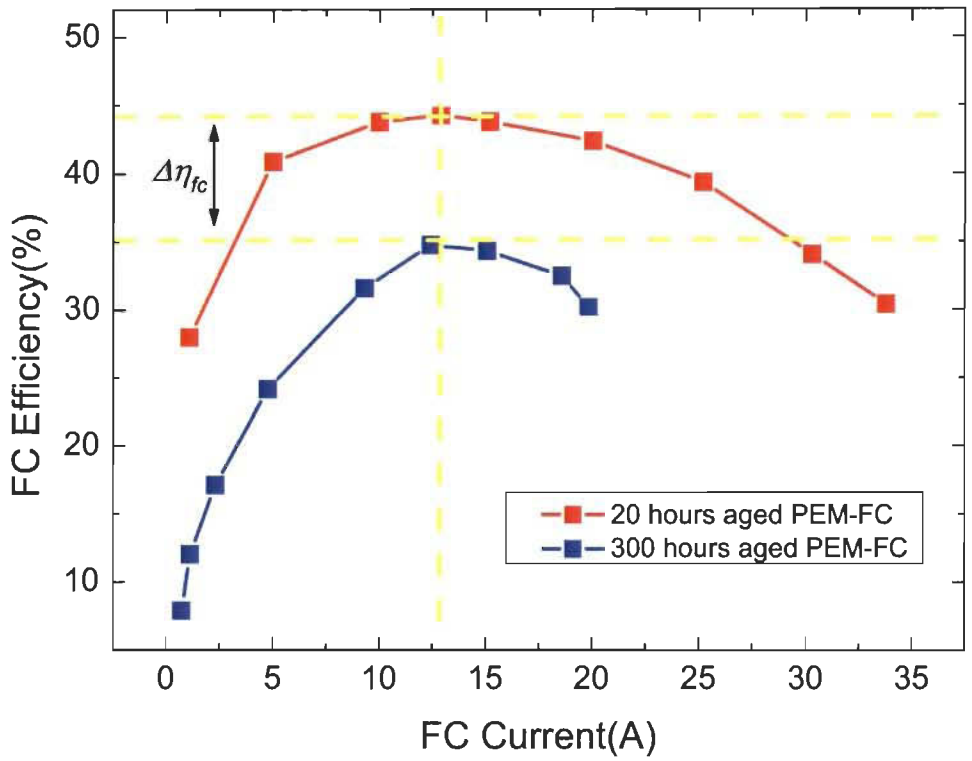

Figure 1: Efficiency curves for two PEM-FCs with different degrees of degradation at T_{fc}=35°C

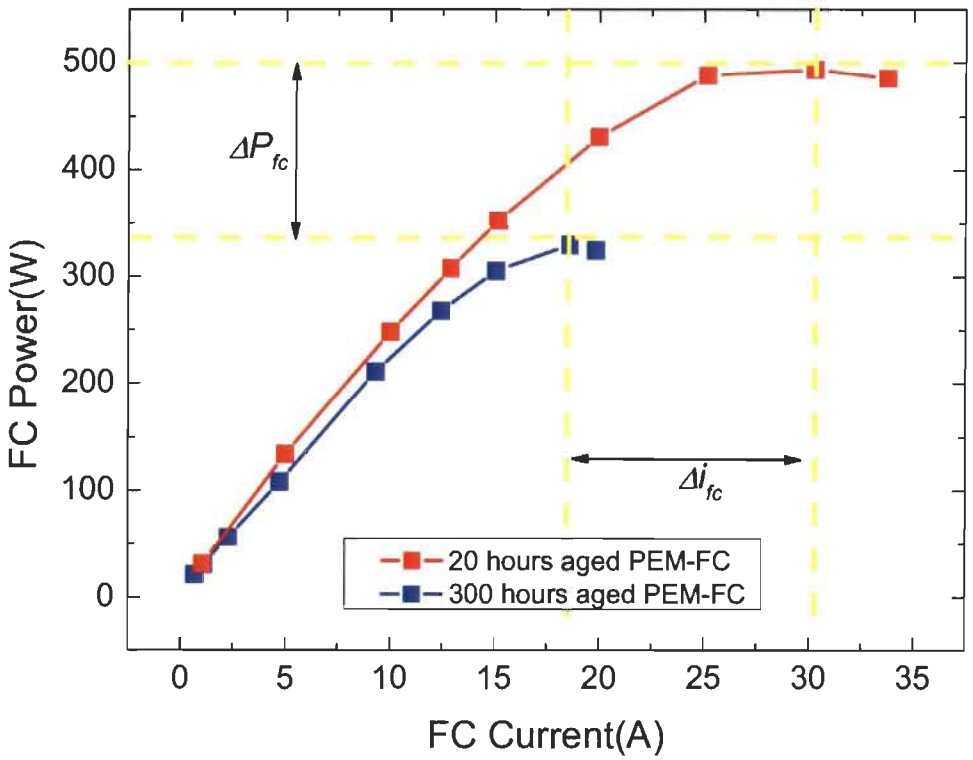

Figure 2: Power curves for two PEM-FCs with different degrees of degradation at T_{fc}=35°C

The rest of the paper is organized as follows. Section **Erreur ! Source du renvoi introuvable.** presents the architecture of the hybrid system, whereas the three steps EMS is described in Sections **Erreur ! Source du renvoi introuvable.**. The experimental results of optimal seeking are presented in Section **Erreur ! Source du renvoi introuvable.**. The validation study is performed in Section **Erreur ! Source du renvoi introuvable.**. The conclusion and perspectives are discussed in Section **Erreur ! Source du renvoi introuvable.**.

4.2 Architecture of the hybrid system

4.2.1 The PEM-FC low speed vehicle némo

The system used in this paper is based on the Némo FC-HEV (Fig.**Erreur ! Source du renvoi introuvable.**). The DC bus is built around a 335 *Ah* battery pack and a 2.5 *kW* Axane PEM-FC is used as a range extender [28]. The powertrain is based on a 5 *kW* induction machine [29].

(a)

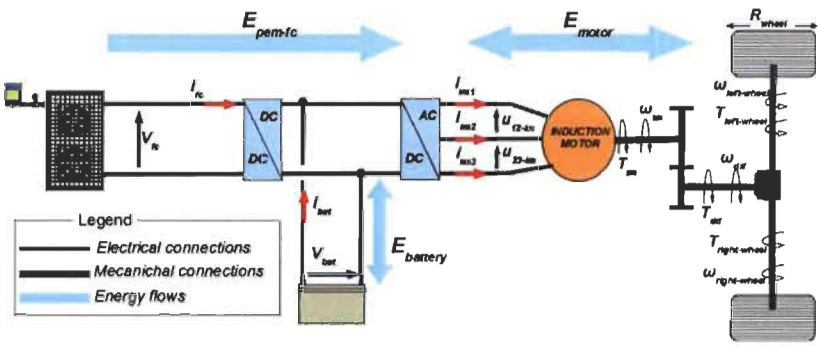

(b)

Figure 3: (a) The FC-HEV of the Hydrogen Research Institute (HRI); (b) Architecture of the FC-HEV of the HRI

4.2.2 Global view of the designed EMS

For the purpose of this work, a reduced-scale experimental test bench is designed (Fig.4). The experiments are performed with a 36 cell air-breathing Horizon PEM-FC (0.5 *kW*). The oxygen supply, relative humidity and temperature are managed by the fans. The hydrogen side operates in dead-end mode with a regulated pressure (0.05 *MPa*). The electric connection between the PEM-FC and the DC bus is realized by using a Zahn Electronics DC/DC converter to control the PEM-FC current i_{fc}. An electronic load (Dynaload Series WCL 488 Water Cooled) and a controllable source (Sorensen SGI 100) are used to emulate the power profile recorded on the real vehicle. The designed A-PMP-EMS is based on three layers. Fig.4 provides a global view of the designed A-PMP-EMS with:

- The power split based on the PMP that gives the optimal PEM-FC current i_{fc}.
- The online identification parameters of the PEM-FC based on the RLS algorithm
- The sequential optimization step that seeks the optimal operating point based on the power and efficiency estimation

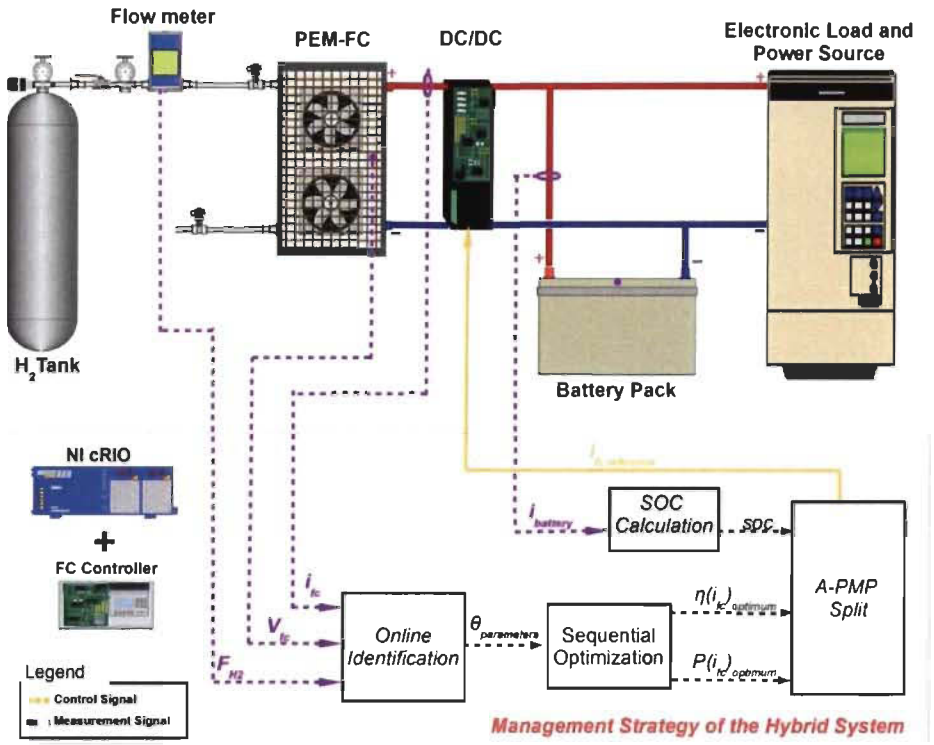

Figure 4: Global view of the applied A-PMP-EMS on the test bench

4.3 Real time optimization process

4.3.1 Optimal strategy based on the PMP: Formulation

This step allows a power distribution between the battery and the PEM-FC. The optimization of hybrid system aims to determine an optimal trajectory of the control variable (i_{fc}) in order to minimize a criterion under constraints [30, 31]. In the vehicle context, the objective of the optimization must meet these conditions:

- Minimize the hydrogen consumption throughout the cycle
- Maintain a state of charge (*soc*) of the battery pack within the limits set by the constraints
- Provide an optimal fuel cell power trajectory which is within the bounds set

- Meet the power demand of the driver along the speed cycle

Note that in the formulation of the optimization problem, the power of the battery pack is considered as the control variable. However, as shown in the architecture of the system, the actual control variable is the current of the PEM-FC. In summary, the optimal battery power is obtained by recombination as explained below in Section **Erreur ! Source du renvoi introuvable.**. In this case, the optimization based on PMP is well suited to this optimization problem [32]. First to define the optimization problem the consumption of hydrogen is described in Fig.5 by the following equation:

$$F_{h_2}(t) = f_1 i_{fc}(t) + f_2 \tag{1}$$

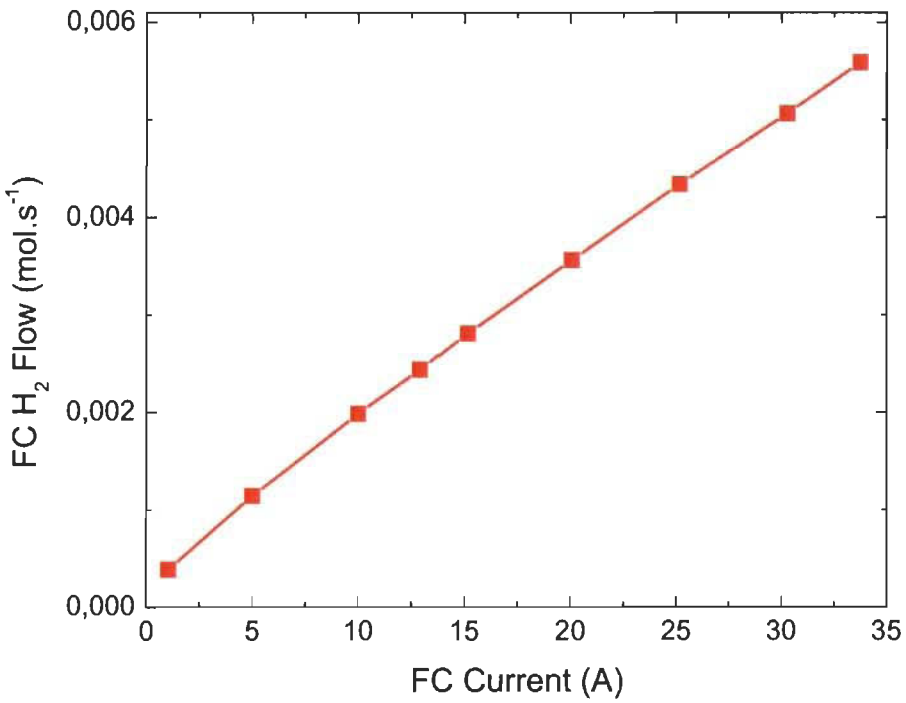

Figure 5: Experimental curve of the hydrogen flow (mol.s-1) of the 20 hour aged PEM-FC

where f_1 f_2 are fitting parameters and i_{fc} is the PEM-FC current. Based on the architecture of the system, the distribution of power between the two sources, PEM-FC and battery pack is governed by the energy conservation equation system:

$$P_{load}(t)=P_{bat}(t)+\eta_{dc-dc}P_{fc}(t) \tag{2}$$

where P_{load} is the power required by the driver during the trip, P_{bat}, P_{fc} and η_{dc-dc} the power supplied by the battery pack, the PEM-FC and the DC/DC converter efficiency, respectively. It is thus possible to express the equation of the hydrogen consumption to highlight the P_{bat} variable and define the performance criteria:

$$F_{h_2}(t) = f_1\left(\frac{P_{load}(t) - P_{bat}(t)}{\eta_{dc-dc}V_{fc}(t)}\right) + f_2 = Q(P_{bat}(t),t) \tag{3}$$

Then to obtain to optimal P_{bat}, the performance criteria can be defined as:

$$\min\ J(P_{bat}) = \min\left[J = \int_{t_0}^{t_f} Q(P_{bat}(t),t)dt\right] \tag{4}$$

This system is subject to constraints of the PEM-FC power level, of the PEM-FC power change rate, and of the battery pack *soc*. The inequality constraints of the system are defined as:

$$P_{fc,\min}(t)\leqslant P_{fc}(t)\leqslant P_{fc,\max}(t) \tag{5}$$

$$\Delta P_{fc,decrease}\leqslant \frac{dP_{fc}(t)}{dt}\leqslant \Delta P_{fc,increase} \tag{6}$$

$$soc_{\min}\leqslant soc(t)\leqslant soc_{\max} \tag{7}$$

where $P_{fc,\min}(t)$ and $P_{fc,\max}(t)$ are the minimum and the maximum power of the PEM-FC estimated by the algorithm developed in section **Erreur ! Source du renvoi introuvable.**. The *soc* is limited between $soc_{\min}$ and $soc_{\max}$. The $\Delta P_{fc,decrease}$ and $\Delta P_{fc,increase}$ are the dynamic limitations of the PEM-FC power change rate. The state of the system is represented by the *soc* of the battery pack and is calculated by:

$$soc(t) = soc_0 - \frac{1}{C_n}\int_0^t I_{bat}(t)dt \tag{8}$$

where C_n and soc_0 are the battery charge capacity and the initial *soc*, respectively. In this study, it is assumed to know the initial value of the *soc* (for example in the vehicle, the information would come from the battery management system). The *soc* time derivative can be expressed using the battery pack power and by modeling the battery with an equivalent model [33]. An internal resistance battery model is used in order to focus on the EMS and to simplify the simulation [10]. It is composed of an internal resistance R_{bat} and an open circuit voltage V_{oc}. This gives the following derivative:

$$\frac{dsoc(t)}{dt} = -\frac{1}{2R_{bat}C_n}\left[V_{oc} - \sqrt{V_{oc}^2 - 4R_{bat}P_{bat}(t)}\right] = f(soc(t), P_{bat}(t), t) \tag{9}$$

An attention must be paid to the power range of the FCS. In this paper, the PEM-FC power range is bounded by the maximum efficiency and the maximum power currents. This choice is motivated by the higher degradation rate of the cells at low (under the maximum efficiency) or high (over the maximum power) currents [8, 34] (Fig.6).

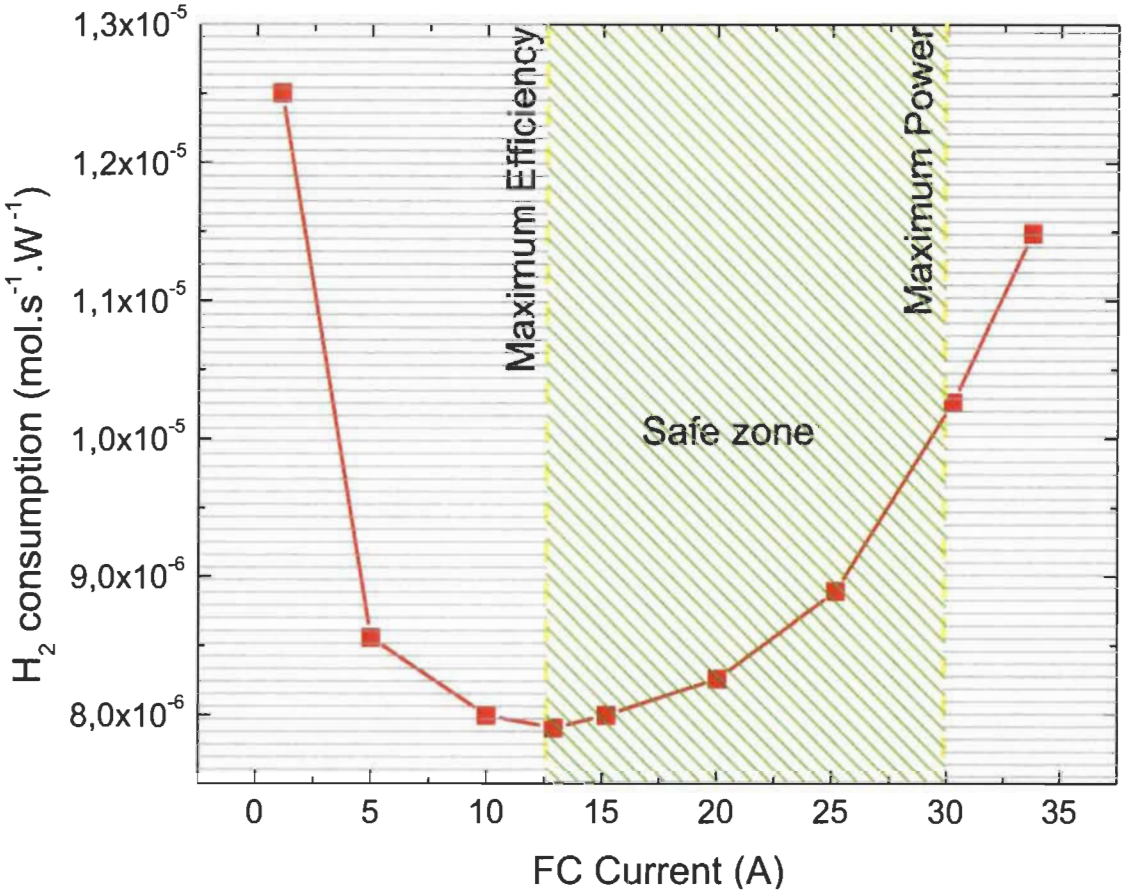

Figure 6: Experimental curve of the hydrogen flow (mol.s-1.W-1) of the 20 hour aged PEM-FC

According to the PMP, the Hamiltonian of the system is expressed as follows:

$$H(Pbat, soc, \lambda, t) = Q(Pbat(t), t) + \lambda f(soc(t), P_{hat}(t)) \tag{10}$$

where λ is the co-state. According to the PMP, the necessary conditions for optimality are set out as follows:

$$\frac{dsoc(t)}{dt} = \frac{\delta H(Pbat(t), soc(t), \lambda(t), t)}{\delta \lambda} = f(soc(t), P_{hat}(t), t) \tag{11}$$

$$\frac{d\lambda(t)}{dt} = -\frac{\delta H(Pbat(t), soc(t), \lambda(t), t)}{\delta soc} = -\lambda \frac{\delta f(soc(t), P_{hat}(t), t)}{\delta soc} \tag{12}$$

$$H(P^*_{hat}(t), soc(t)^*, \lambda(t)^*, t) \leq H(P_{hat}(t), soc(t)^*, \lambda(t)^*, t) \tag{13}$$

where the superscript * denotes optimal trajectories. The final condition of the state *soc* is bounded on the driving cycle and is defined by:

$$soc(t_0)=soc(t_f) \tag{14}$$

4.3.2 Constant co-state definition

The co-state defined in Equation (12) acts as a weighting factor for the derivative of the *soc*. In addition, the second term of Equation (12) which includes the co-state can be seen as a factor of equivalent fuel consumption. It is used to maintain the *soc* level and its value must be set to satisfy the condition described in Equation (14). Equation (9), represent the derivative of the *soc* shows a dependence on the *soc* levels. As the range of variation of the *soc* is low (the battery pack operates between 75% and 85% for a sustaining mode), it is assumed that the influence of the *soc* level is negligible on the OCV and the internal resistance R_{bat} of the battery [30]. This allows rewriting the expression for the variation of the *soc* in the following manner:

$$\frac{dsoc}{dt} = f(P_{bat},t) \tag{15}$$

At this state the *soc* level depends only on battery power P_{bat} then the co-state Equation (12) is expressed as follows:

$$\frac{d\lambda(t)}{dt} = -\lambda\frac{\delta f(P_{bat}(t),t)}{\delta soc} = 0 \rightarrow \lambda^*(t) = \text{constant} \tag{16}$$

The result is a constant co-state in this optimization problem. Furthermore, this hypothesis has two advantages. The first is that the computation time is reduced since the Equation (12) is no longer calculated. The second is that as the co-state λ is constant

throughout the speed cycle then the optimal solution of the PMP, if it exists, is globally optimal.

4.3.3 Reformulation for optimality

The purpose of this section is to reformulate the problem of constrained optimization in an unconstrained problem. For this, the penalty function method is used [35, 36]. The constraints defined above in Equations (5) and (7), are rewritten as follows:

$$g_1(t) = \frac{P_{load}(t) - P_{bat}(t)}{\eta_{dc-dc}} - P_{fc,\min}(t) \geq 0 \tag{17}$$

$$g_2(t) = P_{fc,\max}(t) - \left(\frac{P_{load}(t) - P_{bat}(t)}{\eta_{dc-dc}} \right) \geq 0 \tag{18}$$

$$g_3(t) = soc(t) - soc_{min} = 0 \tag{19}$$

$$g_4(t) = soc_{max} - soc(t) = 0 \tag{20}$$

$$g_5(t) = \frac{d}{dt}\left(\frac{P_{load}(t) - P_{bat}(t)}{\eta_{dc-dc}} \right) - \Delta P_{fc,decrease} \geq 0 \tag{21}$$

$$g_6(t) = \Delta P_{fc,increase} - \frac{d}{dt}\left(\frac{P_{load}(t) - P_{bat}(t)}{\eta_{dc-dc}} \right) \geq 0 \tag{22}$$

Using this penalty functions, the optimization problem is reconsidered in the following manner:

$$\min\ J' = \min\ J + \frac{s}{2}\sum_{i=1}^{6}\int_{t_0}^{t_f} g_i(P_{bat}(t), soc(t), t)h(g_i)dt \tag{23}$$

The term s defines the penalty factor and should be set at a higher value to be close to the optimal solution (s=100). The term $h(x)$ is the Heaviside function defined in Equation

(24). Note that the Heaviside function is discontinuous. So when the Hamiltonian is derived to determine the optimal battery power the solution tends to infinity. To solve this problem the Heaviside function is regularized to be continuous [37]. Thus, in the optimization problem, the Heaviside *h(x)* is represented by Equation (25):

$$h(x)=\begin{cases}1, if\ x \geqslant \varsigma \\ 0, if\ x < \varsigma\end{cases} \tag{24}$$

$$h(x)=\frac{1}{2}\left(1+\frac{2}{\pi}\arctan\left(\frac{x}{\varsigma}\right)\right) \tag{25}$$

where $\varsigma = 2$ in this case. The augmented Hamiltonian is therefore rewritten as follows to take into account the constraints:

$$H(Pbat, soc, \lambda, t) = Q(Pbat(t), t) + \lambda f(soc(t), P_{bat}(t)) + \frac{s}{2}\sum_{i=1}^{6} g_i(P_{bat}(t), soc(t), t)h(g_i) \tag{26}$$

Finally, using the Hamiltonian, the optimal control means determining the optimal battery power P_{bat}^{*} as:

$$P_{bat}^{*}(t) = \arg\min\ H(P_{bat}, soc, \lambda, t) \tag{27}$$

The Hamiltonian in Equation () is shown in the Fig.7 for different load power P_{load} and a constant co-state λ. Clearly note that for different load power P_{load} the Hamiltonian is convex. This means that for each power load during the cycle, there is a unique optimal battery power P_{bat}^{*} respecting the bounds set.

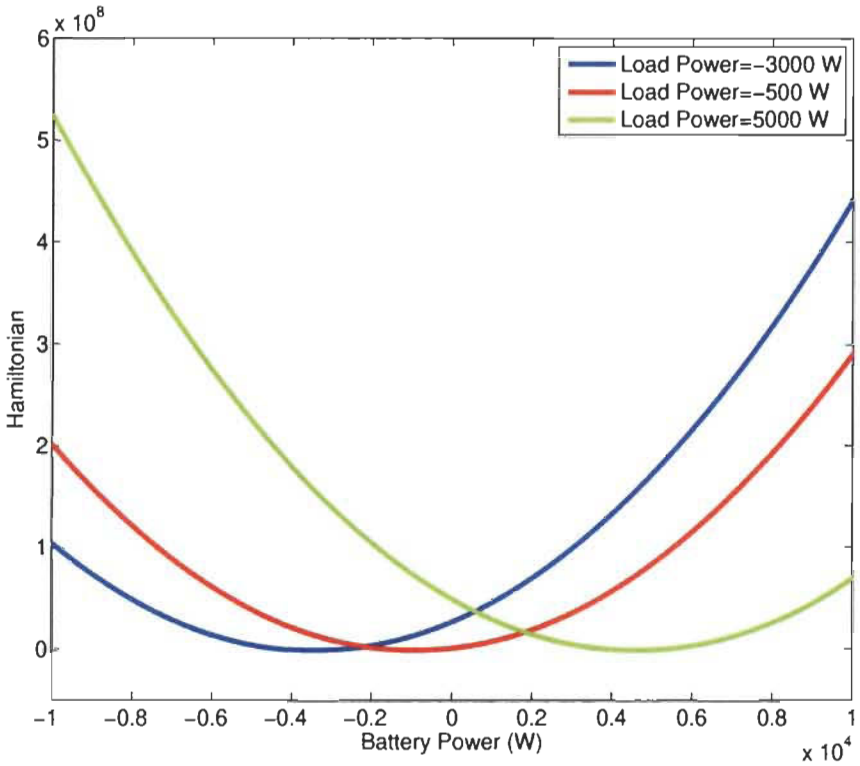

Figure 7: Three representations of the Hamiltonien with constant co-state λ for different P_{load}

4.3.4 Real-time implementation of the optimization

In this work, the role of the co-state λ is to balance the change in *soc* level to satisfy the Equation (14) in a given cycle. This means that for each cycle there is an optimal value for the constant co-state [38, 39]. To find the co-state on a given speed cycle, a method of iterative search over the entire speed cycle is employed. A method that works well is the iterative search [39]. This determines the constant value of the co-state λ knowing the speed cycle. The problem with this method is that it requires knowing the driving cycle in advance, making it difficult for real-time implementation. Kessels et al. [38] proposes using a state feedback control by determining the real-time co-state to approach the optimum, see Fig.8. A proportional integral controller is used to set the co-state λ to maintain the soc level around the real-time reference value and satisfy the final condition on the *soc*:

$$\hat{\lambda}(t) = \lambda_0 + K_P e(t) + K_I \int_0^t e(v)\,dv \tag{28}$$

where λ_0 is an initial co-state , K_P and K_I the proportional and integral gains of the correction, respectively.

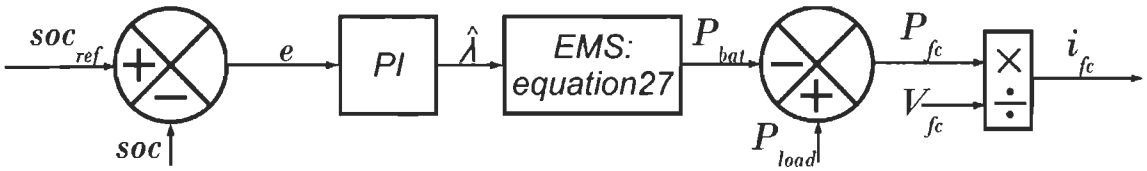

Figure 8: Feedback control for estimating λ

4.4 Online extremum seeking process

In this part, the experimental results of the real-time identification of the PEM-FC characteristic curves are shown. These experiments are carried out on the test bench with a healthy PEM-FC. This step is a key to the A-PMP algorithm because it identifies online variation of maximum power and maximum efficiency over time. The adaptive recursive least square (ARLS) algorithm is used to identify the parameters of the PEM-FC model that are suitable for real-time applications, and it is based on the successive update of the model parameters [21].

4.4.1 Adaptive recursive least square algorithm

In this section, the ARLS step is described [21]. As shown in Fig.9, a single-input single-output system defined by Equation (29) is considered:

$$[y(k)] = [\phi(k)][\theta(k)]^T + [\xi(k)] \tag{29}$$

where ϕ is the regressor vector, θ is the system parameter vector, ξ is a stochastic noise variable with normal distribution and zero mean and k is the time step. The ARLS algorithm minimizes the objective function J_k defined by the prediction error ε squared as shown in Equation (30):

$$J(k) = \sum_{i=1}^{k} \psi^{k-i} \varepsilon_i^2 \tag{30}$$

where ψ (a value between [0; 1]) is the forgetting factor, which is necessary to track the variation of the parameters over time (ageing drift). The implementation of the ARLS algorithm is performed by using the following equations:

$$K(k+1) = \frac{P(k)\phi(k+1)}{1+\phi^T(k+1)P(k)\phi(k+1)} \tag{31}$$

$$P(k+1) = P(k) - \frac{\left(P(k) - K(k+1)\phi^T(k+1)P(k)\right)}{\left(\mu(k)^{-1} + \phi^T(k+1)P(k)\phi(k+1)\right)} \tag{32}$$

$$\varepsilon(k+1) = y(k+1) - \phi^T(k+1)\theta(k) \tag{33}$$

$$\theta(k+1) = \theta(k) + K(k+1)\varepsilon(k+1) \tag{34}$$

where K is the Kalman gain, P is the covariance matrix of the prediction error ε and θ are the identified parameters.

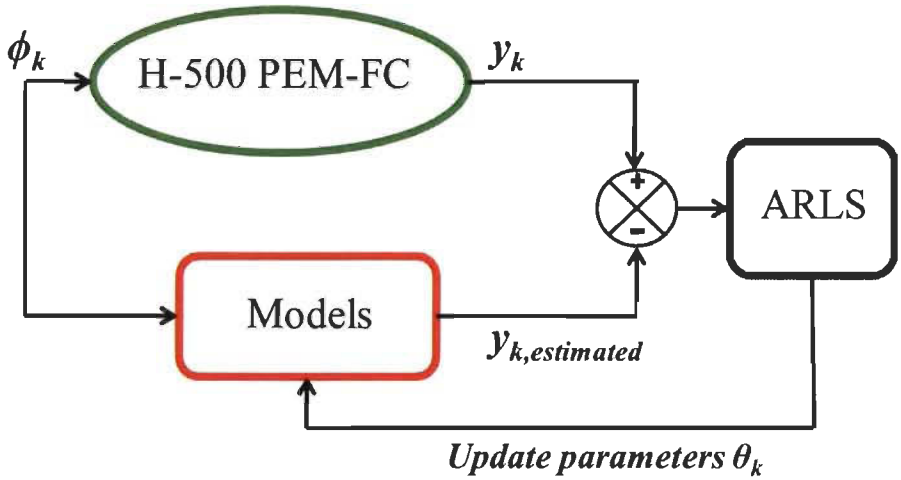

Figure 9: Flowchart of the PEM-FC voltage identification with the ARLS algorithm

4.4.2 Experimental identification of the hydrogen molar flow

As defined in Bagotsky et al.[40], the operating efficiency of a PEM-FC is the ratio between the electrical power produced and the chemical power of the hydrogen oxidation. Typically, not all of the molar flow of the reactant supplied to the PEM-FC is used for current production, and it is difficult to predict. The reasons could be due to an incomplete reactant oxidation or a diffusion of the reactant through the electrolyte. So, the hydrogen molar flow has been estimated to predict the chemical power of the hydrogen oxidation. $f_{2,est}$ is the estimated hydrogen molar flow and it is determined online using an ARLS algorithm. The linear expression described in Equation (1) is used in the ARLS algorithm to estimate $f_{1,est}$ and $f_{2,est}$ as shown in Equation (35). The fitting curve is compared with the experimental data (Fig.10).

$$F_{h_2,est}(t) = f_{1,est} i_{fc}(t) + f_{2,est} \tag{35}$$

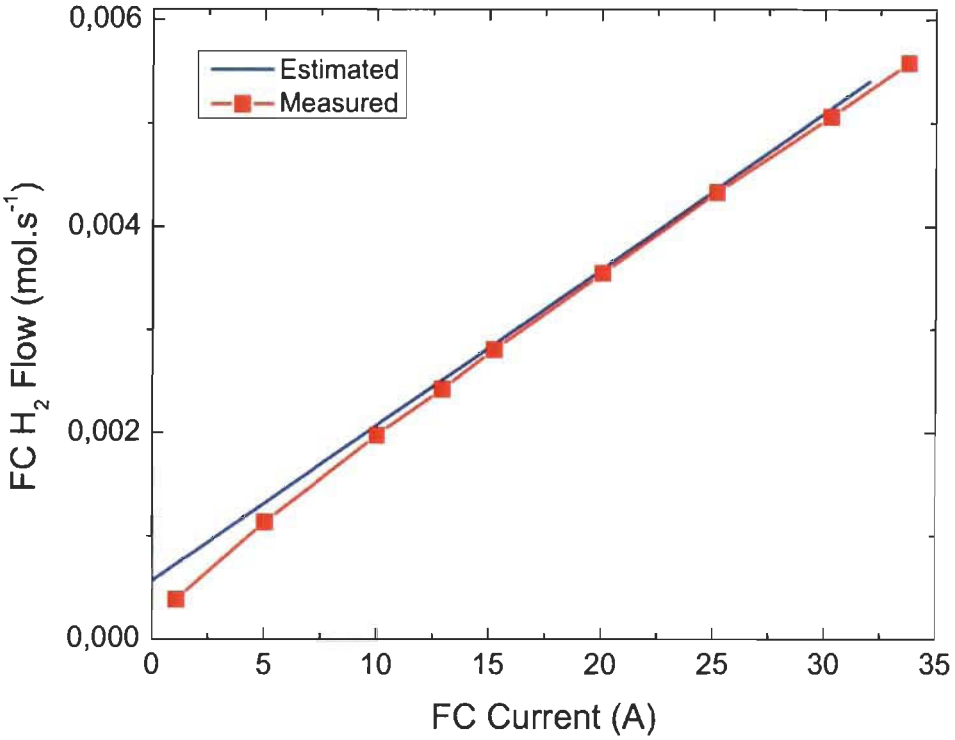

Figure 10: Experimental flow curve of the 20 hour aged PEM-FC compared with the estimated flow curve

4.4.3 Experimental estimation of the FC characteristics

This part describes how to estimate the polarization curve $V_{fc,est}$ of the PEM-FC, by updating a model using the algorithm by measuring the voltage V_{fc} and the current i_{fc} of the PEM-FC. A semi-empirical model is considered because it describes the PEM-FC voltage with a physical meaning (important for the analysis of the relevance of the identification results). Furthermore, it is necessary that the model take into account the overvoltages in order to characterize the PEM-FC for its entire measurement range. In a previous study, it was demonstrated that the Squadrito et al. model [41] is well suited for on-line identification [21]. Squadrito et al. defines a static semi-empirical model of the PEM-FC on the basis of reference [42] (**Erreur ! Source du renvoi introuvable.**):

$$V_{fc_k} = Vo_k - b_k \log(i_{fc_k}) - r_k i_{fc_k} + \alpha_k i_{fc_k}^{\sigma} \log(1 - \beta i_{fc_k}) \quad (36)$$

where V_o, b, r and β are the open circuit voltage, the Tafel slope, the ohmic resistance and the inverse of the limiting current, respectively (see Table 1). Pisani et al. [43] provides a semi-empirical model on the same basis [41] and relates the parameters σ with the water flooding phenomena and α to the diffusion mechanism. For this model, literature provides the values of σ (between 1 and 4) and β ($0.99 A.cm^{-2}$). The model parameters were used to plot the power and efficiency curves for the next step (extremum-seeking algorithm based on sequential optimization). Fig.11 and Fig.12 show that the semi-empirical model coupled with the ARLS algorithm was able to track the performance of the healthy H-500 PEM-FC. The PEM-FC power and efficiency are determined by using the following Equations:

$$P_{fc,est} = V_{fc,est} i_{fc} \quad (37)$$

$$\eta_{fc} = \frac{P_{fc,est} - P_{aux}}{P_{H2,est}} \quad (38)$$

where P_{aux} (W) is the auxiliary power (assumed as constant) and $P_{H2,est}$ (W) is the estimation of the consumed hydrogen power during the electricity production expressed as (39):

$$P_{H2,est} = P_{H2,est} HHV \quad (39)$$

where HHV is the high heating value of hydrogen ($286\ kJ.mol^{-1}$). The estimated power curve for the healthy PEM-FC (Fig.11) provides a maximum power for a current close to 30 A and a good fitting with the measured PEM-FC characteristics. Additionally, Fig.12 shows that the estimated efficiency curve of the new PEM-FC provides a maximum

efficiency for a current near 13 A. These results confirm that the extreme-seeking algorithm can find the optimal set point of the PEM-FC.

Table 1: Initialization of the parameters

Empirical parameters	Vo	b	R	α
Value	33.0694	-0.02594	-26.0395	0.2492

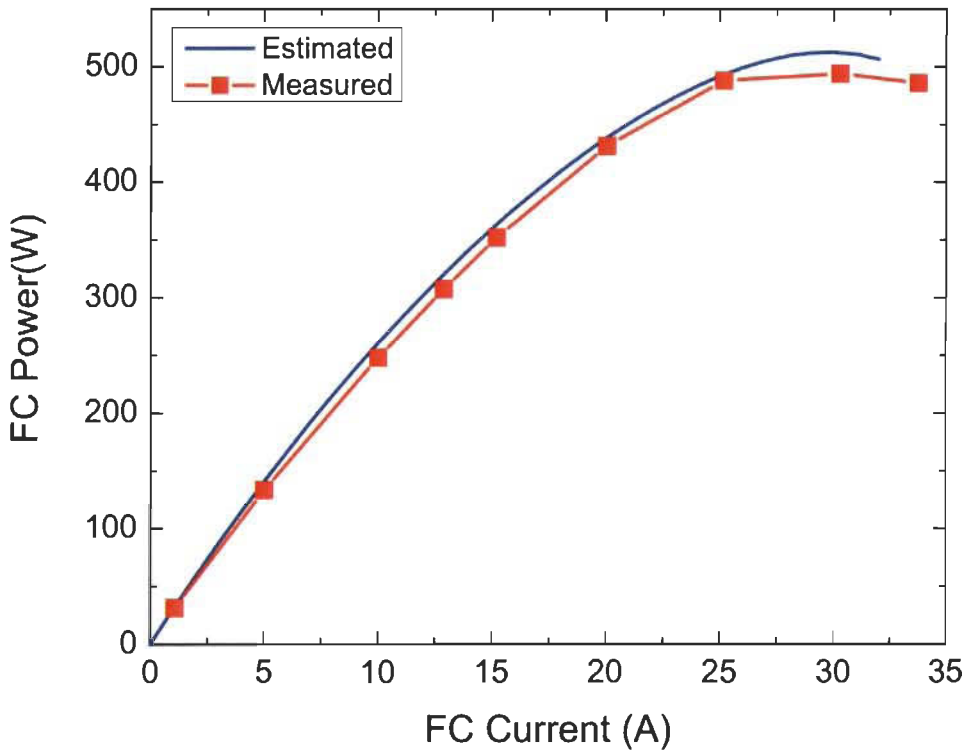

Figure 11: Experimental power curve of the 20 hour aged PEM-FC compared with the estimated power curve

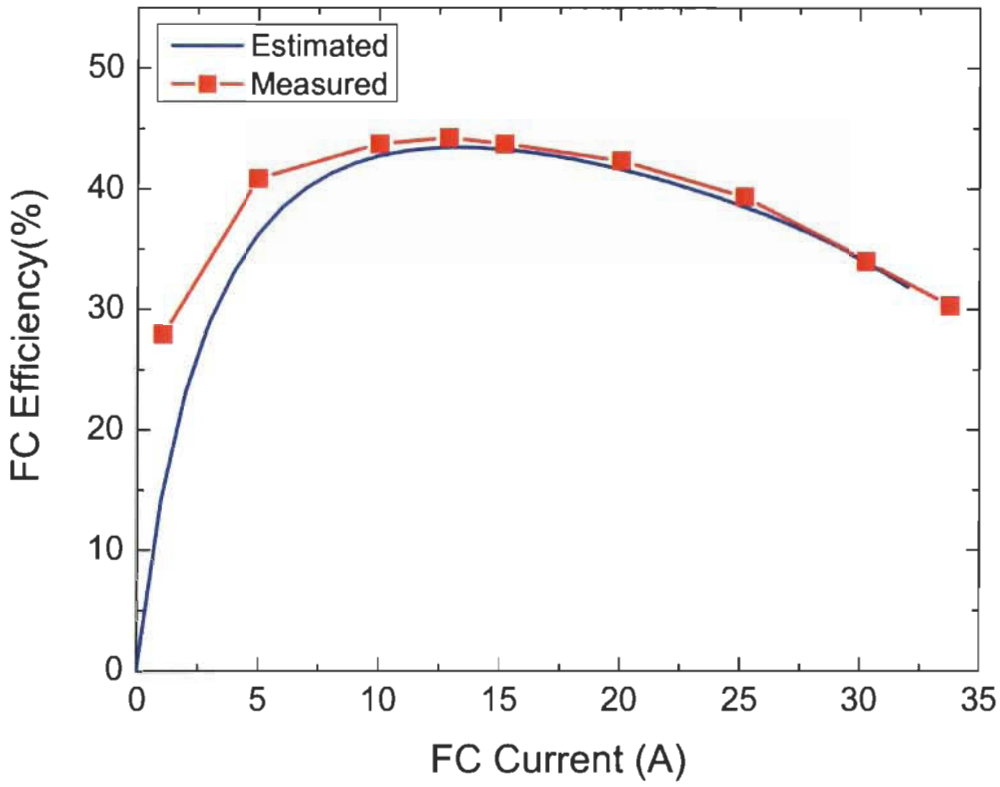

Figure 12: Experimental efficiency curve of the 20 hour aged PEM-FC compared with the estimated efficiency curve

4.4.4 Sequential optimization

The extremum-seeking control is the step in which the optimum PEM-FC power and efficiency are estimated from the characteristic curves obtained using the ARLS in Section **Erreur ! Source du renvoi introuvable.**. So, two optimization problems are formulated each with an objective function (power and efficiency). The sequential quadratic programming (SQP) algorithm is one of the most popular methods for solving optimization problems (especially the convex problems). The local optimization is sufficient because the two objective functions are unimodal and smooth and contain one maximum. To obtain the current i_{fc} that yields the optimal power or efficiency, the problem is set ()-():

$$J(x) = P_{fc}(x) \quad \varphi :\rightarrow x_{\min} \leqslant x \leqslant x_{\max} \tag{40}$$

$$J(x) = \eta_{fc}(x) \quad \varphi :\rightarrow x_{\min} \leqslant x \leqslant x_{\max} \tag{41}$$

where x is the optimal current and x_{min} and x_{max} are the lower and upper bounds of the PEM-FC currents.

4.5 Energy management results

The validation is performed using a model of the FC-HEV developed in a previous work [21]. This model was used to plot the powers of load from a standard Artemis cycle [44]. The results of the identification based adaptive PMP developed in this paper will be compared to a classical online PMP EMS given in the literature [10]. In a first part, the online PMP is based on a model closed to the real PEM-FC (the healthy model parameters are used on the healthy PEM-FC). These results are considered as optimal and the aim is to show the good performances of the developed A-PMP. In a second part, the online PMP is based on a model far from the real PEM-FC (the healthy model parameters are used on the degraded PEM-FC). This case highlights the using of a non-adaptive EMS on the drifting performances of a real PEM-FC. Then, A-PMP performances are shown.

4.5.1 A-PMP versus PMP: validation with healthy FC

The aim of this part is to highlight that the EMS allows the *soc* level to be sustained around the reference (soc_{ref}=80%). Moreover, it will be shown that the A-PMP strategy gives results closed to the online PMP EMS based on maps (classical PMP). On a standard Artemis cycle online PMP and A-PMP EMSs are simulated with healthy PEM-FC. Fig.13

show the results of the online PMP algorithm based on the mapping of the healthy PEM-FC. The objectives are achieved since the *soc* level is sustained and the power of the PEM-FC is maintained between the maximum efficiency and power (P_{max} = 497 W and P_{min} = 308 W) during the cycle as shown in Fig.13. Furthermore, the PEM-FC dynamics is respected since it is under 50 $W.s^{-1}$ as described by Thounthong et al.[45]. Therefore the constraints on the PEM-FC power are also satisfied.

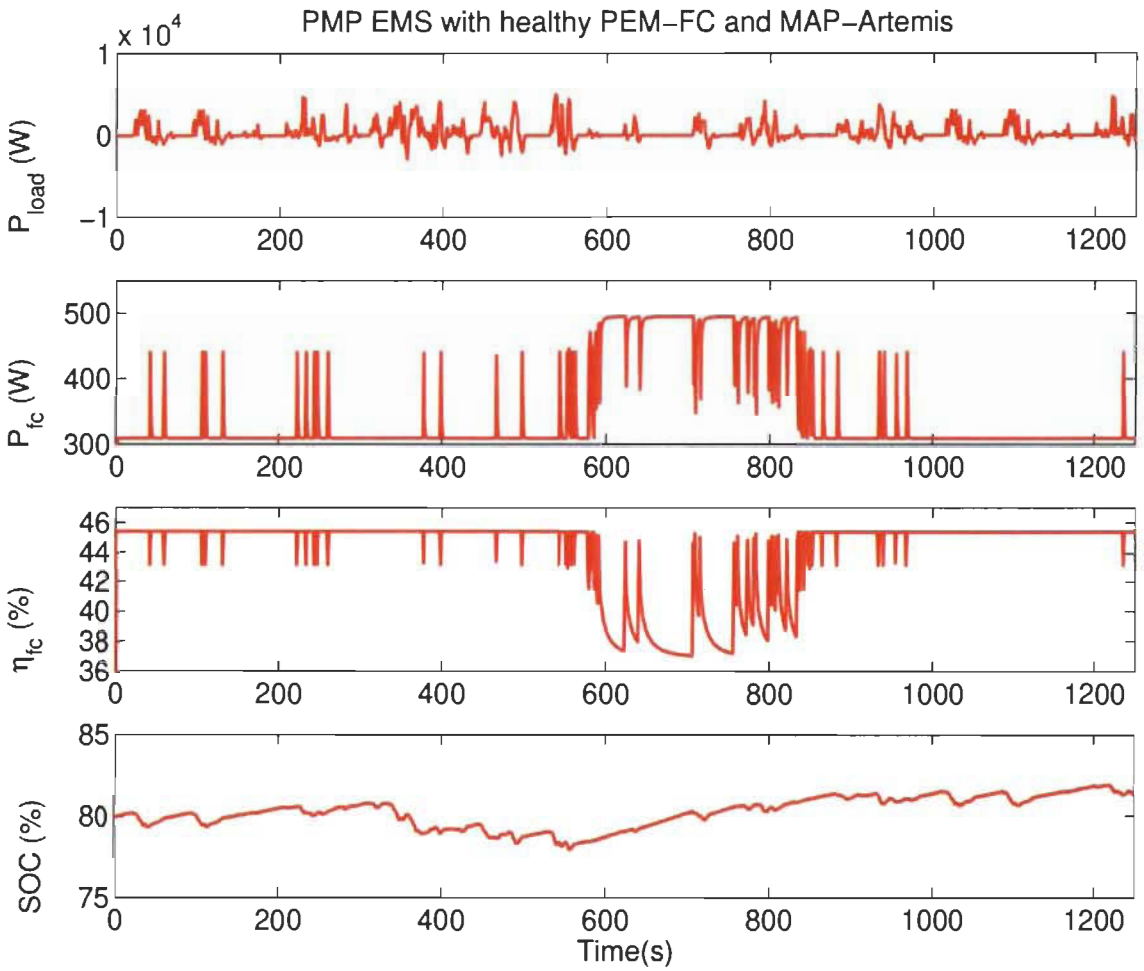

Figure 13: Trajectory of the power splitting obtained by the online PMP based strategy on the 20 hour aged PEM-FC

The A-PMP EMS is now simulated and the results show that the constraints on the soc level (sustained at 80%) and on the power of the PEM-FC are satisfied (Fig.14). The

obtained results show that the online PMP and A-PMP EMS developed in this work, gives similar results. Indeed, when comparing the hydrogen consumption for this case, the online PMP EMS gives a hydrogen consumption of 0.797 $g.km^{-1}$ and the A-PMP EMS give a consumption of 0.805 $g.km^{-1}$. For this study case, the online PMP uses the real map of the FC while the A-PMP uses estimations of the maximum efficiency and power points (provided by the adaptive layer). The online estimated efficiency is slightly below the map value (2.3%) and the estimated power is slightly above (2%).

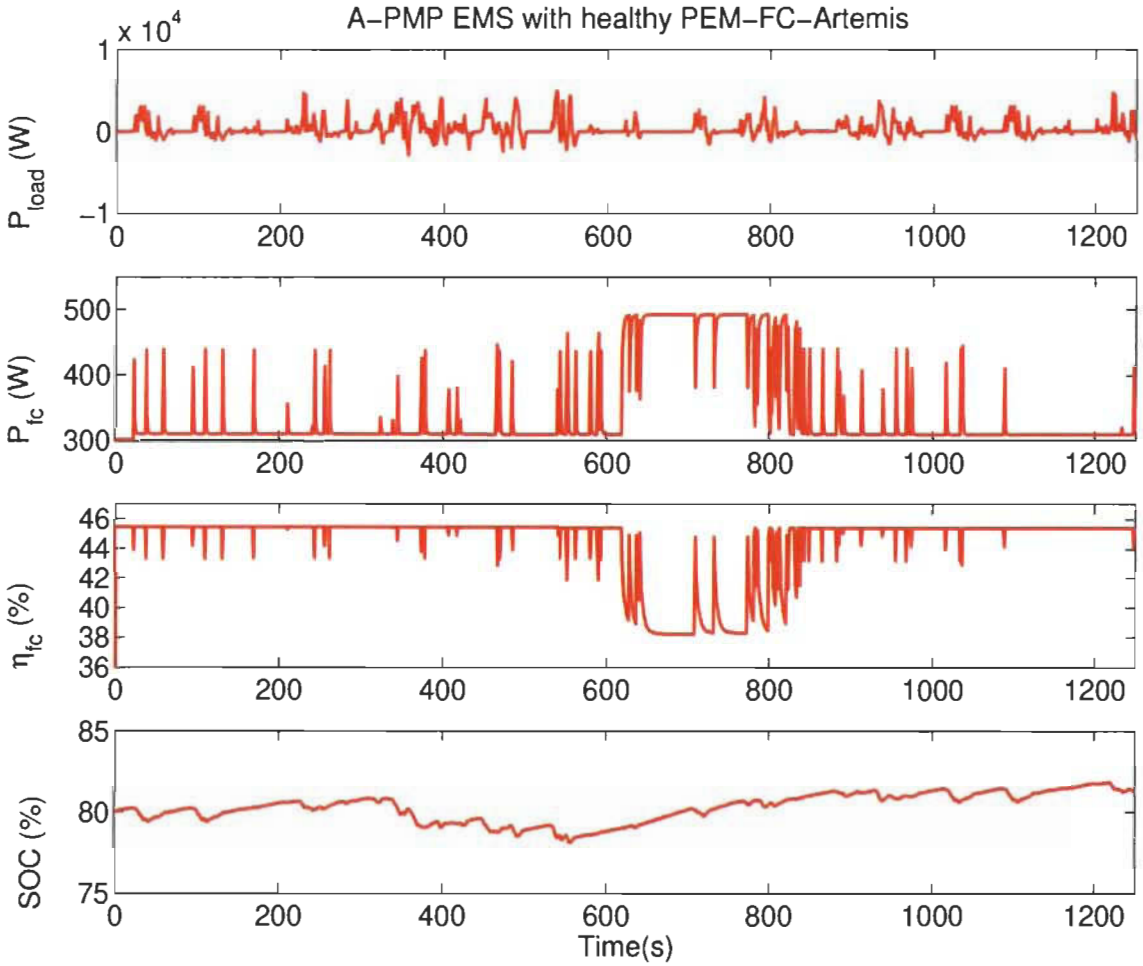

Figure 14: Trajectory of the power splitting obtained by the A-PMP based strategy on the 20 hour aged PEM-FC

4.5.2 Validation of online EMSs with degradation effect

In this section, we highlight the shortcomings of conventional mapping strategy when the maps are poorly calibrated. There are two objectives in these simulations. The first is to show that when degradation of the PEM-FC occurs, the A-PMP EMS allows taking into account this variation. The second objective is to highlight the classical online PMP lead to a mismanagement of energy. On a standardized Artemis cycle, the system is simulated for the two EMSs under the condition where the PEM-FC is degraded. But, the online PMP is still based on the healthy map. For reasons related to the safety of the PEM-FC, a cut-off is used (Fig.15). It avoids staying a long time beyond mass transport area if too much power is requested for the PEM-FC. In the case of the degraded PEM-FC cut-off is observed around 16.3 *V*. The protocol used to manage the cut-off is defined as indicated by the manufacturer, see Fig.16.

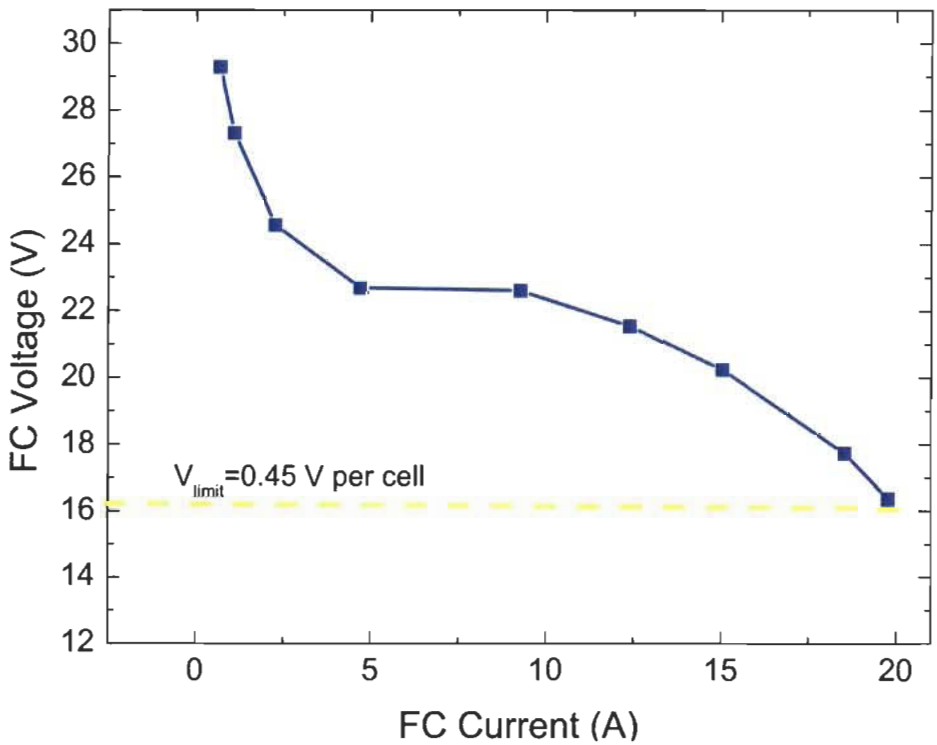

Figure 15: Polarization curve of the 300 hour aged PEM-FC H-500 with a cut-off voltage of *16.3V*

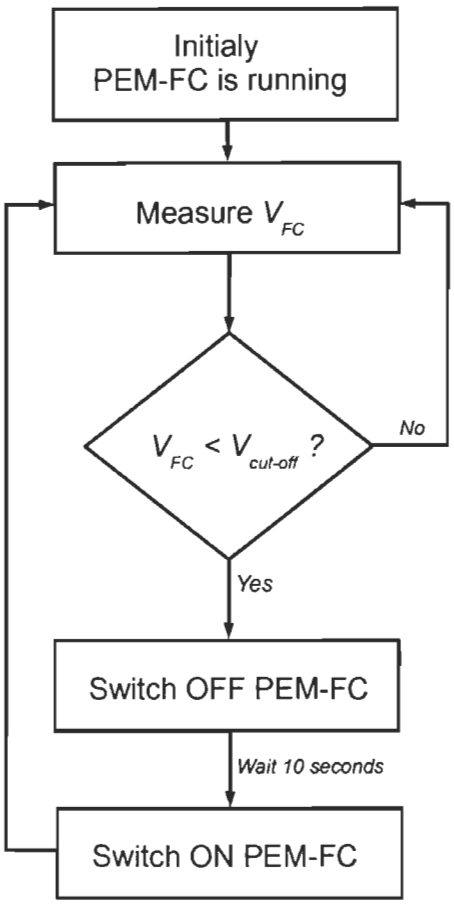

Figure 16: Chart of the cut-off management of the PEM-FC H-500

PMP strategy is realized with a degraded PEM-FC given the data of the healthy PEM-FC (P_{max} = 497 W and P_{min} = 308 W, Fig.17). In a first step, the first 500 seconds the PEM-FC operates at 308 W, which corresponds to the maximum efficiency from the data of the healthy PEM-FC. However, after 500 seconds, the power load request increases and the battery *soc* falls. The EMS based on PMP responds by requesting more power to the PEM-FC. The required power is based on the healthy PEM-FC map and it is greater than the degraded PEM-FC power limit (330 W): the cut-off is engaged. The *soc* level continues to fall and as the power required to sustain the soc level is still beyond the limit power, the PEM-FC oscillates between On and Off mode (Fig.17).

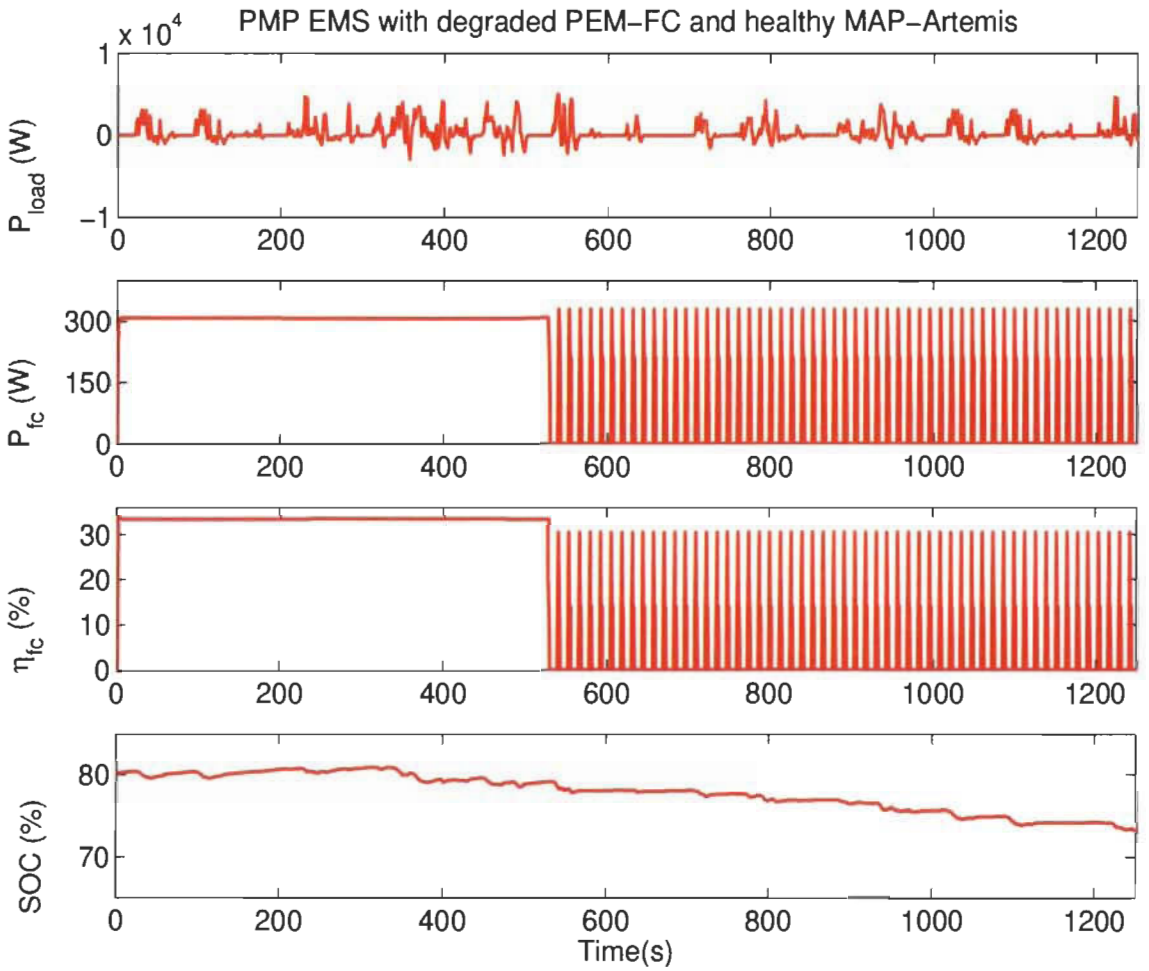

Figure 17: Trajectory of the power splitting obtained by the PMP based EMS with the 300 hour aged PEM-FC

The EMS based on A-PMP is applied (Fig.18) and the identification stage tracks the boundary powers (a maximum efficiency of 35% corresponding to the power of 275 *W* and a maximum power of 330 *W*, as indicated in Fig.1 and Fig.2). The A-PMP EMS allows fulfilling the objectives that are to maintain the *soc* level and to respect the constraints of power of the PEM-FC. The identification algorithm section coupled with the search for maximum, developed allows both to identify online maximum efficiency and power of the degraded PEM-FC. Indeed, we note that the power of the maximum efficiency is close to 275 *W* and maximum power is close to 330 *W*. So A-PMP EMS meets the capability to

track the variation of the operating conditions. Furthermore, the A-PMP EMS converges fast due to the speed of convergence of the ARLS algorithm. In a previous article, it has been shown that this algorithm coupled with the Squadrito et al. model converged after 300 milliseconds when activated [21].

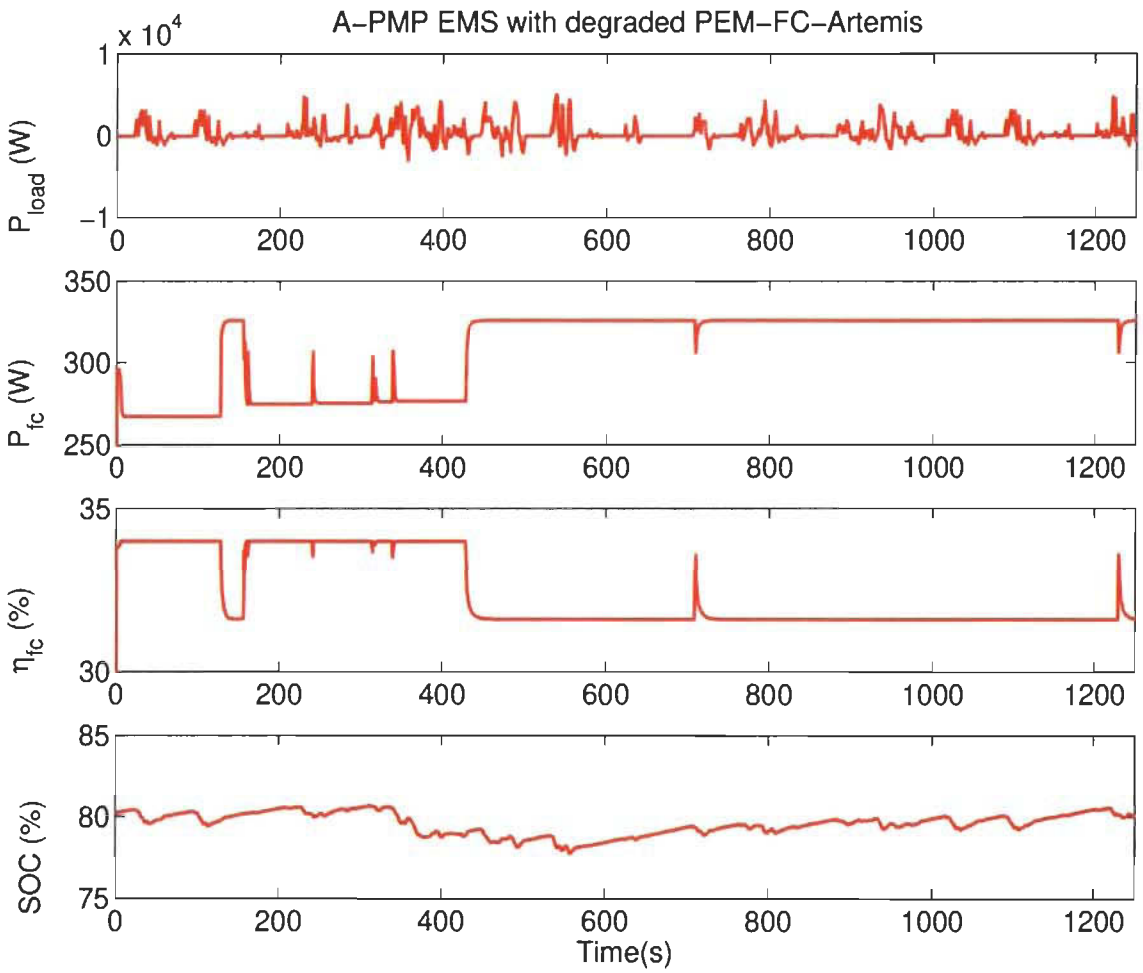

Figure 18: The trajectory of the PEM-FC power with the A-PMP based EMS with the 300 hour aged PEM-FC

4.5.3 Adaptation behavior of strategy with degradation

We propose to study in this part the adaptation of the power sharing with the A-PMP EMS according to the degree of degradation of the PEM-FC. The factors that cause degradation are many and difficult to predict. They are generated by the different operating

modes of the PEM-FC. So, for the purpose of this work, it is assumed that for a constant power PEM-FC degrades exponentially with time [46]. Even if a variable power level is used this assumption allows us to determine the intermediate values of power and efficiency of the PEM-FC. It is considered that the healthy PEM-FC represents the case where the PEM-FC is new and the degraded PEM-FC (300 hours) is the PEM-FC at the end of life. The Equation (42) and (43) represent the behavior of the efficiency according to this law of evolution.

$$\eta_{fc}(k) = \eta_{fc}^{0} e^{-D_{\eta fc}\Delta T} \tag{42}$$

$$D_{Pfc} = \frac{1}{t_{fc}} \ln\left(\frac{P_{fc}^{end}}{P_{fc}^{0}}\right) \tag{43}$$

Where η_{fc}^{0} and D_{Pfc} represent the initial efficiency given by the healthy PEM-FC map Fig.1 and the efficiency decay rate, respectively. ΔT and η_{fc}^{end} are the sampling time and the efficiency at end of life represented by the efficiency of the degraded PEM-FC (300 hours) in Fig.1. The parameter t_{fc} represent the PEM-FC lifetime corresponding to 300 hours. The same equations are used for the power degradation as shown in the equation (44) and (45):

$$P_{fc}(k) = P_{fc}^{0} e^{-D_{Pfc}\Delta T} \tag{44}$$

$$D_{Pfc} = \frac{1}{t_{fc}} \ln\left(\frac{P_{fc}^{end}}{P_{fc}^{0}}\right) \tag{45}$$

where P_{fc}^{0} , $P^{end,fc}$ and D_{Pfc} represent the initial power given by the healthy PEM-FC map Fig.2, the power at end of life and the power decay rate, respectively. Simulations are carried out on four levels of degradation (Fig.19). The used hydrogen energy is evaluated as

a function of the battery energy variation between the beginning and the end of the Artemis cycle. The data are collected for different initial *soc* between 76% and 83% (8 simulations) for each level of degradation. Fig.19 highlights the hydrogen overconsumption related to the PEM-FC degradation. Indeed, for a given battery energy threshold (-25 *kJ*), 100 hours PEM-FC consumes 12% more energy than a healthy PEM-FC to support the batteries. Nevertheless, the main objective is filled since the A-PMP EMS adjusts the power of the PEM-FC in order to maintain the *soc* and according to the degradation of the PEM-FC.

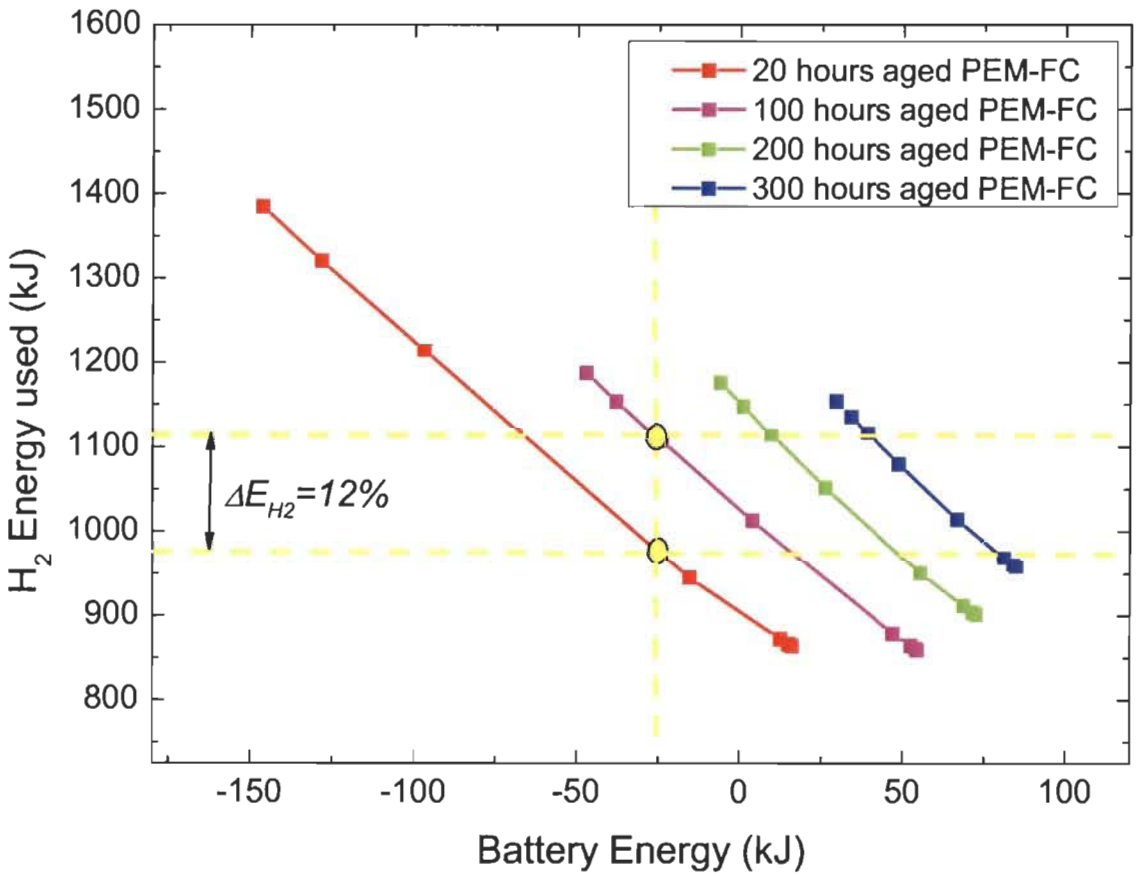

Figure 19: Hydrogen energy used versus the battery energy available for different level of degradation of the PEM-FC

4.6 Conclusion

The optimal adaptive power splitting problem is divided within two separate parts. (i) The global EMS to split power between two sources in a hybrid system. The drawback is that it is often based on a map or a model valid in a given operating range. (ii) In this work, maximum tracking techniques are introduced to determine the best performance of the PEM-FC when the operating conditions change. The aim was to show how to track the best performances of the PEM-FC regarding operating conditions and putting the tracked performances in a global EMS for hybrid sources. An online optimization problem based on the Pontryagin's Minimum Principle was developed to minimize the hydrogen consumption. An online identification layer is added to the global EMS to track the best performances of the PEM-FC. The online identification algorithm is based on an adaptive recursive least square algorithm and is applied to a semi-empirical model of a PEM-FC. Then the identified model is used to seek the optimal performances (power and efficiency) of the PEM-FC. The operating point is set between the maximum efficiency (to avoid an operation closes to the open circuit voltage) and the maximum power (to avoid the high concentration loss zone). It has been shown that the classical power splitting based only on the Pontryagin's Minimum Principle can led to mismanagement because of the variation of performances due to ageing. The developed adaptive management A-PMP can provide the power demand (i.e. sustain the *soc*) while adapting to changes in operating conditions (e.g. ageing effect). The A-PMP is able to track real behavior of the PEM-FC and to request a relevant power. Future works will be focused on an extension of the method in order to control several operating parameters as as temperature, stoichiometry, and pressure. This

extension is not realized by conventional MPPT or MEPT algorithms, which are limited to the tracking of one parameter.

Acknowledgements

This work has been supported by the "Bureau de l'efficacité et de l'innovation énergétique", the "Ministère des Ressources naturelles et de la Faune du Québec", the Natural Sciences and Engineering Research Council of Canada, LTE Hydro-Québec, the "Fonds de Recherche Québécois Nature et Technologie" (FRQNT).

References

[1] O. Z. Sharaf and M. F. Orhan, "An overview of fuel cell technology: Fundamentals and applications," *Renewable and Sustainable Energy Reviews,* vol. 32, pp. 810-853, April 2014.

[2] B. Olateju, J. Monds, and A. Kumar, "Large scale hydrogen production from wind energy for the upgrading of bitumen from oil sands," *Applied Energy,* vol. 118, pp. 48-56, 4/1/ 2014.

[3] X. Feng, L. Wang, and S. Min, "Industrial emergy evaluation for hydrogen production systems from biomass and natural gas," *Applied Energy,* vol. 86, pp. 1767-1773, 9// 2009.

[4] O. Erdinc and M. Uzunoglu, "Recent trends in PEM fuel cell-powered hybrid systems: Investigation of application areas, design architectures and energy management approaches," *Renewable and Sustainable Energy Reviews,* vol. 14, pp. 2874-2884, 2010.

[5] Y. Tang, W. Yuan, M. Pan, and Z. Wan, "Experimental investigation on the dynamic performance of a hybrid PEM fuel cell/battery system for lightweight electric vehicle application," *Applied Energy,* vol. 88, pp. 68-76, 1// 2011.

[6] L. Barelli, G. Bidini, and A. Ottaviano, "Optimization of a PEMFC/battery pack power system for a bus application," *Applied Energy,* vol. 97, pp. 777-784, 9// 2012.

[7] S. G. Wirasingha and A. Emadi, "Classification and Review of Control Strategies for Plug-In Hybrid Electric Vehicles," *Vehicular Technology, IEEE Transactions on,* vol. 60, pp. 111-122, 2011.

[8] D. Feroldi, M. Serra, and J. Riera, "Energy Management Strategies based on efficiency map for Fuel Cell Hybrid Vehicles," *Journal of Power Sources,* vol. 190, pp. 387-401, 2009.

[9] J. Bernard, S. Delprat, T. M. Guerra, and F. N. Büchi, "Fuel efficient power management strategy for fuel cell hybrid powertrains," *Control Engineering Practice,* vol. 18, pp. 408-417, 2010.

[10] O. Farouk, R. Jürgen, W. Lars, and H. Angelika, "Power management optimization of fuel cell/battery hybrid vehicles with experimental validation," *Journal of Power Sources,* vol. 252, pp. 333 - 343, 2014.

[11] M. S. Ismail, D. B. Ingham, K. J. Hughes, L. Ma, and M. Pourkashanian, "An efficient mathematical model for air-breathing PEM fuel cells," *Applied Energy,* vol. 135, pp. 490-503, 12/15/ 2014.

[12] C.-W. Yang and Y.-S. Chen, "A mathematical model to study the performance of a proton exchange membrane fuel cell in a dead-ended anode mode," *Applied Energy,* vol. 130, pp. 113-121, 10/1/ 2014.

[13] A. Gomez, A. Raj, A. P. Sasmito, and T. Shamim, "Effect of operating parameters on the transient performance of a polymer electrolyte membrane fuel cell stack with a dead-end anode," *Applied Energy,* vol. 130, pp. 692-701, 10/1/ 2014.

[14] P. Pei and H. Chen, "Main factors affecting the lifetime of Proton Exchange Membrane fuel cells in vehicle applications: A review," *Applied Energy,* vol. 125, pp. 60-75, 7/15/ 2014.

[15] Z.-d. Zhong, H.-b. Huo, X.-j. Zhu, G.-y. Cao, and Y. Ren, "Adaptive maximum power point tracking control of fuel cell power plants," *Journal of Power Sources,* vol. 176, pp. 259-269, 2008.

[16] N. Bizon, "Energy harvesting from the FC stack that operates using the MPP tracking based on modified extremum seeking control," *Applied Energy,* vol. 104, pp. 326-336, 2013.

[17] Z. Guo-Rong, K. H. Loo, Y. M. Lai, and C. K. Tse, "Quasi-Maximum Efficiency Point Tracking for Direct Methanol Fuel Cell in DMFC/Supercapacitor Hybrid Energy System," *Energy Conversion, IEEE Transactions on,* vol. 27, pp. 561-571, 2012.

[18] C. Raga, A. Barrado, A. Lazaro, C. Fernandez, V. Valdivia, I. Quesada, *et al.*, "Black-Box Model, Identification Technique and Frequency Analysis for PEM Fuel Cell With Overshooted Transient Response," *Power Electronics, IEEE Transactions on,* vol. 29, pp. 5334-5346, 2014.

[19] M. Meiler, O. Schmid, M. Schudy, and E. P. Hofer, "Dynamic fuel cell stack model for real-time simulation based on system identification," *Journal of Power Sources,* vol. 176, pp. 523-528, 2008.

[20] Y.-P. Yang, F.-C. Wang, H.-P. Chang, Y.-W. Ma, and B.-J. Weng, "Low power proton exchange membrane fuel cell system identification and adaptive control," *Journal of Power Sources,* vol. 164, pp. 761-771, 2007.

[21] K. Ettihir, L. Boulon, M. Becherif, K. Agbossou, and H. S. Ramadan, "Online identification of semi-empirical model parameters for PEMFCs," *International Journal of Hydrogen Energy,* vol. 39, pp. 21165-21176, 2014.

[22] R. N. Methekar, S. C. Patwardhan, R. D. Gudi, and V. Prasad, "Adaptive peak seeking control of a proton exchange membrane fuel cell," *Journal of Process Control,* vol. 20, pp. 73-82, 2010.

[23] L. Dazi, Y. Yadi, J. Qibing, and G. Zhiqiang, "Maximum power efficiency operation and generalized predictive control of \{PEM\} (proton exchange membrane) fuel cell," *Energy,* vol. 68, pp. 210 - 217, 2014.

[24] C. A. Ramos-Paja, G. Spagnuolo, G. Petrone, and E. Mamarelis, "A perturbation strategy for fuel consumption minimization in polymer electrolyte membrane fuel cells: Analysis, Design and FPGA implementation," *Applied Energy,* vol. 119, pp. 21-32, 4/15/ 2014.

[25] A. B. Gene, W. Zacharie, F. Grégory, N. Arata, T. Leonidas, and B. Dominique, "Experimental real-time optimization of a solid oxide fuel cell stack via constraint adaptation," *Energy,* vol. 39, pp. 54 - 62, 2012.

[26] S. Kelouwani, K. Adegnon, K. Agbossou, and Y. Dube, "Online System Identification and Adaptive Control for PEM Fuel Cell Maximum Efficiency Tracking," *Energy Conversion, IEEE Transactions on,* vol. 27, pp. 580-592, 2012.

[27] K. Ettihir, L. Boulon, and K. Agbossou. (2016, Energy management strategy for a fuel cell hybrid vehicle based on maximum efficiency and maximum power identification. *IET Electrical Systems in Transportation 6(4),* 261-268. Available: http://digital-library.theiet.org/content/journals/10.1049/iet-est.2015.0023

[28] H. B. Jensen, E. Schaltz, P. S. Koustrup, S. J. Andreasen, and S. K. Kaer, "Evaluation of Fuel-Cell Range Extender Impact on Hybrid Electrical Vehicle Performance," *Vehicular Technology, IEEE Transactions on,* vol. 62, pp. 50-60, 2013.

[29] K. Ettihir, L. Boulon, K. Agbossou, S. Kelouwani, and M. Hammoudi, "Design of an Energy Management Strategy for PEM Fuel Cell Vehicles," *2012 IEEE International Symposium on Industrial Electronics (ISIE),* pp. 1714-1719, 2012.

[30] A. Chasse and A. Sciarretta, "Supervisory control of hybrid powertrains: An experimental benchmark of offline optimization and online energy management," *Control Engineering Practice,* vol. 19, pp. 1253-1265, 11// 2011.

[31] Z. Chen, B. Xia, C. You, and C. C. Mi, "A novel energy management method for series plug-in hybrid electric vehicles," *Applied Energy,* vol. 145, pp. 172-179, 5/1/ 2015.

[32] Y. Hou, C. Shen, Z. Yang, and Y. He, "A dynamic voltage model of a fuel cell stack considering the effects of hydrogen purge operation," *Renewable Energy,* vol. 44, pp. 246-251, 2012.

[33] Z. Song, H. Hofmann, J. Li, J. Hou, X. Han, and M. Ouyang, "Energy management strategies comparison for electric vehicles with hybrid energy storage system," *Applied Energy,* vol. 134, pp. 321-331, 12/1/ 2014.

[34] J. Wu, X.-Z. Yuan, J. J. Martin, H. Wang, D. Yang, J. Qiao, *et al.*, "Proton exchange membrane fuel cell degradation under close to open-circuit conditions:

Part I: In situ diagnosis," *Journal of Power Sources,* vol. 195, pp. 1171-1176, 2/15/ 2010.

[35] W.-S. Lin and C.-H. Zheng, "Energy management of a fuel cell/ultracapacitor hybrid power system using an adaptive optimal-control method," *Journal of Power Sources,* vol. 196, pp. 3280-3289, 3/15/ 2011.

[36] A.-Q. Xing and C.-L. Wang, "Applications of the exterior penalty method in constrained optimal control problems," *Optimal Control Applications and Methods,* vol. 10, pp. 333-345, 1989.

[37] W. Lin, D. Tao, J. Kacprzyk, Z. Li, E. Izquierdo, and H. Wang, *Multimedia analysis, processing and communications* vol. 346: Springer Science & Business Media, 2011.

[38] M. Koot, J. T. B. A. Kessels, B. de Jager, W. P. M. H. Heemels, P. P. J. Van den Bosch, and M. Steinbuch, "Energy management strategies for vehicular electric power systems," *Vehicular Technology, IEEE Transactions on,* vol. 54, pp. 771-782, 2005.

[39] S. Delprat, J. Lauber, T. M. Guerra, and J. Rimaux, "Control of a parallel hybrid powertrain: optimal control," *Vehicular Technology, IEEE Transactions on,* vol. 53, pp. 872-881, 2004.

[40] V. S. Bagotsky, "The Working Principles of a Fuel Cell," in *Fuel Cells*, ed: John Wiley & Sons, Inc., 2012, pp. 5-24.

[41] G. Squadrito, G. Maggio, E. Passalacqua, F. Lufrano, and A. Patti, "An empirical equation for polymer electrolyte fuel cell (PEFC) behaviour," *Journal of Applied Electrochemistry,* vol. 29, pp. 1449-1455, 1999.

[42] G. Squadrito, O. Barbera, G. Giacoppo, F. Urbani, and E. Passalacqua, "Polymer electrolyte fuel cell stack research and development," *International Journal of Hydrogen Energy,* vol. 33, pp. 1941-1946, 4// 2008.

[43] L. Pisani, G. Murgia, M. Valentini, and B. D'Aguanno, "A new semi-empirical approach to performance curves of polymer electrolyte fuel cells," *Journal of Power Sources,* vol. 108, pp. 192-203, 2002.

[44] M. André, R. Joumard, R. Vidon, P. Tassel, and P. Perret, "Real-world European driving cycles, for measuring pollutant emissions from high- and low-powered cars," *Atmospheric Environment,* vol. 40, pp. 5944-5953, 10// 2006.

[45] P. Thounthong, S. Raël, and B. Davat, "Test of a PEM fuel cell with low voltage static converter," *Journal of Power Sources,* vol. 153, pp. 145-150, 1/23/ 2006.

[46] S. Kelouwani, K. Agbossou, Y. Dubé, and L. Boulon, "Fuel cell Plug-in Hybrid Electric Vehicle anticipatory and real-time blended-mode energy management for battery life preservation," *Journal of Power Sources,* vol. 221, pp. 406-418, 1/1/ 2013.

Conclusion générale et perspectives

Ce travail consistait à l'élaboration d'une SGE globale et locale dans un VHPAC. Deux axes d'études se sont dégagés dans ce travail pour:

a) Développer une méthode de recherche des maximums de puissance et de rendement basée sur l'identification en ligne nécessaire à la prise en compte des performances variables de la pile PEM en temps réel

b) Réaliser une SGE optimale en temps réel sur la base de modèles semi-empiriques physiques adaptatifs afin de minimiser la consommation d'hydrogène et donc, d'augmenter l'autonomie du VHPAC

La littérature traite en général ces deux axes de manières indépendantes. En effet, les méthodes de recherche des maximums de rendement ou de puissance destinées à la pile à combustible et la SGE pour la répartition énergétique entre les sources sont traitées de manière isolée. De plus, les SGE optimales pour les sources hybrides se basent sur des modèles fixes pour la plupart. Les deux axes développés ont permis de faire le lien entre la gestion globale de l'énergie et les méthodes de recherche de maximums au niveau du système.

La réflexion de cette thèse se scinde en trois étapes valorisées par la présentation de trois articles de revues [34-36] et soutenue par des articles de conférence [32, 37]. Un premier article [35] a permis d'identifier les modèles candidats à la satisfaction des exigences liées aux besoins d'identification des performances de la pile PEM en temps réel. Cet article a validé l'hypothèse qu'un modèle semi-empirique pouvait aboutir à

l'identification des performances de la pile à combustible en fonction des conditions opératoires. Dans le cas de cette première étude, une étude expérimentale selon différentes températures de fonctionnement a permis de mettre en lumière que l'algorithme d'identification couplé au modèle semi-empirique adapte bien les paramètres du modèle face à la variation des performances vis-à-vis des conditions opératoires de la pile.

Dans un deuxième article [36], une réflexion est posée sur le fonctionnement de la méthode d'identification des performances de la pile PEM en ligne dans une SGE simple. La réflexion se positionne dans une problématique VHPAC. En outres, l'objectif est de prouver par une étude expérimentale que la méthode développée identifie bien les maximums de puissance et de rendement en temps réel en fonction des conditions opératoires de la pile. La SGE développée dans cet article permet simplement de basculer entre les modes de fonctionnement de maximum de puissance ou de maximum de rendement selon le niveau de charge des batteries sur un parcours routier adapté. Une étude expérimentale et comparative a été réalisée avec la SGE couplée à la méthode d'identification développée et la SGE sans la méthode. Les résultats démontrent que la SGE sans la méthode développée n'est plus valide quand la pile PEM est dégradée, la pile à combustible s'arrête et se met en défaut de fonctionnement. Alors qu'avec la méthode d'identification couplée à l'optimisation de la pile à combustible continue de fonctionner en mode dégradé.

Finalement, un troisième article [34] apporte une solution concrète à la problématique générale de ce travail de thèse. Une SGE optimale en temps réel est développée et intègre la méthode d'identification développée. Cet article démontre que la méthode développée peut s'inscrire dans une SGE optimale en temps réel qui prend en compte la variation des

conditions opératoires de la pile. De la même manière que l'article précédent, le troisième article permet de démontrer que l'utilisation de cartographie de la pile PEM est obsolète quand les conditions opératoires changent. Dans une SGE optimale classique la répartition est traduite par l'utilisation de systèmes modélisés par des relations mathématiques avec des paramètres constants. Ces paramètres des modèles du système constant affectent le critère d'optimisation, en particulier les bornes de fonctionnement en termes de puissances ou de courants. Les paramètres du modèle définissant le critère optimale sont valides dans une plage de conditions opératoires spécifique. Lorsque la pile à combustible se dégrade le critère d'optimisation n'est plus valide et la trajectoire n'est plus optimale.

Ce travail a poursuivi les travaux initiés par Kelouwani et al. [29] au sein de l'Institut de Recherche sur l'Hydrogène sur l'optimisation multiparamétrique d'une pile PEM. Ce travail ouvre des perspectives pour des travaux futurs et doit maintenant converger vers cette optique multiparamétrique. En effet, les travaux de cette thèse traitent d'un unique paramètre : le courant de la pile à combustible. Une étape suivante est l'optimisation multiparamétrique. Pour cela, des modèles incluant les phénomènes physiques tels que la température, pression et humidité par exemple doivent être explorés. Cependant, une emphase doit être mise sur des modèles qui découplent l'interaction des paramètres sur les performances de la pile PEM. Dans ce cas, utiliser plusieurs modèles pour chaque paramètre à optimiser peut être une solution. Cependant, la technique des moindres carrés employée dans ce travail requiert un temps de calcul supplémentaire à mesure que le nombre de paramètres augmente. Une solution est d'utiliser le filtrage de Kalman pour l'estimation paramétrique et coupler plusieurs modèles simples de la pile. Par exemple,

dans le cas où l'on optimise la pile PEM en température et en courant, le modèle sélectionné dans ce travail peut être couplé à un modèle thermique de la pile à combustible.

Une deuxième perspective est l'utilisation de ce travail sur le projet multistack de l'IRH et développé par Marx et al. [38]. Le système multistack est redondant, en conséquence, l'utilisation de ce travail de thèse est très utile pour anticiper l'utilisation d'une pile à combustible en fonction des conditions opératoires de l'ensemble du système. Des SGE permettraient d'estimer la puissance disponible au niveau des piles et donc d'optimiser leurs mises en marche et leurs modes de fonctionnement afin de réduire la consommation et préserver leur durée de vie.

Une troisième perspective est de faire converger les travaux développés dans cette thèse avec les travaux de Martel et al. [39] sur la gestion du vieillissement des batteries. Un travail complet peut être mené pour étudier la possibilité d'une SGE qui tient compte des conditions opératoires des batteries et de la pile à combustible dans le cadre du VHPAC. Les algorithmes appliqués à la pile PEM sont transposables à la batterie puisque les équations caractéristiques sont similaires. Le modèle de Martel et al. développé à l'IRH s'intégrerait au processus d'identification en ligne des paramètres non modélisable afin de s'adapter aux variations des performances de la batterie. Ainsi, localement, les performances de la batterie seraient identifiées en ligne pour être remontées dans une SGE globale et optimale.

Bibliographies

[1] IEA (2014), "World Energy Outlook 2014."

[2] *Gouvernement du Québec. Inventaire québécois des émissions de gaz à effet de serre en 2012 et leur évolution depuis 1990*, 2015.

[3] C. C. Chan, A. Bouscayrol, and K. Chen, "Electric, Hybrid, and Fuel-Cell Vehicles: Architectures and Modeling," *Vehicular Technology, IEEE Transactions on,* vol. 59, pp. 589-598, 2010.

[4] C. E. Thomas, "Fuel cell and battery electric vehicles compared," *International Journal of Hydrogen Energy,* vol. 34, pp. 6005-6020, 2009.

[5] B. M. Besancon, V. Hasanov, R. Imbault-Lastapis, R. Benesch, M. Barrio, and M. J. Mølnvik, "Hydrogen quality from decarbonized fossil fuels to fuel cells," *International Journal of Hydrogen Energy,* vol. 34, pp. 2350-2360, 3// 2009.

[6] R. H. Borgwardt, "Platinum, fuel cells, and future US road transport," *Transportation Research Part D: Transport and Environment,* vol. 6, pp. 199-207, 5// 2001.

[7] J. J. Hwang, "Transient power characteristic measurement of a proton exchange membrane fuel cell generator," *International Journal of Hydrogen Energy,* vol. 38, pp. 3727-3740, 3/27/ 2013.

[8] S. F. Tie and C. W. Tan, "A review of energy sources and energy management system in electric vehicles," *Renewable and Sustainable Energy Reviews,* vol. 20, pp. 82-102, 2013.

[9] A. Payman, S. Pierfederici, and F. Meibody-Tabar, "Energy control of supercapacitor/fuel cell hybrid power source," *Energy Conversion and Management,* vol. 49, pp. 1637-1644, 2008.

[10] D. Feroldi, M. Serra, and J. Riera, "Energy Management Strategies based on efficiency map for Fuel Cell Hybrid Vehicles," *Journal of Power Sources,* vol. 190, pp. 387-401, 2009.

[11] H. Hemi, J. Ghouili, and A. Cheriti, "Combination of Markov chain and optimal control solved by Pontryagin's Minimum Principle for a fuel cell/supercapacitor vehicle," *Energy Conversion and Management,* vol. 91, pp. 387-393, 2015.

[12] J. Bernard, S. Delprat, T. M. Guerra, and F. N. Büchi, "Fuel efficient power management strategy for fuel cell hybrid powertrains," *Control Engineering Practice,* vol. 18, pp. 408-417, 2010.

[13] O. Farouk, R. Jürgen, W. Lars, and H. Angelika, "Power management optimization of fuel cell/battery hybrid vehicles with experimental validation," *Journal of Power Sources,* vol. 252, pp. 333 - 343, 2014.

[14] T. Jahnke, G. Futter, A. Latz, T. Malkow, G. Papakonstantinou, G. Tsotridis, *et al.*, "Performance and degradation of Proton Exchange Membrane Fuel Cells: State of the art in modeling from atomistic to system scale," *Journal of Power Sources,* vol. 304, pp. 207-233, 2/1/ 2016.

[15] M. Meiler, O. Schmid, M. Schudy, and E. P. Hofer, "Dynamic fuel cell stack model for real-time simulation based on system identification," *Journal of Power Sources,* vol. 176, pp. 523-528, 2008.

[16] C. Raga, A. Barrado, A. Lazaro, C. Fernandez, V. Valdivia, I. Quesada, *et al.*, "Black-Box Model, Identification Technique and Frequency Analysis for PEM Fuel Cell With Overshooted Transient Response," *Power Electronics, IEEE Transactions on,* vol. 29, pp. 5334-5346, 2014.

[17] V. Valdivia, A. Barrado, A. Lazaro, M. Sanz, D. Lopez del Moral, and C. Raga, "Black-Box Behavioral Modeling and Identification of DC–DC Converters With Input Current Control for Fuel Cell Power Conditioning," *Industrial Electronics, IEEE Transactions on,* vol. 61, pp. 1891-1903, 2014.

[18] J. P. Torreglosa, F. Jurado, P. García, and L. M. Fernández, "PEM fuel cell modeling using system identification methods for urban transportation applications," *International Journal of Hydrogen Energy,* vol. 36, pp. 7628-7640, 7// 2011.

[19] C. Kunusch, "Online identification of time varying parameters in PEM fuel cells," 2013.

[20] L. Xu, J. Li, J. Hua, X. Li, and M. Ouyang, "Adaptive supervisory control strategy of a fuel cell/battery-powered city bus," *Journal of Power Sources,* vol. 194, pp. 360-368, 2009.

[21] L. Qi, C. Weirong, W. Youyi, L. Shukui, and J. Junbo, "Parameter Identification for PEM Fuel-Cell Mechanism Model Based on Effective Informed Adaptive Particle Swarm Optimization," *Industrial Electronics, IEEE Transactions on,* vol. 58, pp. 2410-2419, 2011.

[22] A. Askarzadeh and A. Rezazadeh, "An Innovative Global Harmony Search Algorithm for Parameter Identification of a PEM Fuel Cell Model," *Industrial Electronics, IEEE Transactions on,* vol. 59, pp. 3473-3480, 2012.

[23] J. Wu, X.-Z. Yuan, J. J. Martin, H. Wang, D. Yang, J. Qiao, *et al.*, "Proton exchange membrane fuel cell degradation under close to open-circuit conditions: Part I: In situ diagnosis," *Journal of Power Sources,* vol. 195, pp. 1171-1176, 2/15/ 2010.

[24] Z.-d. Zhong, H.-b. Huo, X.-j. Zhu, G.-y. Cao, and Y. Ren, "Adaptive maximum power point tracking control of fuel cell power plants," *Journal of Power Sources,* vol. 176, pp. 259-269, 2008.

[25] N. Benyahia, H. Denoun, A. Badji, M. Zaouia, T. Rekioua, N. Benamrouche, *et al.*, "MPPT controller for an interleaved boost dc–dc converter used in fuel cell electric vehicles," *International Journal of Hydrogen Energy,* vol. 39, pp. 15196-15205, 2014.

[26] R. N. Methekar, S. C. Patwardhan, R. D. Gudi, and V. Prasad, "Adaptive peak seeking control of a proton exchange membrane fuel cell," *Journal of Process Control,* vol. 20, pp. 73-82, 2010.

[27] M. Becherif and D. Hissel, "MPPT of a PEMFC based on air supply control of the motocompressor group," *International Journal of Hydrogen Energy,* vol. 35, pp. 12521-12530, 2010.

[28] L. Dazi, Y. Yadi, J. Qibing, and G. Zhiqiang, "Maximum power efficiency operation and generalized predictive control of \{PEM\} (proton exchange membrane) fuel cell," *Energy,* vol. 68, pp. 210 - 217, 2014.

[29] S. Kelouwani, K. Adegnon, K. Agbossou, and Y. Dube, "Online System Identification and Adaptive Control for PEM Fuel Cell Maximum Efficiency Tracking," *Energy Conversion, IEEE Transactions on,* vol. 27, pp. 580-592, 2012.

[30] C. A. Ramos-Paja, G. Spagnuolo, G. Petrone, and E. Mamarelis, "A perturbation strategy for fuel consumption minimization in polymer electrolyte membrane fuel cells: Analysis, Design and FPGA implementation," *Applied Energy,* vol. 119, pp. 21-32, 4/15/ 2014.

[31] B. Somaiah and V. Agarwal, "Recursive Estimation-Based Maximum Power Extraction Technique for a Fuel Cell Power Source Used in Vehicular Applications," *Power Electronics, IEEE Transactions on,* vol. 28, pp. 4636-4643, 2013.

[32] K. Ettihir, L. Boulon, K. Agbossou, S. Kelouwani, and M. Hammoudi, "Design of an Energy Management Strategy for PEM Fuel Cell Vehicles," *2012 IEEE International Symposium on Industrial Electronics (ISIE),* pp. 1714-1719, 2012.

[33] D. Fares, R. Chedid, F. Panik, S. Karaki, and R. Jabr, "Dynamic programming technique for optimizing fuel cell hybrid vehicles," *International Journal of Hydrogen Energy,* 2015.

[34] K. Ettihir, L. Boulon, and K. Agbossou, "Optimization-based energy management strategy for a fuel cell/battery hybrid power system," *Applied Energy,* vol. 163, pp. 142-153, 2/1/ 2016.

[35] K. Ettihir, L. Boulon, M. Becherif, K. Agbossou, and H. S. Ramadan, "Online identification of semi-empirical model parameters for PEMFCs," *International Journal of Hydrogen Energy,* vol. 39, pp. 21165-21176, 2014.

[36] K. Ettihir, L. Boulon, and K. Agbossou. (2016, Energy management strategy for a fuel cell hybrid vehicle based on maximum efficiency and maximum power identification. *IET Electrical Systems in Transportation 6(4),* 261-268. Available: http://digital-library.theiet.org/content/journals/10.1049/iet-est.2015.0023

[37] K. Ettihir, L. Boulon, K. Agbossou, and S. Kelouwani, "MPPT control strategy on PEM Fuel Cell Low Speed Vehicle," in *Vehicle Power and Propulsion Conference (VPPC), 2012 IEEE*, 2012, pp. 926-931.

[38] N. Marx, L. Boulon, F. Gustin, D. Hissel, and K. Agbossou, "A review of multi-stack and modular fuel cell systems: Interests, application areas and on-going

research activities," *International Journal of Hydrogen Energy,* vol. 39, pp. 12101-12111, 8/4/ 2014.

[39] F. Martel, S. Kelouwani, Y. Dubé, and K. Agbossou, "Optimal economy-based battery degradation management dynamics for fuel-cell plug-in hybrid electric vehicles," *Journal of Power Sources,* vol. 274, pp. 367-381, 1/15/ 2015.